



Theses and Dissertations

2006-12-01

Development of Methods for the Study of Phosphoproteins

Zhaoyuan Chen

Brigham Young University - Provo

Follow this and additional works at: <https://scholarsarchive.byu.edu/etd>



Part of the [Biochemistry Commons](#), and the [Chemistry Commons](#)

BYU ScholarsArchive Citation

Chen, Zhaoyuan, "Development of Methods for the Study of Phosphoproteins" (2006). *Theses and Dissertations*. 1041.

<https://scholarsarchive.byu.edu/etd/1041>

This Dissertation is brought to you for free and open access by BYU ScholarsArchive. It has been accepted for inclusion in Theses and Dissertations by an authorized administrator of BYU ScholarsArchive. For more information, please contact scholarsarchive@byu.edu, ellen_amatangelo@byu.edu.

**DEVELOPMENT OF METHODS
FOR
THE STUDY OF PHOSPHOPROTEINS**

by

Zhaoyuan Chen

A dissertation submitted to the faculty of
Brigham Young University

In partial fulfillment of the requirement for the degree of

Doctor of Philosophy

Department of Chemistry and Biochemistry
Brigham Young University

December 2006

BRIGHAM YOUNG UNIVERSITY
GRADUATE COMMITTEE APPROVAL

Of a dissertation submitted by

Zhaoyuan Chen

This dissertation has been read by each member of the following graduate committee and by majority vote has been found to be satisfactory

Date _____ Craig D. Thulin, Chair

Date _____ Barry M. Willardson

Date _____ Milton L. Lee

Date _____ Allen R. Buskirk

Date _____ Gerald D. Watt

BRIGHAM YOUNG UNIVERSITY

As Chair of the candidate's graduate committee, I have read the dissertation of Zhaoyuan Chen in its final form and have found that (1) its format, citations, and bibliographical style are consistent and acceptable and fulfill university and department style requirement;(2) its illustrative materials including figures, tables, and charts are in place; and (3) the final manuscript is satisfactory to the graduate committee and is ready for submission to the university library.

Date

Craig D. Thulin
Chair, Graduate Committee

Accepted for the Department

David V. Dearden
Graduate Coordinator

Accepted for the College

Thomas W. Sederberg, Associate Dean
College of Physical and Mathematical Sciences

ABSTRACT

DEVELOPMENT OF METHODS FOR THE STUDY OF PHOSPHOPROTEINS

Zhaoyuan Chen

Department of Chemistry and Biochemistry

Doctor of Philosophy

Characterization of phosphoproteins—including detection, identification of phosphoproteins and identification of phosphorylation sites—is mostly done with radiolabeling and proteomic techniques. Three main topics related to phosphoprotein characterization are included in this dissertation. First, large-scale characterization of the CHO (Chinese hamster ovary) cell phosphoproteome was done using two dimensional gel electrophoresis (2DE) separation, visualization of phosphoproteins by radiolabeling or a phosphoprotein specific dye, followed by MALDI-TOF identification. Because radiolabeling of phosphoproteins is very sensitive and straightforward to quantify, such analysis can give a clear picture of the relative phosphosphorylation of proteins present in a sample. But there are also limitations to this approach, such as the inability of 2DE to separate hydrophobic, acidic and large proteins and the poor detection limits of common protein stains such as Coomassie stain. Additionally, it is difficulty to excise the right spots for identification because of the low abundance of phosphoproteins which have been visualized by radiolabeling. Furthermore, there are problems associated with metabolic radiolabeling.

A second topic of the dissertation is the development of a novel strong cation exchange monolithic column for MudPIT (multidimensional protein identification technology) and phosphopeptide isolation. This column, a poly(AMPS-*co*-PEGDA) monolith containing as high as 40% AMPS, has several favorable features, such as high binding capacity, extraordinarily high resolution, and high peak capacity, making it ideal for resolving complex peptide samples. Application of this novel column to isolate model phosphopeptides was shown. More general use of this column in MudPIT (strong cation exchange column followed by reverse-phased MS/MS) is probably somewhat limited, due to the hydrophobicity of the AMPS monomer. A better monolith could be obtained if a more hydrophilic monomer was used.

In the third area of the dissertation, several individual protein phosphorylation sites were analyzed, employing different strategies. Phosphorylation sites of one multiply phosphorylated tryptic peptide from CK2-phosphorylated phosphoducin-like protein (PhLP) was well characterized using enrichment with a MonoTip® TiO Pipette Tip. Analysis of syntaxin 1a phosphorylation by AMPK (AMP-activated protein kinase) was done by peptide level mapping for potential phosphopeptides after its unsuccessful trial with enrichment using the MonoTip® TiO Pipette Tip. Several criteria such as existence of non-phosphorylated forms of potential phosphopeptides, controls and reasonable retention times were used to rule out false positives. Phosphorylation of syntaxin 1a by AMPK was narrowed down to tryptic peptide T32 with evidence from different sources. Three phosphorylation sites of syntaxin 4 by AMPK were identified within the same peptide (Q₆₅QVTILATPLPEESMK₈₀). Further pinpointing of phosphorylation site(s) for syntaxin 1a by AMPK and further confirmation of these phosphorylation sites in syntaxin

4 by AMPK are required *in vivo*. The role of phosphorylation in syntaxin 4 by AMPK is the next step toward elucidation of AMPK activation and regulation of the glucose uptake mechanism.

ACKNOWLEDGEMENTS

First and foremost, I thank Dr. Craig Thulin, for his continuous guidance and support throughout my graduate study. I also admire and respect him as a kind and caring person with a great sense of humor. I also want to thank my committee members, Dr. Lee, Dr. Willardson, Dr. Buskirk and Dr. Watt for their valuable suggestions and thorough review of this dissertation. Dr. Lee was especially helpful in the collaborative effort with the monolithic strong cation exchange column project. I also thank Dr. William Winder and Dr. Dixon Woodbury for their help and effort in the syntaxin phosphorylation project. My lab mates and other friends in the department have been helpful and have made the experience enjoyable. I thank my wife, Yanchen, for her tremendous patience, sacrifice and her help on the editing of this dissertation. I want to thank my family, especially my parents, for their unconditioned love for me from day one of my life.

TABLE OF CONTENTS

LIST OF FIGURES	III
LIST OF TABLES	V
LIST OF ACRONYMS AND ABBREVIATIONS	VI
CHAPTER ONE INTRODUCTION	1
1.1 PROTEIN PHOSPHORYLATION	1
1.2 PROTEIN PHOSPHORYLATION ANALYSIS.....	3
1.2.1 Protein Phosphorylation Detection	4
1.2.2 Phosphopeptide Recognition	8
1.2.3 Phosphorylation Site Identification.....	12
1.3 PHOSHOPEPTIDE/PHOSPHOPROTEIN ENRICHMENT METHODS	18
1.3.1 Phosphoprotein Enrichment.....	19
1.3.2 Phosphopeptide Enrichment	20
1.4 REFERENCES.....	25
CHAPTER TWO CHARACTERIZATION OF PHOSPHOPROTEINS BY TWO DIMENSIONAL GEL ELECTROPHORESIS AND MASS SPECTROMETRY... 33	
2.1 INTRODUCTION	33
2.2 MATERIALS AND METHODS	34
2.2.1 ³² P-Labeling of Chinese Hamster Ovary Cell Phosphoproteins	34
2.2.2 2D Electrophoretic Analysis	35
2.2.3 Identification of Proteins from Excised Gel Spots	35
2.2.4 Pro-Q Diamond Stain of Chinese Hamster Ovary Cell Extract.....	36
2.2.5 2D Gel Image Processing.....	36
2.3 RESULTS AND DISCUSSION	37
2.3.1 Overview of the Phosphoproteome Compared with the Entire Proteome	37
2.3.2 Effects of Labeling Time on the Phosphoproteome Observed	39
2.3.3 Effect of a Specific Phosphatase Inhibitor.....	42
2.3.4 Identifying Phosphoproteins from 2D gels	42
2.3.5 Use of a Phosphoprotein Stain for Visualization.....	44
2.4 CONCLUSIONS.....	45
2.5 REFERENCES.....	46
CHAPTER THREE NOVEL STRONG CATION EXCHANGE MONOLITHIC COLUMN AND PHOSHOPEPTIDE ISOLATION	47
3.1 INTRODUCTION	47
3.2 MATERIALS AND METHODS	51
3.2.1 Chemicals and Reagents	51
3.2.2 Polymer Monolith Preparation.....	52
3.2.3 Capillary Liquid Chromatography (CLC)	53
3.2.4 Synthesis and Characterization of Acrylamidomethanesulfonic Acid	55

3.2.5 Safety Considerations	55
3.3 RESULTS AND DISCUSSION	56
3.3.1 Polymer Monolith Preparation.....	56
3.3.2 Effect of Acetonitrile on the Elution of Synthetic Peptides.....	60
3.3.3 Effect of Buffer pH on the Resolution of Synthetic Peptides.....	64
3.3.4 Dynamic Binding Capacity.....	65
3.3.5 SCX Chromatography of a Complex Peptide Mixture.....	67
3.3.6 SCX Chromatography of Protein Standards.....	72
3.3.7 SCX Chromatography Application for the Separation of Model Phosphopeptides	73
3.3.8 Stability of the Poly(AMPS-co-PEGDA) Monolith	73
3.3.9 Tentative Explanation of the Sharp Peaks Obtained.....	75
3.3.10 Synthesis of Acrylamidomethanesulfonic Acid.....	77
3.4 CONCLUSIONS.....	78
3.5 REFERENCES.....	79
CHAPTER FOUR ANALYSIS OF PHOSPHORYLATION OF SYNTAXIN 1A AND 4A BY AMPK	83
4.1 INTRODUCTION	83
4.2 MATERIALS AND METHODS	86
4.2.1 Syntaxin 1a (1a1, 1a7, 1a9, 1a11, 1a12) Expression and Protein Purification	86
4.2.2 PhLP Expression and Purification	86
4.2.3 In vitro Phosphorylation of PhLP, Syntaxin 1a and Syntaxin 4a	87
4.2.4 In-gel Digestion of Syntaxin 1a Containing Gel Bands.....	87
4.2.5 Enrichment of Phosphopeptides from Tryptic Peptides	88
4.2.6 LC-MS/MS Analysis of Tryptic Peptides or Enriched Samples	88
4.3 RESULTS AND DISCUSSION	89
4.3.1 Study of PhLP Phosphorylation with Phosphopeptide Enrichment	89
4.3.2 Study of Syntaxin 1a Phosphorylation.....	92
4.4 CONCLUSIONS.....	98
4.5 REFERENCES.....	99
CHAPTER FIVE FUTURE WORK.....	101
5.1 APPLIED SITE-DIRECTED MUTAGENESIS TO CONFIRM THE IDENTIFIED PHOSPHORYLATION SITES IN VIVO AND ROLES OF PHOSPHORYLATION ON THESE SITES	101
5.1.1 Confirmation of the Identified Phosphorylation Sites in vivo.....	101
5.1.2 Role of Phosphorylation on the Identified Sites	101
5.1.3 Examination of the Possibility of other SNARE Proteins Involved in This Vesicle-membrane Fusion Process	102
5.2 FUTURE WORK ON THE MONOLITHIC SCX COLUMN.....	102

LIST OF FIGURES

Figure 1. Detection of phosphoproteins employing λ -phosphatase (λ PPase).....	7
Figure 2. Schematic view of a triple quadrupole mass analyzer operating in precursor ion scanning (PIS) or neutral loss scanning (NLS) modes.	11
Figure 3. Different techniques for the enrichment and analysis of phosphoproteins based on MS procedures [D'Ambrosio et al., 2006b].	20
Figure 4. Various strategies for the enrichment of phosphopeptides based on different chemical modification reactions.	24
Figure 5. Two-dimensional electrophoresis of proteins and phosphoproteins of Chinese hamster ovary cells.	37
Figure 6. Number of spots in different categories. Proteins are grouped according to their appearance in phosphorimage, Coomassie-stained gel, or both.	38
Figure 7. Effect of labeling time.	39
Figure 8. Spot intensities as a function of labeling time.	40
Figure 9. Effect of phosphatase inhibitor.....	41
Figure 10. Spot intensities as a function of phosphatase inhibitor.	41
Figure 11. Comparison of radiolabeling and phosphoprotein staining for visualizing the phosphoproteome.....	44
Figure 12. SEM photographs of several monoliths synthesized.....	59
Figure 13. SCX chromatography of synthetic peptides.....	61
Figure 14. SCX chromatography of natural peptides.	68
Figure 15. SCX chromatography of a β -casein digest.....	71
Figure 16. SCX chromatography of an old synthetic peptide sample.	71

Figure 17. SCX chromatography of proteins.....	72
Figure 18. SCX chromatography of a phosphopeptide and a mixture of three peptides..	74
Figure 19. LC-MSD-TOF confirmation of acrylamidomethanesulfonic acid.....	77
Figure 20. Two mechanisms for stimulation of glucose uptake in skeletal muscle, one mediated by insulin and one triggered by muscle contraction.....	85
Figure 21. MS/MS spectra of T3 of phosphorylated PhLP by CKII.....	90
Figure 22. Ion extractions of m/z (1118.7-1119.7) of TOF MS experiments from syntaxin 1a phosphorylation samples and controls.....	94
Figure 23. Autoradiography of <i>in vitro</i> phosphorylated syntaxin 1a and its truncated forms by activated AMPK.....	95
Figure 24. MS/MS spectrum of unphosphorylated T32 (1637.7, +2,) with strong b, y ions labeled.....	96
Figure 25. MS/MS spectrum of T12 of syntaxin 4a (1012.5, +2, Mowse score, 20) with strong b, y and their de-ammonia (b*) form labeled.....	97

LIST OF TABLES

Table 1. Comparison of mass spectrometry-based techniques with other methods for phosphorylation analysis of peptides.....	13
Table 2. Identification of phosphoprotein spots cut from Coomassie-stained gel (Figure 5).	43
Table 3. Properties of Synthetic Peptides.	60
Table 4. Properties of the Nine Peptides in the P2693 Standard.	67
Table 5. Permeability of the Poly(AMPS-co-PEGDA) Monolith	75
Table 6. Sequence alignments of syntaxin 4a (syn4a) and syntaxin 1a (syn1a) by Sim software program	92
Table 7. <i>In vitro</i> phosphorylation of syntaxin 1a for in-gel digestion.	95

LIST OF ACRONYMS AND ABBREVIATIONS

2DE	two-dimensional gel electrophoresis
AMPK	AMP-activated protein kinase
AMPS	2-acrylamido-2-methyl-1-propanesulfonic acid
CE	capillary zone electrophoresis
CHO	Chinese hamster ovary
CK2	Casein kinase II
CLC	capillary liquid chromatography
CID	collision-induced dissociation
DHB	5-dihydroxybenzoic acid
DMEM	Dulbecco's modified eagle's medium
DMPA	2-dimethoxy-2-phenylacetophenone
ECD	electron capture dissociation
EDMA	ethylene glycol dimethacrylate
ETD	electron transfer dissociation
FTICR	Fourier transform ion cyclotron resonance
ICP	inductively coupled plasma
IDA	information-dependent acquisition
MCA	multiple channel analyzer
IMAC	Immobilized metal affinity chromatography
MALDI	matrix-assisted laser desorption/ionization
MALDI-ion trap	MALDI source coupled to ion trap MS
MALDI-q-TOF	MALDI source coupled to quadrupole-TOF

MALDI-TOF-TOF MS ³	MALDI source coupled to TOF-TOF tandem MS MS/MS/MS
MudPIT	multidimensional protein identification technology
NLS	neutral loss scan (neutral lost scan)
NTA	nitriloacetic acid
oMALDI	orthogonal MALDI
PEGDA	poly(ethylene glycol) diacrylate
PPase	phosphoprotein phosphatase
pSer/pThr/pTyr	phosphoamino acid content ratio
PIS	precursor ion scan
PSI	phosphorylation site identification
Q1	quadrupole 1
RSD	relative standard deviation
SCX	strong cation exchange
SDS	sodium dodecyl sulfate
SDS-PAGE	SDS-polyacrylamide gel electrophoresis
SEM	scanning electron microscopy
Ser/Thr PPases	phosphoprotein Serine/Threonine phosphatases
TED	Tris-(carboxymethyl)-ethylendiamine
Tyr PPase	phosphotyrosine phosphatases
XIC	ion extraction chromatogram
λ PPase	λ phosphoprotein phosphatase

CHAPTER ONE

INTRODUCTION

1.1 PROTEIN PHOSPHORYLATION

Reversible protein phosphorylation was first discovered by Krebs and Fisher who demonstrated that the interconversion of phosphorylase b to phosphorylase a involved a phosphorylation/dephosphorylation mechanism [Fisher et al., 1955]. It was through the 1970s and 1980s that the general significance of protein phosphorylation came to be appreciated. Many protein kinase cascades were identified during the 1990s. Now we realize that protein phosphorylation is an integral part of all biological systems. No one will doubt the statement that the reversible phosphorylation of proteins regulates nearly every aspect of cell life. It is vital to many protein functions that are important to cellular processes spanning the range from signal transduction, differentiation and development, to cell cycle control and metabolism. The phosphorylation status of proteins is controlled by two different classes of enzymes: protein kinases which catalyze the transfer of phosphoryl groups from a high-energy compound to a nucleophilic acceptor on an amino acid side-chain of proteins, and protein phosphatases which catalyze water-driven hydrolysis of phosphoester bonds. Kinases and phosphatases modulate the protein phosphorylation status of proteins in a cell. Kinases have been classified according to their substrate specificity, being either tyrosine kinases, serine/threonine kinases, or dual specificity kinases (which have both tyrosine as well as serine/threonine kinase

activities). Just like their kinase counterparts, the protein phosphatases have been categorized into two groups, the phosphoprotein Ser/Thr phosphatases (Ser/Thr PPases) and the phosphotyrosine phosphatases (Tyr PPase), based upon substrate specificity. The importance of these two classes of enzymes is also supported by their high number of genes in the genome, constituting approximately 2% of the proteins encoded by the human genome [Amit et al., 2002; Antonsson et al., 1998]. There are more kinases than phosphatases due to their specificities (e.g. there are ~500 kinases and 100 phosphatases in humans) [Venter et al., 2001]. It is estimated that one out of every three proteins is phosphorylated at some point in its life cycle [Sickmann et al., 2001]. Several amino acids in proteins can be phosphorylated by the four known types of phosphorylation [Venter et al., 2001]. O-phosphates are the most common class and they are usually attached to serine, threonine and tyrosine residues, but also to unusual amino acids such as hydroxy-proline. Serine and threonine residues undergo phosphorylation more often than tyrosine residues. The phosphoamino acid content ratio (pSer/pThr/pTyr) of a vertebrate cell is approximately 1800:200:1. There is a higher gain in signals involving tyrosine phosphorylation because it is less abundant and more tightly regulated [Hunter et al., 1995]. N-, S- and acyl-phosphorylation are far less widespread and occur mostly on histidine and lysine (N-phosphates), cysteine (S-phosphates) and aspartic and glutamic acid residues (acyl-phosphates). In this dissertation, I will focus on o-phosphate type phosphorylation on serine, threonine and tyrosine residues which are most common in eukaryotic cells.

Phosphorylation leads to heterogeneity. Most phosphoproteins undergo phosphorylation on more than one residue – this means that all the molecules of a given

protein are not identically phosphorylated. Another characteristic of phosphorylation is the ratio of phosphorylated to non-phosphorylated protein present in the cell [Schlessinger et al., 1993-1994]. Some protein residues may be always quantitatively phosphorylated, while others may only be transiently phosphorylated. The abundance of phosphorylated forms of a protein can be as low as 1-2% of the total amount of that protein [Kalume et al., 2003]. Phosphorylation is highly dynamic and intensely regulated, and phosphorylation cycles may take place on a very short timescale. In addition to problems concerning regulation, dynamics and abundance of phosphorylation, the analysis is complicated by the complexity of phosphorylation patterns and the sheer number of phosphorylation sites. There are more than 100,000 estimated phosphorylation sites in the human proteome [Kalume et al., 2003].

1.2 PROTEIN PHOSPHORYLATION ANALYSIS

Despite a growing knowledge of many phosphorylation consensus sequences, this posttranslational modification cannot usually be predicted accurately from translated gene sequences alone. Additionally, we cannot predict when a site will be phosphorylated. Thus, the experimental determination of sites of phosphorylation is an important task. Analysis of protein phosphorylation usually includes phosphorylation detection, phosphoprotein/phosphopeptide isolation and phosphorylation site identification (PSI) by Edman degradation or MS-based methods. Various strategies for protein phosphorylation detection have been developed throughout the years. Detection of the phosphoprotein usually is the first step towards PSI.

1.2.1 Protein Phosphorylation Detection

Based on an extra phosphate group on an amino acid residue, several methods have been developed to visualize phosphoproteins.

1.2.1.1 Isotopic Label of Phosphoprotein

The use of the inorganic phosphate isotopes ^{32}P or ^{33}P (as in $[\gamma\text{-}^{32}\text{P}] \text{ATP}$, for example) to radiolabel phosphorylated proteins is probably the oldest method used to study protein phosphorylation. It is still largely employed because it is simple, reliable and sensitive for studying phosphorylation events *in vitro* and in cellular models. This strategy takes advantage of cells taking up phosphates in media during metabolic processes. So the usual procedure for this strategy is feeding cells with a radioactive phosphorus isotope containing phosphate, lysing the cells, separating the cell lysate in SDS-PAGE gel or a two-dimensional gel electrophoresis (2DE) and detection of phosphorylation by autoradiography or a PhosphorImager system. The high sensitivity of this method usually makes it a good choice to determine if a given protein is phosphorylated particularly when stoichiometry of phosphorylation is low. Requirements of *in vitro* metabolic labeling also bring problems for those situations when viable cells are not available, for example with human biopsies, or when phosphoproteins have a quick turnover rate. It also brings problems of different detection limits between gel electrophoresis (SDS-PAGE gels or 2DE gels) and radiolabeling. Some proteins are detected as phosphoproteins in gels by PhosphoImaging but not amenable to downstream analysis such as PSI by MS because of the low amount of proteins present in gels. Another disadvantage of the isotopic labeling is the safety and environmental concern.

1.2.1.2 Direct Staining of Phosphoprotein

It would be fairly simple to visualize a phosphoprotein if there were reagents that selectively detect phosphoproteins directly in SDS-PAGE gels. In this case, no viable cells are required, and no safety or environmental issues are involved compared to isotopic labeling method. Several methods have been described [Debruyne et al., 1983; Cutting et al., 1973] to stain phosphoproteins directly in gels, but low specificity and sensitivity have prevented these methods from being routinely applied. A recently introduced fluorescent-based dye system called Pro-Q DiamondTM [Steinberg et al., 2003; Schulenberg et al., 2003] makes direct staining more practical. Although the mechanism for this stain is unknown due to proprietary patents, this dye selectively stains phosphorylated proteins employing a very simple experimental protocol. The sensitivity of staining depends on the number of phosphorylated residues present in the protein. About 16 ng for pepsin (1 phosphorylated residue) and 2 ng for alpha-casein (8 phosphorylated residues) were the detection limits. Although it is quite sensitive, it is not sufficient for comprehensive analysis of the phosphoproteome. Because of compatibility of this dye with mass spectrometry analysis, it allows detection of phosphorylated proteins and total proteins (with the SYPRO Ruby dye) on the same gel.

1.2.1.3 Western Blot Employing Phosphospecific Antibodies

Western blotting is a technique for identifying a certain protein in a sample by using an antibody specific to that protein, in which proteins are separated by electrophoresis, transferred to nitrocellulose and reacted with the antibody [Towbin et al., 1979]. The development of antibodies against common protein epitopes allows the identification of proteins sharing the same characteristics. In the case of the

phosphoproteome, the common epitopes are phosphoserine, phosphothreonine and phosphotyrosine. The basic elements of this approach are the resolution of proteins in gels, the selectivity and sensitivity of the antibodies and the sensitivity of the detection system. All these elements were improved with the availability of high-resolution 2DE, highly selective antibodies and high sensitivity detection systems [Kaufmann et al., 2001; Buonocore et al., 1999]. Better anti p-Tyr antibodies are available because of the larger size of p-Tyr compared to p-Ser or p-Thr. P-Ser or p-Thr specific antibodies are mostly dependent on surrounding sequences in addition to the phosphorylated residue and are thus more likely to be less specific and of lower affinity. The specificity and affinity of antibodies play a key role in the applicability of this approach due to false positive detection in this process. This is part of the reason that anti p-Tyr containing phosphoproteins are much better studied [Godovac-Zimmermann et al., 1999; Soskic et al., 1999] with this approach, although they are less abundant than their counterparts. Better anti p-Ser and anti p-Thr antibodies are needed to achieve the same result as anti p-Tyr antibodies [Wagner et. al 1991; Yang et al., 2001]. A fairly exhaustive evaluation of the specificity and reliability of commercially available anti p-Ser and anti p-Thr antibodies has been done [Grønberg et al., 2002]. Although Western blotting has a very low detection limit for phosphoproteins, this method is not very suitable for quantitative analysis due to the variability of the amount of proteins transferred to the membrane from one SDS gel to another, which necessitates an internal standard.

1.2.1.4 Detection of Phosphoproteins Employing Phosphatases

Phosphatases hydrolyze phosphate groups off phosphoproteins, which change the net charge and molecular weight of the proteins and, thus, the migration behavior during

2D gel electrophoresis. These changes have been exploited to discriminate phosphorylated from unphosphorylated proteins. The specific enzymatic activity of λ -phosphatase (λ PPase) on p-Ser, p-Thr, p-Tyr and p-His residues, combined with the high

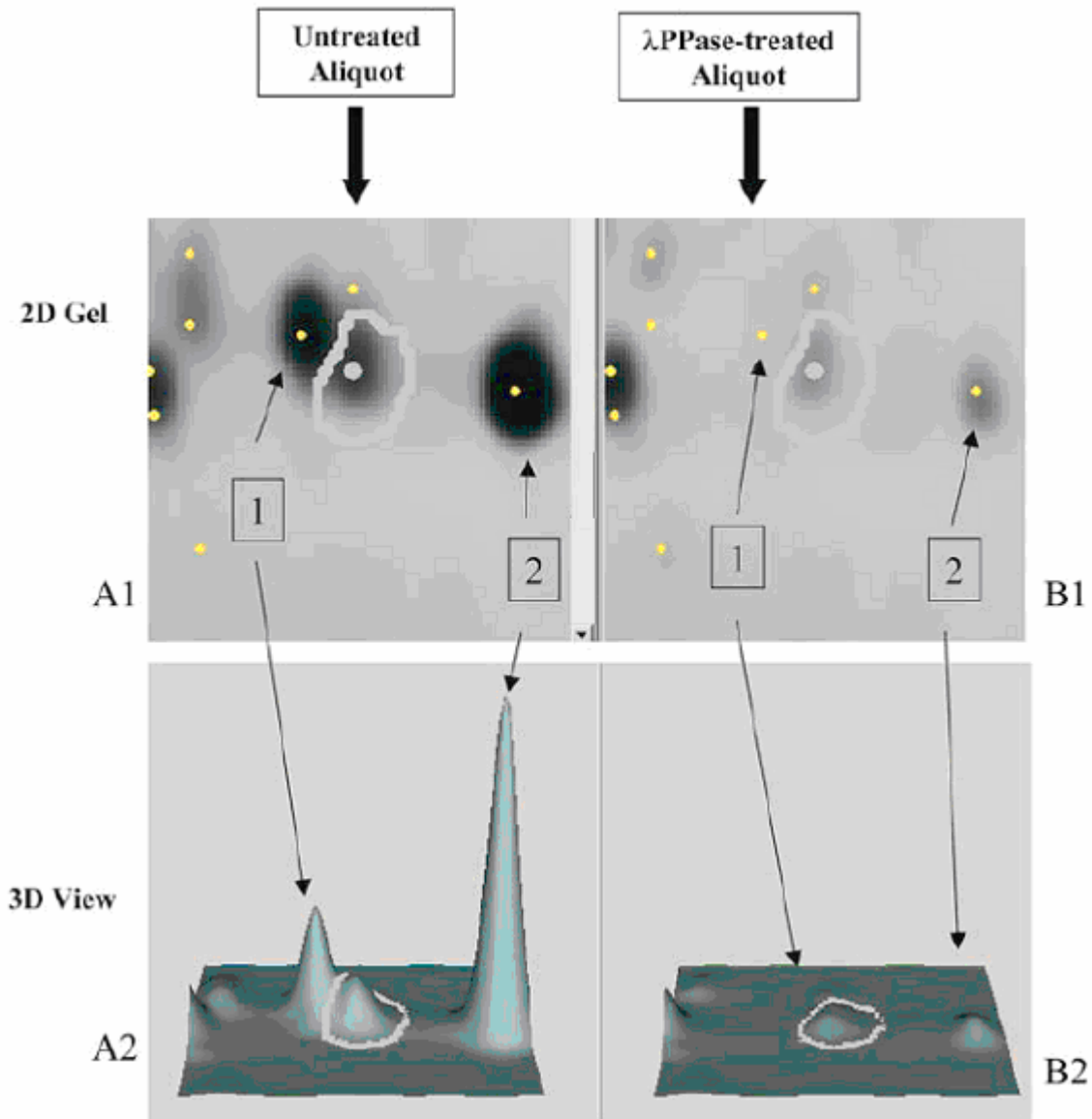


Figure 1. Detection of phosphoproteins employing λ -phosphatase (λ PPase). The starting sample is divided in two aliquots, one of which is treated with λ -PPase. Subsequently, both samples are analysed by 2D gel electrophoresis. Phosphorylated proteins are identified by comparison of the 2D protein patterns exploiting the different migration 'behaviour' due to loss of phosphate groups as can be seen by comparing spots 1 and 2 in parts A1 and B1 of this figure which represent enlarged views of a 2D gel. Comparing these spots in a 3D view (see A2 and B2), differences in spot volume are even more evident [Reproduced from Yamagata et al., 2002].

resolution power of 2D gel electrophoresis has led to the identification of some novel phosphoproteins in cultured rat fibroblasts [Yamagata et al., 2002]. The strategy is shown in Figure 1. [Reproduced from Yamagata et al., 2002].

1.2.2 Phosphopeptide Recognition

Once the nature of a protein has been identified, its phosphorylation status can be ascertained by revealing the occurrence of phosphopeptides within its proteolytic digest. Detection of protein phosphorylation may be done by MS based methods, but it is usually done by other aforementioned non-MS based methods. Recognition of phosphorylation of peptides, on the other hand, is mostly done by MS based methods. The following are some most common techniques used to recognize phosphopeptides.

1.2.2.1 Molecular Mass Shift and Phosphatase Treatment

The basic idea of this method is measurement of all the tryptic peptides usually with MALDI-TOF-MS, which has a wide range of m/z detection limits and then compare these values with theoretically expected values. A molecular mass shift by single or multiples of +80 Da ($HPO_3 = 80$ Da) indicates that it is a phosphopeptide [Mann et al., 2003]. Practically, this method has many difficulties. It is hard to obtain m/z values of all the peptides in the tryptic mixture. Detection of phosphopeptides is worse because of the usual low stoichiometry of phosphopeptides, weak ionization of phosphopeptides in the positive ion mode due to the extra negative charge brought by phosphate group(s) and signal suppression from non-phosphopeptides. Several strategies have been used to alleviate these negative effects. Enrichment of phosphopeptides can alleviate both problems of low stoichiometry of phosphopeptides and the suppression from non-

phosphopeptides. Details of the enrichment of phosphopeptides are discussed in a later chapter. Addition of phosphoric acid and ammonium salts to conventional 2',4',6'-trihydroxy-acetophenone based MALDI-matrices [Kjellstrom et al., 2004; Asara et al., 1999; Yang et al., 2004] improves suppression in the MALDI spectrum. Negative ion mode can also be used to improve poor ionization of phosphopeptides [Janek et al., 2001; Ma et al. 2001].

Even with these improvements, MALDI-TOF-MS recognition of phosphopeptides is complicated by the isobaric peptides in the sample. Using phosphatases combined with MALDI-TOF-MS has been popular to solve this problem. By comparing sample spectra with and without phosphatase treatment, a characteristic shift of one multiple of -80 Da in molecular mass indicates phosphopeptides due to the cleavage of HPO_3 from the phosphopeptides by phosphatases [Stensball et al., 2001; Larsen et al., 2001a; Larsen et al., 2001b]. Major drawbacks of this approach are again related to the decreased ionization of phosphopeptides in complex mixtures due to ionization suppression effects. Different chemical derivatization approaches based on β -elimination/Michael addition chemistry have been developed to alleviate problems related to weak ionization/suppression phenomena for phosphopeptides in the positive ion mode [Molloy et al., 2001; Thompson et al., 2003 Knight et al., 2003].

1.2.2.2 Precursor Ion Scan (PIS)

PIS and neutral loss scan (NLS) for detection of phosphopeptides both require collision induced dissociation (CID) in their detection. The specific fragmentation behavior of phosphopeptides can be used to recognize a phosphopeptides by mass spectrometers capable of PIS and neutral loss scanning (NLS). Briefly, monitoring the

small negative ions such as phosphate (PO_3^-) ($m/z = -79$) from p-Ser, p-Thr or p-Tyr in the negative ion mode is called precursor ion scanning. Detection of PO_3^- identifies the corresponding precursor phosphopeptide ion by its m/z value as performed in Figure 2 [Steen et al., 2001b; Reinders et al., 2005]. This method is very sensitive with a nano-ESI source [Wilm et al., 1996; Carr et al., 1996; Watty et al., 2000; Verma et. al; 1997]. If further MS/MS fragmentation of phosphopeptides is desired, the third MS must be switched back to the positive ion mode and the buffer must be switched to an acidic buffer as well. A strategy to separate the LC eluant for both phosphopeptide detection and phosphopeptide tandem MS fragmentation has been reported [Zappacosta et. al; 2002]. The positive ion mode in PIS was also used to scan and detect p-Tyr-containing peptides [Steen et al., 2001a; Steen et al., 2001b]. P-Tyr-containing peptides have the characteristic fragment under CID, the immonium ion (an internal fragment with just a single side chain formed by a combination of *a* type and *y* type cleavage) containing p-tyrosine side chain with $m/z=216.043$. But this method requires high-resolution MS [Chernushevich et al., 2001] to distinguish this immonium ion from other peptide fragment ions such as b-ions AsnThr or GlySer (both $m/z=216.098$ Da) and y_2 -ion- NH_3 AspVal ($m/z=216.069$ Da), etc. Because the scan happens in the positive ion mode, there is no need to change the ion polarity for the further fragmentation. Subpicomolar sensitivity for detection of tyrosine phosphorylation sites from protein digests has been reached.

A similar, not commonly performed process called stepped skimmer potential in ESI was also used to fragment phosphopeptides and monitor the characteristic m/z -63

(PO^-) and -79 (PO_3^-) ions to recognize phosphopeptides [Huddleston et al., 1993; Ding et al., 1994; Jedrzejewski et al., 1997].

1.2.2.3 Neutral Loss Scan (NLS)

Compared to PIS, which scans the negative phosphate (PO_3^-), the neutral loss of phosphoric acid (-98 Da) or a dephosphorylation (-80 Da) [122] during gas-phase β -elimination of pSer/pThr-containing peptides can not be detected by MS directly. But characteristic ions with m/z shifts of 49, 32.6 and 24.5 (for doubly, triply and quadruply charged ions, respectively) with respect to parent ions indicate phosphopeptides. This method is called neutral loss scan. This scan generally is not applicable to pTyr-containing peptides because β -elimination usually does not happen for them. Method drawbacks are the incidence of false-positive signals in automatic visualization of peptides affected by neutral loss events as well as the dominant occurrence of phosphate-loss specific fragment ions in the MS/MS spectra [Beausoleil et al., 2004]. Both PIS and NLS can be used as driving information for automated data-dependent acquisition in MS

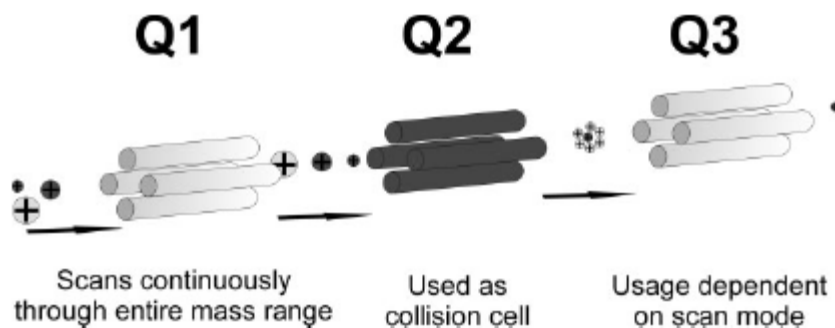


Figure 2. Schematic view of a triple quadrupole mass analyzer operating in precursor ion scanning (PIS) or neutral loss scanning (NLS) modes. Quadrupole 1 (Q1) scans repeatedly through the entire mass range while Q2 is used as a collision cell. In PIS mode Q3 is used to monitor a certain fragment ion mass, e.g., $m/z = 216.043$ Da for the immonium ion of phosphotyrosine. However, in NLS mode Q3 scans through the mass range with a distinct offset to Q1 corresponding to a neutral loss of the peptide such as loss of the phosphate-group of pSer or pThr ($\Delta m = 298$ Da/280 Da) [Reinders et al., 2005].

with sufficient resolution and fast scanning rate, i. e. triple quadrupole [Schlosser et al., 2001], ion trap [Beausoleil et al., 2004, D'Ambrosio et al., 2006a] and q-TOF mass spectrometers [Trinidad et al., 2006; Nousiainen et al., 2006].

1.2.2.4 ^{31}P Detection

Usually no other places other than phosphate groups in proteins/peptides will ^{31}P be found, under conditions that no ^{31}P -containing inorganic contaminants are present. So inductively coupled plasma (ICP) ionization-based instruments [Wind et al., 2001b], such as element mass spectrometry can be used to monitor ^{31}P occurrence, thus, recognizing phosphopeptides. ICP ionization and detection of ^{31}P is not affected by suppression effects as in ESI/MALDI ionization, so absolute quantitation can be achieved. The average phosphate content of proteins can also be determined with ICP-MS by measuring the $^{31}\text{P}/^{32}\text{S}$ ratio [Wind et al., 2001a].

1.2.3 Phosphorylation Site Identification

After the detection of phosphorylation of proteins/peptides, localization of the exact phosphorylation site becomes important. Methods for PSI are compared to reveal their advantages and drawbacks. MS-based methods are discussed in more detail than non-MS based methods for practical reasons and the sake of this dissertation.

1.2.3.1 Comparison Among PSI Methods

Before the availability of MS-based methods for accurate pinpointing of phosphorylation sites, methods that involved ^{32}P -labeled phosphoproteins using phosphopeptide mapping [Van der Geer et. al 1994; Boyle et. al 1991; Nagahara et. al 1999] and Edman degradation [Van der Geer et al., 1994] were well-established, but not

without their limitations. Briefly, phosphopeptide mapping for identification of phosphorylation sites is based on digestion of ^{32}P -labeled proteins with site-specific proteases and separation of the digestion products in two dimensions on thin-layer cellulose plates using electrophoresis in the first dimension followed by chromatography. Phosphopeptide maps are obtained after autoradiography of the two dimensional cellulose plates. The position of the spot on the image indicates the specific peptide that is phosphorylated, which potentially gives the phosphorylation site assignment. The Edman degradation approach is based on Edman sequencing of purified phosphopeptides, which result from the digestion of ^{32}P -labeled protein with a protease and purification of resulting phosphopeptides by reversed-phase HPLC or thin-layer chromatography. Phosphorylation sites can be determined by measuring the radioactivity of each fraction from each Edman cycle using a scintillation counter.

	^{32}P-labelling and phosphopeptide mapping	Edman sequencing	Mass spectrometry
Requirement for radioactivity	Large amounts required	May be used	Not required
Sensitivity	Most sensitive	Less sensitive (pmol)	Highly sensitive (fmol)
Localization of sites	Difficult without mutagenesis experiments	Possible. Tyrosine residues are problematic	Definitive localization is possible
Coverage	Full coverage is difficult	Full coverage is possible, provided sufficient material is available	Full coverage is difficult. FTMS may provide full coverage
High-throughput operation	Not possible. Very labor intensive	Difficult	Possible with automated LC-MS/MS setups
Purified protein required	Yes	Yes	No

Table 1. Comparison of mass spectrometry-based techniques with other methods for phosphorylation analysis of peptides [Kalume, et. al 2003].

The MS-based methods have become popular recently, and will be discussed in detail in the next section. The advantages and limitations of each method are clearly shown in Table 1 [Kalume, et. al 2003]. With the advantages of no radiolabeling required, no protein purification required, high sensitivity, decent coverage and high-throughput; MS-based methods are becoming the methods of choice for PSI. However, in many cases, more than one method may be employed for the study of phosphorylation site identification [Loyet et al., 2003].

1.2.3.2 MS-based Identification Methods

All MS-based PSI methods are based on the fragmentation of phosphopeptides and the use of algorithms to determine the phosphorylation site(s). A tandem MS is usually required for this purpose. After ionization of peptides from a proteolytically digested phosphoprotein of interest with one of the two most popular ionization sources (MALDI and ESI), the first MS scans through the entire mass range and allows a specific m/z species to proceed into the collision cell for fragmentation with an inert gas. The fragments are then scanned by the second MS and sent to a detector to measure its m/z . With two ionization sources, many MS/MS combinations, different fragmentation methods and several different types of detectors, the possible combinations for phosphorylation studies are large. Discussion of all the possibilities is beyond the scope of this introduction. Based on the different fragmentation methods, only popular combinations used for novel PSI study are discussed.

1.2.3.2.1 Collision Induced Dissociation (CID) and LC-ESI-MS/MS

CID is the most common fragmentation method used in PSI so far. CID uses inert gases, such as argon or nitrogen to collide with accelerated peptides to produce peptide

fragments for *de novo* sequencing. Several factors make LC-ESI-MS/MS the most popular combination for PSI in this category. In this combination, an ESI source is used for peptide ionization after separation by on-line LC. The use of LC greatly reduces the sample complexity by first resolving it chromatographically. There are other important methods to reduce non-phosphopeptides and enrich phosphopeptides, and they will be further discussed in the phosphopeptide/phosphoprotein enrichment chapter. One reason ESI is a preferred ionization source is due to the different natures of ionization of MALDI and ESI. MALDI ionization tends to produce singly charged peptides, while ESI tends to produce doubly and triply charged peptides. Generally, modification assignment is achieved more easily with doubly or triply charged parent ions produced by an ESI source. The specific m/z species selected by the first MS will be fragmented by CID. There are two more recently developed fragmentation methods: electron capture dissociation (ECD) and electron transfer dissociation (ETD). Because of the specialized tandem MS required, these will be discussed in a later section. Fragmented species will be scanned for their m/z by “the second” MS, which is actually the third MS because the second MS serves as a collision cell. Many types of tandem MS are used for this combination and they are the dominant methods for novel phosphorylation site identification, for example, triple quadrupole [Neubauer et al., 1999; Zappacosta et al., 2002], ion trap- [Beausoleil et al., 2004; D’Ambrosio et al., 2006a], hybrid q-TOF [Trinidad et al., 2006; Merrick et al., 2001] and Fourier transform ion cyclotron resonance (FTICR) [Haas et al., 2006; Chalmers et al., 2003] instruments have been used. Several popular algorithms such as Analyst, Sequest and SALSA are used to map the sequence of phosphopeptides and phosphorylation site(s). It is difficult and unwise to

analyze all peptides eluted (including phosphopeptides) even after improved resolution of peptides in a complex proteolytic mixture using LC.

Strategies have been developed to selectively fragment peptides eluted from on-line LC columns. In fact, MS/MS analysis is usually carried out automatically by repeated MS scanning of the chromatographic peaks and subsequent multiple selections of the most intense ions from a given scan for CID-generated fragmentation data for many peptides (including phosphopeptides) in the sample. This is called information-dependent acquisition (IDA), or more accurately, intensity-dependent acquisition. In the IDA mode, the achievement of good fragmentation data for phosphopeptides may be hindered by the presence of more co-eluting peptides (limiting the time available for recording good MS/MS spectra of each species) and their occurrence as sub-stoichiometric species (limiting the relative parent ion MS signal intensity) [Steen et al., 2006]. Thus, PIS or NLS-driven (in the positive ion mode) automated information-dependent acquisitions are routinely used during analysis of phosphopeptide containing mixtures [Steen et al., 2006; Beausoleil et al., 2004; Haas et al., 2006; Chalmers et al., 2003]. With software capable of predicting precursor and neutral loss fragment ion m/z values, NLS-driven IDA of product ion scans and MS/MS/MS (MS^3) experiments are conducted on hybrid quadrupole linear ion trap instruments to generate informative data from further fragmentation of fragment ions generated by neutral loss in MS^2 -spectra [Jin et al., 2004] in the study of phosphorylation of pSer/pThr-containing phosphoproteins. The resulting MS^3 - spectrum provides significantly more structural information than the MS^2 -spectrum, with a spacing of 69 Da (owing to dehydroalanine, Dha) or 83 Da (owing

to dehydroaminobutyric acid, Dhb) indicative of the exact location of pSer and pThr residues, respectively [Lalle et al., 2006; Gruhle et al., 2005].

In addition to the ESI source, the MALDI source has also been coupled to tandem mass spectrometers for PSI, especially with the availability of instruments such as the quadrupole-TOF (MALDI-q-TOF), TOF-TOF (MALDI-TOF-TOF), or ion trap (MALDI-ion trap). This allows increased efficiency and sample throughput because identification of phosphopeptides and assignment of the modification sites based on MS/MS sequencing can be performed on a single sample spot [Laiko et al., 2000; Bennett et al., 2002]. As compared to the ESI source, the weaknesses associated with MALDI source ionization (limited sequence coverage and weak ionization/suppression effects for phosphopeptides) have not been obviated with the introduction of these instruments.

1.2.3.2.2 Post Source Decay and MALDI-TOF-MS

PSD refers to the fragmentation of molecular ions during their flight times in the MS, subsequent to ionization and acceleration away from the ionization source. All precursor ions leaving the ion source have approximately the same kinetic energy. During the flight time, the precursor ions fragment, resulting in smaller product ions. The product ions have almost the same velocity as their precursors, but differ in their kinetic energies (corresponding to their m/z). MALDI-TOF is the combination of choice for coupling to PSD because of high sensitivity, simple instrumentation and much higher tolerance of MALDI to buffer and salt contaminants in comparison to ESI. Without tandem MS fragmentation, it is hard to directly assign phosphorylation sites. However, there are some successful examples of assigning low intensity signals to polypeptide backbone fragments observed in the course of PSD experiments [Annan et al., 1996; Neville et al.,

1997; Vener et al., 2001]. When phosphorylation occurs within the target sequences of Pro-directed kinases (Ser-Pro and Thr-Pro motifs), cleavage of the intervening amide bond is highly preferred, making characterization much easier [Hoffmann et al., 1999].

1.2.3.2.3 Latest Developments

Recently two similar fragmentation methods were introduced. These are electron capture dissociation (ECD) and electron transfer dissociation (ETD). ECD is a method of fragmenting gas phase ions for structural elucidation in MS. It involves introduction of low energy electrons to trapped gas phase ions and produces significantly different types of fragment ions (mostly c and z ions) than other fragmentation methods such as CID (mostly b and y ions) [Shi et al., 2001; McLafferty et al., 2001]. The unique (and complementary to CID) fragmentation of phosphopeptides, including maintaining phosphorylated amino acid side chains intact and obtaining efficient peptide backbone fragmentation [Stensballe et al., 2000], make it much easier to assign a modification. It also has the ability to fragment large peptides or proteins, for which no proteolytic digestion is needed [Shi et al., 2001; Jebanathirajah et al., 2005]. Drawbacks are the necessity of high resolution, expensive FTICR MS and skilled personnel.

Different from ECD, which uses direct electrons, ETD uses anions, such as singly charged anthracene anions, to transfer electrons to protonated peptides, which leads to a similar fragmentation of the peptide backbone [Syka et al., 2004]. ETD enables the use of this type of fragmentation in a lower resolution ion trap MS [Schroeder et al., 2005].

1.3 PHOSHOPEPTIDE/PHOSPHOPROTEIN ENRICHMENT METHODS

Only a fraction of the total proteins in a proteome are phosphorylated at any given time. This not only means that only a fraction of the total protein species are

phosphorylated, but also means that only a fraction of any given species is phosphorylated, which is often as low as 1%. The normal procedure of MS-based PSI involves the protease digestion of phosphoproteins, which gives mostly non-phosphopeptides and a few phosphopeptides. Even starting with 100% phosphoproteins, the phosphopeptides are still the minority among proteolytically digested peptides. Negatively charged phosphate side chains on phosphopeptides prevent them from ionizing as well as non-phosphopeptides with MS performed in its usual positive ion mode. All of these facts, combined with the detection of phosphopeptides by MS often being hindered because of suppression effects, necessitate the enrichment of phosphoproteins or phosphopeptides. Many different strategies for separating unphosphorylated species from phosphopeptides have been established. The three major strategies are immunoprecipitation, affinity chromatography and chemical derivatization.

1.3.1 Phosphoprotein Enrichment

The above mentioned three strategies have been all applied to enrich phosphoproteins. A survey of the different strategies for phosphoprotein enrichment is shown in Figure 3 [D'Ambrosio et al., 2006b].

Although there are examples for enrichment of phosphoproteins by IMAC/MOAC [Anderson et al., 1986; Metodiev et al., 2004] or anti-pSer/pThr antibody immunoprecipitation [Carty et al., 2002; Stannard et al., 2003], they are not that commonly performed. On the other hand, the use of SDS-PAGE/2DE or anti-pTyr antibody immunoprecipitation to isolate or enrich phosphopeptides is routine [Pandey et al., 2000].

1.3.2 Phosphopeptide Enrichment

Phosphopeptide enrichment is still a necessary step for most phosphoproteins due to suppression effects from the large amount of non-phosphopeptides. In a large scale study of phosphorylation, such as in a phosphoproteome, good phosphopeptide

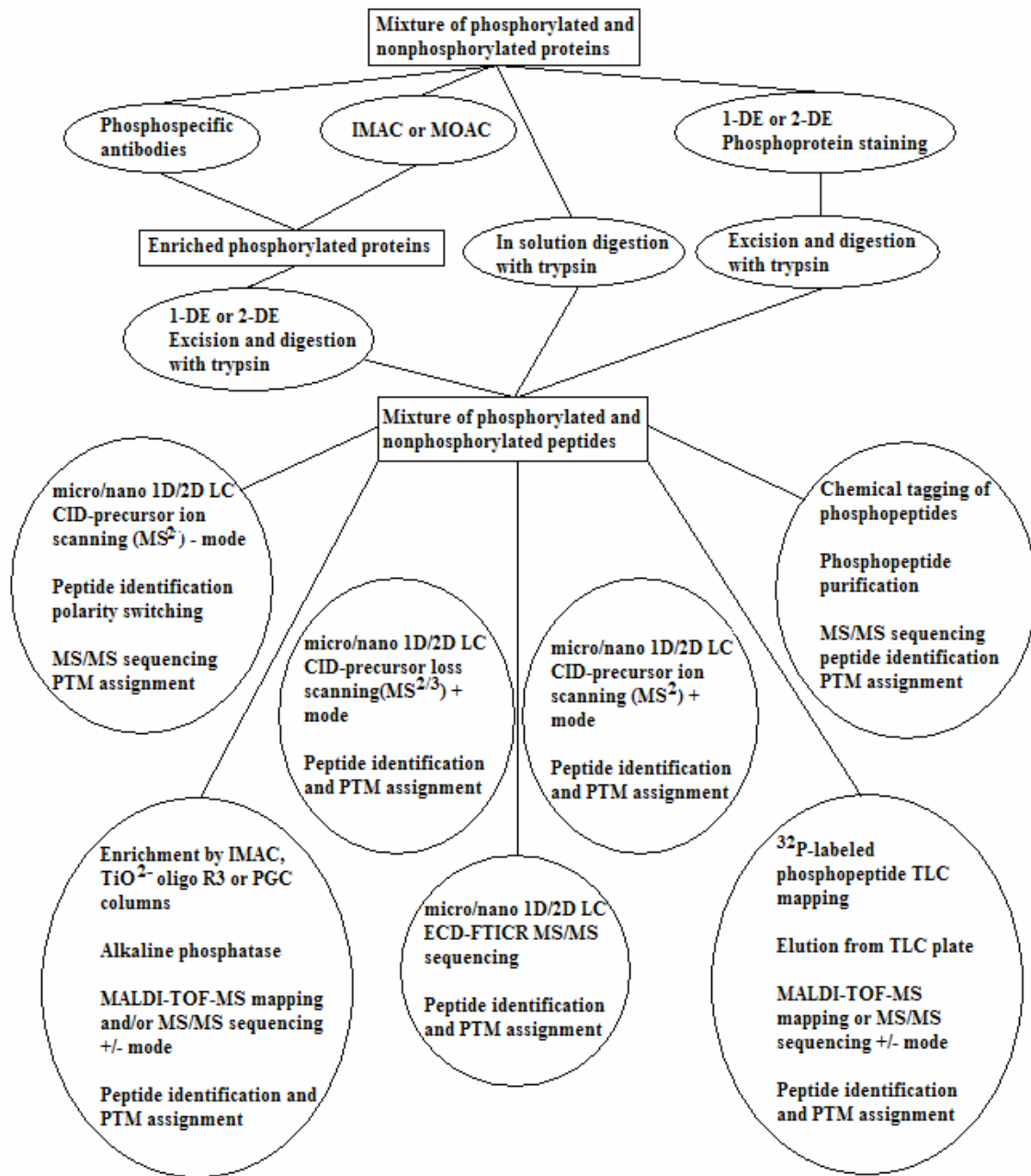


Figure 3. Different techniques for the enrichment and analysis of phosphoproteins based on MS procedures [D'Ambrosio et al., 2006b].

enrichment methods serve at once for all purposes, and no intermediate phosphoprotein enrichment is needed. It enriches all the phosphopeptides from all phosphoproteins digested in a complex mixture. Most strategies applied to phosphoprotein enrichment can apply to phosphopeptide enrichment as well. Much more effort has been put into phosphopeptide enrichment method improvement and innovation. Only some of the most popular methods will be covered in this introduction.

1.3.2.1 Affinity Methods (IMAC)

Immobilized metal affinity chromatography (IMAC) was originally introduced for purification of His-tagged proteins [Porath et al., 1975] and is the most frequently applied technique for phospho-peptide and -protein enrichment [McLachlin et al., 2001]. The theory behind IMAC is based on the electrostatic interaction between the negatively charged phosphate groups and positively charged metal ions which are immobilized to the column material via iminodiacetic acid (IDA), nitriloacetic acid (NTA) or Tris-(carboxymethyl)-ethylendiamine (TED) chelators. It is obvious that more negatively charged groups, such as multiply phosphorylated peptides and very acidic peptides will be predominantly enriched [Stensballe et al., 2001]. Esterification of the acidic side chains of glutamate and aspartate residues using HCl-saturated, dried methanol has alleviated the problem of interaction with acidic peptides [Conrads et al., 2002; Ficarro et al., 2002]. However, the extra modification step may complicate the samples by incomplete esterification, interfere with subsequent mass spectrometric analysis and encumber automation for large scale phosphoproteome-wide analysis. Another possibility for decreasing the co-purification of acidic peptides is the use of the more selective TiO₂-columns [Sano et al., 2004]. The greatest disadvantage of this IMAC is still non-specific

interaction by other negative groups such as side chain carboxylic acids from aspartate and glutamate. Again, this is because the interaction is between a positively charged metal and any negatively charged group.

Various metal ions such as Fe^{3+} , Ga^{3+} , Al^{3+} or Zr^{4+} have been tested for better selectivity and phosphopeptide recovery [Liu et al., 2003; Nuhse et al., 2003]. Ga^{3+} ions have proven effective [Posewitz et al., 1999] in different studies. However, Fe^{3+} -based methods are still used more often. The good compatibility of IMAC procedures with subsequent separation and detection techniques such as CE and LC-MS/MS make it popular in the large scale analysis of phosphorylation.

Because automation is an important factor for large scale phosphoproteome studies, any extra chemical modification involved will compromise high-throughput. In an effort to reduce the non-specific binding, I have proposed a strategy taking advantage of the high specificity and affinity of bacteriophage λ phosphoprotein phosphatase mutants as affinity reagents for enrichment of phosphopeptides.

1.3.2.2 Immunoprecipitation

Compared to immunoprecipitation of p-Ser/p-Thr antigens using expensive, antibodies of questionable quality, the immunoprecipitation of p-Tyr-containing proteins [Mann et al., 2002] is much more frequently practiced [Gronborg et al., 2002]. As previously mentioned, the smaller size of p-Ser and p-Thr compared to p-Tyr, makes it difficult to raise good antibodies against them. Immunoprecipitation of phosphopeptides using phosphopeptide-specific antibodies is also usually not successful [Marcus et al., 2000; Sun et al., 2001; Oda et al., 2001] and other methods must be applied.

1.3.2.3 Derivatization Methods

Chemical modification methods have been developed and improved over the last five years. The first method in this category used chemical tagging of the phosphate group based on gas-phase β -elimination and Michael addition chemistry [Oda et al., 2001] as in panel A and B of Figure 4. This method only applies to p-Ser/p-Thr residues, because p-Tyr does not undergo β -elimination. Another important innovation was a multi-step derivatization procedure that is capable of enriching not only Ser/Thr-phosphorylated peptides, but all types of phosphorylated peptides [Zhou et al., 2001]. There have been many modifications of these methods since they were originally developed. Most of them are listed in Figure 4. The detection limits were improved as the methods were more finely tuned.

Although many methods have been reported in this category, application of most methods is rarely performed outside method-development laboratories themselves, partly because of the delicate derivatization reactions involved. The necessary extra modification reaction(s) may lead to sample loss, increase of sample complexity and unexpected modification of peptides. Automation is a key factor for phosphoproteome-wide analysis, which is made more difficult by the extra reaction step(s) involved in these modification methods.

1.3.2.4 Recent Developments

TiO₂ particles [Pinkse et al., 2004; Larsen et al., 2005; Liang et al., 2006] and ZrO₂ particles [Kweon et al., 2006] have been recently used to enrich phosphopeptides. These particles work in the same way as IMAC columns, through interaction is between

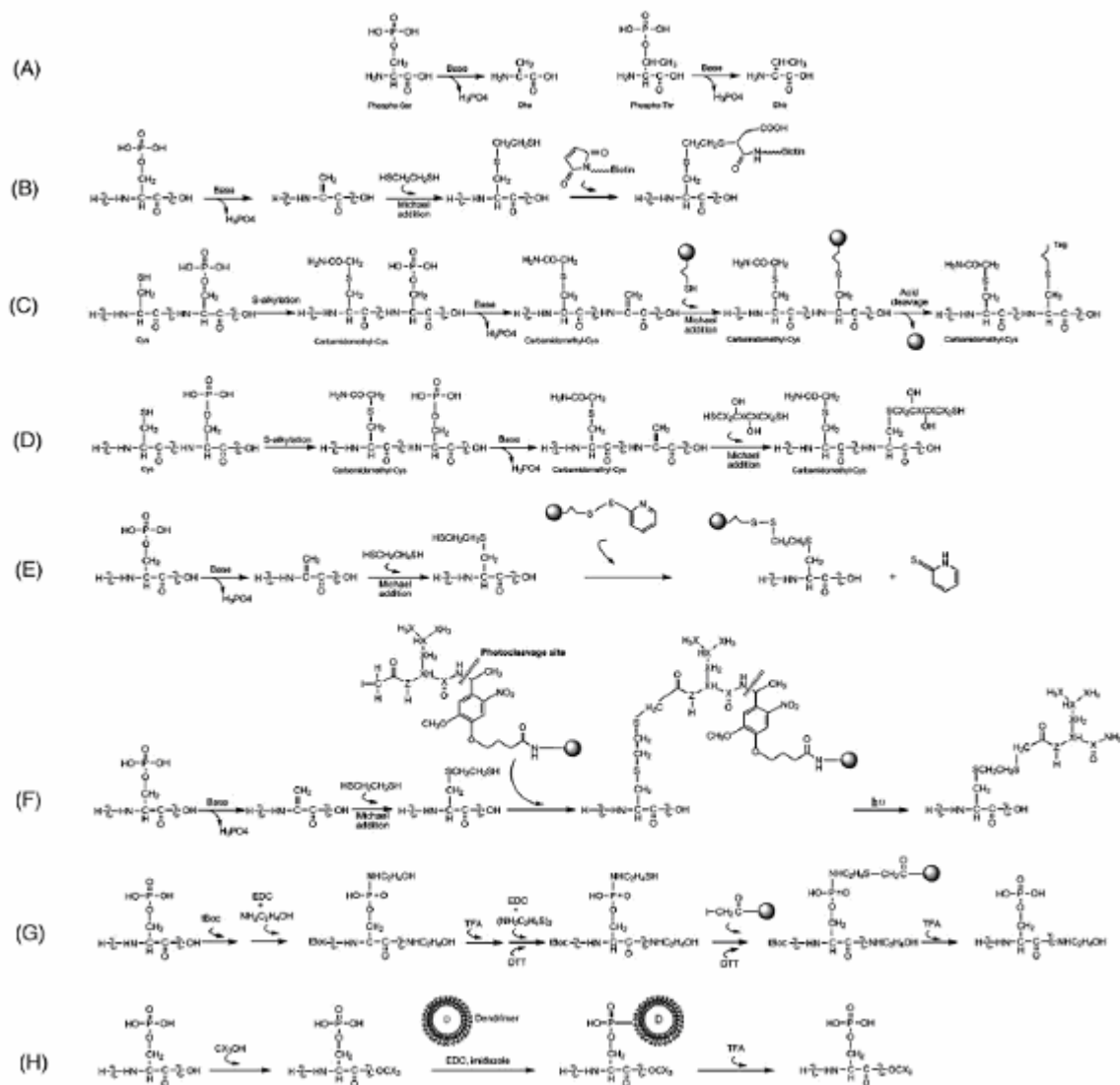


Figure 4. Various strategies for the enrichment of phosphopeptides based on different chemical modification reactions. (Panel A) Base-catalyzed β -elimination of pSer and pThr yielding Dha and Dhb, respectively. Enrichment approaches by chemical tagging of the phosphate group based on a β -elimination/Michael addition chemistry [Oda et al., 2001] (panel B), [Tseng et al., 2005] (panel C), [Vosseller et al., 2005] (panel D), [McLachlin et al., 2003] (panel E), [Qian et al., 2003] (panel F). Enrichment approaches by chemical tagging of the phosphate group based on a carbodiimide condensation chemistry [Zhou et al., 2001] (panel G) and [Tao et al., 2005] (panel H). Depending on the possibility to perform quantitative measurements, X corresponds to H or D (panel D and H); similarly X and Z correspond to ^{12}C or ^{13}C and ^{14}N or ^{15}N , respectively (Panel F) [D'Ambrosio et al., 2006b].

negatively charged phosphates and positively charged ions. With the particle size in the nanometer range, better enrichment efficiency was achieved when used as a precolumn

[Liang et al., 2006]. Specificity is always a big issue with this type of affinity chromatography. The specificity of TiO₂ particles is improved by adding 2, 5-dihydroxybenzoic acid (DHB) in the peptide loading buffer [Larsen et al., 2005]. The reason has been speculated to be the competition between DHB and non-phosphopeptides in one binding mode with TiO₂, while phosphopeptide binding is unaffected in the other mode. Phosphopeptide enrichment microtips made of TiO₂ tend to selectively isolate multiply phosphorylated peptides, while ZrO₂ microtips tend to enrich singly phosphorylated peptides, so these two chromatographic materials possess complementary properties [Kweon et al., 2006].

Application of strong cation exchange columns to separate phosphopeptides from non-phosphopeptides based on the extra negative charge brought by the phosphate group in the phosphopeptide, were also reported [Peng et al., 2003]. Details of this approach will be discussed the third chapter of this dissertation.

1.4 REFERENCES

- Amit, S., Hatzubai, A., Birman, Y., Andersen, J.S., Ben-Shushan, E., Mann, M., Ben-Neriah, Y. and Alkalay, I. (2002) Axin-mediated CKI phosphorylation of beta-catenin at Ser 45: a molecular switch for the Wnt pathway. *Genes Dev.*, **16**, 1066-1076.
- Anderson L. and Porath, J. (1986) Isolation of phosphoproteins by immobilized metal (Fe. 3R.) affinity chromatography. *Anal. Biochem.*, **154**, 250-254.
- Annan, R.S. and Carr, S.A. (1996) Phosphopeptide analysis by matrix-assisted laser desorption time-of-flight mass spectrometry. *Anal. Chem.*, **68**, 3413-3421.
- Antonsson, B., Kassel, D.B., Di Paolo, G., Lutjens, R., Riederer, B.M. and Grenningloh, G. (1998) Identification of in vitro phosphorylation sites in the growth cone protein SCG10. Effect Of phosphorylation site mutants on microtubule-destabilizing activity. *J Biol Chem.*, **273**, 8439-8446.
- Asara, J.M. and Allison, J. (1999) Enhanced detection of phosphopeptides in matrix-assisted laser desorption/ionization mass spectrometry using ammonium salts. *J. Am. Soc. Mass Spectrom.*, **10**, 35-44.

- Beausoleil, S.A., Jedrychowski, M., Schwartz, D., Elias, J.E., Villen, J., Li, J., Cohn, M.A., Cantley, L.C. and Gygi, S.P.(2004) Large-scale characterization of HeLa cell nuclear phosphoproteins. *Proc. Natl. Acad. Sci. USA*, **101**, 12130-12135.
- Bennett, K.L., Stensballe, A., Podtelejnikov, A.V., Moniatte, M. and Jensen, O.N. (2002) Phosphopeptide detection and sequencing by matrix-assisted laser desorption/ionization quadrupole time-of-flight tandem mass spectrometry. *J. Mass Spectrom*, **37**, 179-190.
- Boyle, W.J., van der Geer, P., and Hunter, T.(1991) Phosphopeptide mapping and phosphoamino acid analysis by two-dimensional separation on thin-layer cellulose plates. *Methods Enzymol*, **201**, 110–149.
- Buonocore, G., Liberatori, S., Bini, L., Mishra, O.P., Delivoria-Papadopoulos, M., Pallini, V., and Bracci, R.(1999) Hypoxic response of synaptosomal proteins in term guinea pig fetuses. *J. Neurochem*, **73**, 2139–2148.
- Carr, S.A., Huddleston, M.J. and Annan R.S. (1996) Selective detection and sequencing of phosphopeptides at the femtomole level by mass spectrometry. *Anal. Biochem*. **239**, 180-192.
- Carty, S.M., and Greenleaf, A.L.(2002) Hyperphosphorylated C-terminal repeat domain-associating proteins in the nuclear proteome link transcription to DNA/chromatin modification and RNA processing. *Mol. Cell. Proteomics*, **1**, 598-610.
- Chalmers, M.J., Quinn, J.P., Blakney, G.T., Emmett, M. R., Mischak, H., Gaskell, S.J. and Marshall. (2003) Liquid chromatography-Fourier transform ion cyclotron resonance mass spectrometric characterization of protein kinase C phosphorylation. *J. Proteome Res.*, **2**, 373-382.
- Chernushevich, I.V., Loboda, A.V. and Thomson, B.A.(2001) An introduction to quadrupole-time-of-flight mass spectrometry. *J. Mass Spectrom*, **36**, 849-865.
- Conrads, T.P., Issaq, H.J. and Veenstra, T.D.(2002) New tools for quantitative phosphoproteome analysis. *Biochem. Biophys. Res. Commun*, **290**, 885–890.
- Cutting, J.A. and Roth, T.F.(1973) Staining of phospho-proteins on acrylamide gel electropherograms. *Anal. Biochem*, **54**, 386–394.
- D'Ambrosio, C., Arena, S., Fulcoli, G., Scheinfeld, M.H., Zhou, D., D'Adamio, L. and Scaloni.(2006) Hyperphosphorylation of JNK-interacting protein 1, a protein associated with Alzheimer disease. *Mol. Cell. Proteomics*, **5**, 97-113.
- D'Ambrosio, C., Salzano, A. M., Arena, S., Renzone, G. and Scaloni, A. (2006) Analytical methodologies for the detection and structural characterization of phosphorylated proteins. *J Chromatogr B Analyt Technol Biomed Life Sci.*, Aug 4.
- Debruyne, I.(1983) Staining of alkali-labile phosphoproteins and alkaline phosphatases on polyacrylamide gels. *Anal. Biochem.*, **133**, 110–115.
- Ding, J., Burkhart, W. and Kassel, D.B.(1994) Identification of phosphorylated peptides from complex mixtures using negative-ion orifice-potential stepping and capillary liquid chromatography/electrospray ionization mass spectrometry. *Rapid Commun Mass Spectrom*, **8**, 94-98.
- Ficarro, S.B., McClelland, M.L., Stukenberg, P.T., Burke, D.J., Ross, M.M., Shabanowitz, J., Hunt, D.F. and White, F.M.(2002) Phosphoproteome analysis by mass spectrometry and its application to *Saccharomyces cerevisiae*. *Nature Biotechnol*, **20**, 301–305.

- Fisher, E.H. and Krebs, E.G. (1955) Conversion of phosphorylase b to phosphorylase a in muscle extracts. *J. Biol. Chem*, **216**,121-132.
- Godovac-Zimmermann, J., Soskic, V., Poznanovic, S. and Brianza, F.(1999) Functional proteomics of signal transduction by membrane receptors. *Electrophoresis*, **20**, 952–961.
- Antonsson, B., Kassel, D.B., Di Paolo, G., Lutjens, R., Riederer, B.M. and Grenningloh, G. (1998) Identification of in vitro phosphorylation sites in the growth cone protein SCG10.Effect Of phosphorylation site mutants on microtubule-destabilizing activity. *J. Biol. Chem.*, **273**, 8439-8446.
- Grønborg, M., Kristiansen, T.Z., Stensballe, A., Andersen, J.S., Ohara, O., Mann, M., Jensen, O.N. and Pandey, A. (2002) A mass spectrometry-based proteomic approach for identification of serine/threonine-phosphorylated proteins by enrichment with phospho-specific antibodies: identification of a novel protein, Frigg, as a protein kinase A substrate. *Mol. Cell. Proteomics*, **1**, 517–527.
- Gruhle A. r., Olsen, J.V., Mohammed, S., Mortensen, P., et al., (2005) Quantitative Phosphoproteomics Applied to the Yeast Pheromone Signaling Pathway *Mol. Cell. Proteomics*, **4**, 310-327.
- Haas, W., Faherty, B.K., Gerber, S.A., Elias, J.E., Beausoleil, S.A., Bakalarski, C.E., Li, X., Villen, J. and Gygi, S.P.(2006) Optimization and use of peptide mass measurement accuracy in shotgun proteomics. *Mol. Cell. Proteomics*, **5**, 1326-1337.
- Schlessinger J. (1993-94) Cellular signaling by receptor tyrosine kinases. *Harvey Lect.* **89**, 105-123
- Hoffmann, R., Metzger, S., Spengler, B. and Otvos, L.(1999) Sequencing of peptides phosphorylated on serines and threonines by post-source decay in matrix-assisted laser desorption/ionization time-of-flight mass spectrometry. *J. Mass Spectrom*, **34**, 1195-1204.
- Huddleston M.J., Annan, R.S., Bean, M. and Carr, S.A. (1993) Selective detection of phosphopeptides in complex mixtures by electrospray liquid chromatography/mass spectrometry *J. Am. Soc. Mass Spectrom*, **4**, 710-717.
- Hunter, T.(1995) Protein kinases and phosphatases: The Yin and Yang of protein phosphorylation and signaling. *Cell*, **80**, 225–236.
- Janek, K., Wenschuh, H., Bienert, M. and Krause, E.(2001) Phosphopeptide analysis by positive and negative ion matrix-assisted laser desorption/ionization mass spectrometry. *Rapid Commun Mass Spectrom*, **15**, 1593-1599.
- Jebanathirajah, J.A., Pittman, J.L., Thomson, B.A., Budnik, B.A., Kaur, P., Rape, M., Kirschner, M., Costello, C.E. and O'Connor, P.B.(2005) *J. Am. Soc. Mass Spectrom*, **16**, 1985-1999.
- Jedrzejewski, P.T. and Lehmann, W.D.(1997) *Anal. Chem*, **69**, 294-301.
- Jin W.H., Dai, J., Zhou, H., Xia, Q.C., et al., (2004) Phosphoproteome analysis of mouse liver using immobilized metal affinity purification and linear ion trap mass spectrometry *Rapid Commun. Mass Spectrom.*, **18**, 2169-2176.
- Reinders, J. and Sickmann, A.(2005) State-of-the-art in phosphoproteomics. *Proteomics*, **5**,589-598.
- Kalume, D.E., Molina, H. and Pandey, A.(2003) Tackling the phosphoproteome: tools and strategies. *Curr. Opin. Chem. Biol.*, **7**, 64-69.

- Kaufmann, H., Bailey, J.E., and Fussenegger, M. (2001) Use of antibodies for detection of phosphorylated proteins separated by two-dimensional gel electrophoresis. *Proteomics*, **1**, 194–199.
- Kjellstrom S. and Jensen, O.N.(2004) Phosphoric acid as a matrix additive for MALDI MS analysis of phosphopeptides and phosphoproteins. *Anal. Chem.*, **76**, 5109-5117.
- Knight, Z.A., Schilling, B., Row, R.H., Kenski, D.M., Gibson, B.W. and Shokat, K.M.(2003) Phosphospecific proteolysis for mapping sites of protein phosphorylation. *Nat. Biotechnol.*, **21**, 1047-1054.
- Kweon, H.K. and Hakansson, K.(2006) Selective zirconium dioxide-based enrichment of phosphorylated peptides for mass spectrometric analysis. *Anal Chem.*, **78**, 1743-1749.
- Laiko, V.V., Moyer, S.C. and Cotter, R.J.(2000) Atmospheric pressure MALDI/ion trap mass spectrometry. *Anal. Chem.*, **72**, 5239-5243.
- Lalle, M., Salzano, A.M., Crescenzi, M. and Pozio, E.(2006) The Giardia duodenalis 14-3-3 protein is post-translationally modified by phosphorylation and polyglycylation of the C-terminal tail. *J. Biol. Chem.*, **281**, 5137-5148.
- Larsen, M.R., Sorensen, G.L., Fey, S.J., Larsen, P.M. and Roepstorff, P.(2001) Phosphoproteomics: evaluation of the use of enzymatic de-phosphorylation and differential mass spectrometric peptide mass mapping for site specific phosphorylation assignment in proteins separated by gel electrophoresis. *Proteomics*, **22**, 223-238.
- Larsen, M.R., Thingholm, T.E., Jensen, O.N., Roepstorff, P. and Jorgensen, T.J.(2005) Highly selective enrichment of phosphorylated peptides from peptide mixtures using titanium dioxide microcolumns. *Mol Cell Proteomics*, **4**, 873-886.
- Liang, S.S., Makamba, H., Huang, S.Y. and Chen, S.H.(2006) Nano-titanium dioxide composites for the enrichment of phosphopeptides. *J Chromatogr A.*, **1116**, 38-45.
- Liu, H. L., Ho, Y., Hsu, C. M. (2003) Molecular simulations to determine the chelating mechanisms of various metal ions to the His-tag motif: a preliminary study. *J. Biomol. Struct. Dyn.* **21**, 31–41.
- Loyet, K.M., Stults, J.T., Arnott, D.(2005) Mass spectrometric contributions to the practice of phosphorylation site mapping through 2003: a literature review. *Mol Cell Proteomics*, **4**, 235-245.
- Ma, Y., Lu, Y., Zeng, H., Ron, D. (2001) Characterization of phosphopeptides from protein digests using matrix-assisted laser desorption/ionization time-of flight mass spectrometry and nanoelectrospray quadrupole time-of-flight mass spectrometry *Rapid Commun. Mass Spectrom.*, **15**, 1693-1700.
- Mann, M. and Jensen, O.N.(2003) Proteomic analysis of post-translational modifications. *Nat. Biotechnol.*, **21**, 255-261.
- Mann, M., Ong, S.E., Gronborg, M., Steen, H., Jensen O.N. and Pandey, A.(2002) Analysis of protein phosphorylation using mass spectrometry: deciphering the phosphoproteome. *Trends Biotechnol.*, **20**, 261–268.
- Marcus, K., Immler, D., Sternberger, J. and Meyer, H.E.(2000) Identification of platelet proteins separated by two-dimensional gel electrophoresis and analyzed by matrix assisted laser desorption/ionization-time of flight-mass spectrometry and detection of tyrosine-phosphorylated proteins. *Electrophoresis*, **21**, 2622–2636.

- McLachlin, D.T. and Chait, B.T.(2003) Improved beta-elimination-based affinity purification strategy for enrichment of phosphopeptides. *Anal. Chem.*, **75**, 6826-6836.
- McLachlin, D.T. and Chait, B.T.(2001) Analysis of phosphorylated proteins and peptides by mass spectrometry. *Curr Opin Chem Biol.*, **5**, 591–602.
- McLafferty, F.W., Horn, D.M., Breuker, K., Ge, Y., Lewis, M. A., Cerda, B., Zubarey, R. A., Carpenter, B. K. (2001) Electron capture dissociation of gaseous multiply charged ions by Fourier-transform ion cyclotron resonance. *J. Am. Soc. Mass Spectrom.*, **12**, 245-249.
- Merrick, B.A., Zhou, W., Martin, K.J., Jeyarajah, S., Parker, C.E., Selkirk, J.K., Tomer, K.B. and Borchers, C.H.(2001) Site-specific phosphorylation of human p53 protein determined by mass spectrometry. *Biochemistry*, **40**, 4053-4066.
- Metodiev, M.V., Timanova, A. and Stone, D.E.(2004) Differential phosphoproteome profiling by affinity capture and tandem matrix-assisted laser desorption/ionization mass spectrometry. *Proteomics*, **4**, 1433-1438.
- Molloy, M.P. and Andrews, P.C.(2001) Phosphopeptide derivatization signatures to identify serine and threonine phosphorylated peptides by mass spectrometry. *Anal. Chem.*, **73**, 5387-5394.
- Nagahara, H., Latek, R.R., Ezhevsky, S.A., and Dowdy, S.F.(1999) 2-D hosphopeptide mapping. *Methods Mol. Biol.*, **112**, 271–279.
- Neubauer, G. and Mann, M.(1999) Mapping of phosphorylation sites of gel-isolated proteins by nanoelectrospray tandem mass spectrometry: potentials and limitations. *Anal. Chem.*, **71**, 235-242.
- Neville, D.C., Rozanas, C.R., Price, E.M., Gruis, D.B., Verkman, A.S. and Townsend, R.R.(1997) Evidence for phosphorylation of serine 753 in CFTR using a novel metal-ion affinity resin and matrix-assisted laser desorption mass spectrometry. *Protein Sci.*, **6**, 2436-2445.
- Nousiainen, M., Sillje, H.H., Sauer, G., Nigg, E.A. and Korner, R.(2006) Phosphoproteome analysis of the human mitotic spindle. *Proc. Natl. Acad. Sci. USA*, **103**, 5391-5396.
- Nuhse, T.S., Stensballe, A., Jensen, O.N. and Peck, S.C.(2003) Large-scale analysis of in vivo phosphorylated membrane proteins by immobilized metal ion affinity chromatography and mass spectrometry. *Mol. Cell Proteomics*, **2**, 1234–1243.
- Oda, Y., Nagasu, T. and Chait, B.T.(2001) Enrichment analysis of phosphorylated proteins as a tool for probing the phosphoproteome. *Nat. Biotechnol.*, **19**, 379–382.
- Pandey, A., Podtelejnikov, A.V., Blagoev, B., Bustelo, X.R., Mann, M. and Lodish, H.F.(2000) Analysis of receptor signaling pathways by mass spectrometry: identification of vav-2 as a substrate of the epidermal and platelet-derived growth factor receptors. *Proc. Natl. Acad. Sci. USA*, **97**, 179-184.
- Peng, J., Elias, J.E., Thoreen, C.C., Licklider, L.J. and Gygi, S.P.(2003) Evaluation of multidimensional chromatography coupled with tandem mass spectrometry (LC/LC-MS/MS) for large-scale protein analysis: the yeast proteome. *J Proteome Res.*, **2**, 43-50.
- Pinkse, M.W., Uitto, P.M., Hilhorst, M.J., Ooms, B. and Heck, A.J.(2004) Selective isolation at the femtomole level of phosphopeptides from proteolytic digests using

- 2D-NanoLC-ESI-MS/MS and titanium oxide precolumns. *Anal. Chem.*, **5**, 3935-3943.
- Towbin, H., Staehelin, T. and Gordon, J.(1979) Electrophoretic transfer of proteins from polyacrylamide gels to nitrocellulose sheets: procedure and some applications. *Proc. Natl. Acad. Sci. USA*, **76**, 4350–4354.
- Porath, J., Carlsson, J., Olsson, I. and Belfrage, G.(1975) Metal chelate affinity chromatography, a new approach to protein fractionation. *Nature*, **258**, 598–599.
- Posewitz, M.C. and Tempst, P.(1999) Immobilized gallium(III) affinity chromatography of phosphopeptides. *Anal. Chem.*, **71**, 2883–2892.
- Qian, W.J., Goshe, M.B., Camp, D.G., Yu, L.R., Tang, K. and Smith, R.D.(2003) Phosphoprotein isotope-coded solid-phase tag approach for enrichment and quantitative analysis of phosphopeptides from complex mixtures. *Anal. Chem.*, **75**, 5441-5450.
- Sano, A. and Nakamura, H. (2004) Titania as a chemo-affinity support for the column-switching HPLC analysis of phosphopeptides: application to the characterization of phosphorylation sites in proteins by combination with protease digestion and electrospray ionization mass spectrometry. *Anal. Sci.*, **20**, 861–864.
- Schlosser, A., Pipkom, R., Bossemeyer, D. and Lehmann, W.D.(2001) Analysis of protein phosphorylation by a combination of elastase digestion and neutral loss tandem mass spectrometry. *Anal. Chem.*, **73**, 170-176.
- Schroeder, M.J., Webb, D.J., Shabanowitz, J., Horwitz, A.F. and Hunt, D.F.(2005) Methods for the detection of paxillin post-translational modifications and interacting proteins by mass spectrometry. *J. Proteome Res.*, **4**, 1832-1841.
- Schulenberg, B., Aggeler, R., Beechem, J.M., Capaldi, R.A., and Patton, W.F. (2003) Analysis of steady-state protein phosphorylation in mitochondria using a novel fluorescent phosphosensor dye. *J. Biol. Chem.*, **278**, 27251–27255.
- Shi, S.D., Hemling, M.E., Carr, S.A., Horn, D.M., Lindh, I. and McLafferty, F.W.(2001) Phosphopeptide/phosphoprotein mapping by electron capture dissociation mass spectrometry. *Anal. Chem.*, **73**, 19-22.
- Sickmann, A., Meyer, H.E. (2001) Phosphoamino acid analysis. *Proteomics*, **1**, 200–206.
- Soskic, V., Gorchach, M., Poznanovic, S., Boehmer, F.D., and Godovac-Zimmermann, J. (1999) Functional proteomics analysis of signal transduction pathways of the platelet-derived growth factor beta receptor. *Biochemistry*, **38**, 1757–1764.
- Stannard, C., Soskic, V. and Godovac-Zimmermann, J.(2003) Rapid changes in the phosphoproteome show diverse cellular responses following stimulation of human lung fibroblasts with endothelin-1. *Biochemistry*, **42**, 13919-13928.
- Steen, H., Kuster, B., Fernandez, M., Pandey, A. and Mann, M.(2001) Detection of tyrosine phosphorylated peptides by precursor ion scanning quadrupole TOF mass spectrometry in positive ion mode. *Anal. Chem.*, **73**, 1440-1448.
- Steen, H., Kuster, B. and Mann, M.(2001) Quadrupole time-of-flight versus triple-quadrupole mass spectrometry for the determination of phosphopeptides by precursor ion scanning. *J. Mass Spectrom.*, **36**, 782-790.
- Steen, H., Jebanathirajah, J.A., Rush, J., Morrice, N. and Kirschner, M.W.(2006) *Mol. Cell. Proteomics*, **5**, 172-181.
- Steinberg, T.H., Agnew, B.J., Gee, K.R., Leung, W.Y., Goodman, T., Schulenberg, B., Hendrickson, J., Beechem, J.M., Haugland, R.P. and Patton, W.F.(2003) Global

- quantitative phosphoprotein analysis using Multiplexed Proteomics technology. *Proteomics*, **3**, 1128–1144.
- Stensball, A., Andersen, S. and Jensen, O.N.(2001) Characterization of phosphoproteins from electrophoretic gels by nanoscale Fe(III) affinity chromatography with off-line mass spectrometry analysis. *Proteomics*, **1**, 207-222.
- Stensballe, A., Jensen, O.N., Olsen, J.V., Haselmann, K.F. and Zubarev, R.A.(2000) Electron capture dissociation of singly and multiply phosphorylated peptides. *Rapid Commun. Mass Spectrom*, **14**, 1793-1800.
- Sun, T., Campbell, M., Gordon, W. and Arlinghaus, R.B. (2001) Preparation and application of antibodies to phosphoamino acid sequences. *Biopolymers (Peptide Science)*, **60**, 61-75.
- Syka, J.E., Coon, J.J., Schroeder, M.J., Shabanowitz, J. and Hunt, D.F.(2004) Peptide and protein sequence analysis by electron transfer dissociation mass spectrometry. *Proc. Natl. Acad. Sci. USA*, **101**, 9528-9533.
- Tao, W.A., Wollscheid, B., O'Brien, R., Eng, J.K. Li, X.J., Bodenmiller, B., Watts, J.D., Hood, L. and Aebersold, R.(2005) Quantitative phosphoproteome analysis using a dendrimer conjugation chemistry and tandem mass spectrometry. *Nat. Methods*, **2**, 591-598.
- Thompson, A.J., Hart, S.R., Franz, C., Barnouin, K., Ridley, A. and Cramer, R.(2003) Characterization of protein phosphorylation by mass spectrometry using immobilized metal ion affinity chromatography with on-resin beta-elimination and Michael addition. *Anal. Chem.*, **75**, 3232-3243.
- Towbin, H., Staehelin, T. and Gordon, J.(1979) Electrophoretic transfer of proteins from polyacrylamide gels to nitrocellulose sheets: procedure and some applications. *Proc Natl Acad Sci U S A*, **76**, 4350-4354.
- Trinidad J.C., Specht, C., Thalhammer, A., Schoepfer, R. Burlingame, A. L. (2006) Comprehensive Identification of Phosphorylation Sites in Postsynaptic Density Preparations *Mol. Cell. Proteomics*, **5**, 914-922.
- Tseng, H.C., Ovaa, H., Wei, N.J., Ploegh, H. and Tsai L.H.(2005) Phosphoproteomic analysis with a solid-phase capture-release-tag approach. *Chem. Biol.*, **12**, 769-777.
- Van der Geer, P. and Hunter, T.(1994) Phosphopeptide mapping and phosphoamino acid analysis by electrophoresis and chromatography on thin-layer cellulose plates. *Electrophoresis*, **15**, 544–554.
- Vener, A.V., Harms, A., Sussman, M.R. and Vierstra, R.D.(2001) Mass spectrometric resolution of reversible protein phosphorylation in photosynthetic membranes of *Arabidopsis thaliana*. *J. Biol. Chem.*, **276**, 6959-6966.
- Venter, J.C. et al.(2001)The sequence of the human genome. *Science*, **291**, 1304–1351.
- Verma, R., Annan, R.S., Huddleston, M.J., Carr, S.A., Reynard, G. and deshaies, R.J.(1997) Phosphorylation of Sic1p by G1 Cdk required for its degradation and entry into S phase. *Science*, **278**, 455-460.
- Vosseller, K., Hansen, K.C., Chalkley, R.J., Trinidad, J.C., Wells, L., Hart, G.W. and Burlingame, A.L.(2005) Quantitative analysis of both protein expression and serine / threonine post-translational modifications through stable isotope labeling with dithiothreitol. *Proteomics*, **5**, 388-398.

- Wagner, K., Edson, K., Heginbotham, L., Post, M., Haganir, R.L. and Czernik, A.J.(1991) Determination of the tyrosine phosphorylation sites of the nicotinic acetylcholine receptor. *J Biol Chem.*, **266**, 23784-23789.
- Watty, A., Neubauer, G., Dreger, M., Zimmer, M., Wilm, M. and Burden, S.J.(2000) The in vitro and in vivo phosphotyrosine map of activated MuSK. *Proc. Natl. Acad. Sci. USA*, **97**, 4585-4590.
- Wilm, M., Neubauer, G. and Mann, M.(1996) Parent ion scans of unseparated peptide mixtures. *Anal. Chem.*, **68**, 527-533.
- Wind M., Wesch, H., Lehmann, W.D. (2001) Protein phosphorylation degree: determination by capillary liquid chromatography and inductively coupled plasma mass spectrometry *Anal. Chem.*, **73**, 3006-3010.
- Wind M., Edler, M., Jakubowski, N., Linscheid, M., Wesch, H., Lehmann, W. D. (2001) Analysis of protein phosphorylation by capillary liquid chromatography coupled to element mass spectrometry with ³¹P detection and to electrospray mass spectrometry. *Anal. Chem.*, **73**, 29-35.
- Yamagata, A., Kristensen, D.B., Takeda, Y., Miyamoto, Y., Okada, K., Inamatsu, M. and Yoshizato, K. (2002) Mapping of phosphorylated proteins on two-dimensional polyacrylamide gels using protein phosphatase. *Proteomics*, **2**, 1267–1276.
- Yang, M. and Leonard, J.P.(2001) Identification of mouse NMDA receptor subunit NR2A C-terminal tyrosine sites phosphorylated by coexpression with v-Src. *J Neurochem.*, **77**, 580-588.
- Yang X., Wu, H., Kobayashi, T., Solaro, R.J., van Breemen, R.B.(2004) Enhanced Ionization of Phosphorylated Peptides During MALDI-TOF Mass Spectrometry. *Anal. Chem.*, **76**, 1532-1526.
- Zappacosta, F., Huddleston, M.J., Karcher, R.L., Gelfand, V.I., Carr, S.A. and Annan, R.S.(2002) Improved sensitivity for phosphopeptide mapping using capillary column HPLC and microionspray mass spectrometry: comparative phosphorylation site mapping from gel-derived proteins. *Anal. Chem.*, **74**, 3221-3231.
- Zhou, H., Watts, J. D. and Aebersold, R.(2001) A systematic approach to the analysis of protein phosphorylation. *Nat. Biotechnol.*, **19**, 375–378.

CHAPTER TWO

CHARACTERIZATION OF PHOSPHOPROTEINS BY TWO DIMENSIONAL GEL ELECTROPHORESIS AND MASS SPECTROMETRY

2.1 INTRODUCTION

Since the discovery in 1955 that reversible phosphorylation regulates the activity of glycogen phosphorylase [Fisher et al., 1955] there has been intense interest in studying protein phosphorylation. Phosphorylation and dephosphorylation of proteins regulate a variety of essential biological functions. Generally, the phosphorylation state of a protein cannot be predicted from the gene sequence, and thus needs to be determined at the protein level. Currently there are two popular approaches for examining the phosphoproteins at large scale (the phosphoproteome). Strategy one involves digesting the proteins, detaching the phosphopeptides from non-phosphopeptides by various methods discussed in Chapter one (affinity chromatography, immunoprecipitation and derivatization methods), and then identifying these peptides by tandem mass spectrometry (MS/MS) [Ficarro et al., 2002]. The other strategies involve separation of the proteome first with two-dimensional gel electrophoresis (2DE) [Shevchenko et al., 1966] and then visualization of the phosphoproteins by one of the aforementioned methods [Khan et al., 2005; Hayduk et al., 2004]. Here we apply *in vitro* ^{32}P labeling of phosphoproteins and visualization of phosphoproteins by autoradiography or applying a

phosphate-specific stain directly to the phosphoproteins separated by 2DE. Although protein separation followed by phosphoprotein visualization is not as facile as identification by affinity methods, it does have the advantage of providing a view of the phosphoproteome as a subset of the overall proteome and relative quantification of each visualized phosphoprotein. In view of these advantages, we undertook a cursory examination of the phosphoproteome of Chinese hamster ovary (CHO) cells, including a comparison of radiolabeling and phosphoprotein-specific fluorescence staining.

CHO cell line was chosen because it is easily manipulated genetically and can be adapted to a wide variety of growth conditions including growth in suspension culture and in chemically defined media. As CHO cells are currently the mammalian host of choice for producing human therapeutics [Walsh et al., 2003], the importance of studying CHO cells is known for their generation of glycoproteins with similar oligosaccharide structures to those produced from normal human diploid cells or isolated from human urine glycoproteins [Goochee et al., 1991]. Because the CHO cell genome has not been sequenced, it is likely that proteomics-wide studies such as phosphoproteomics will shed light on signal transduction studies involving phosphorylation.

2.2 MATERIALS AND METHODS

2.2.1 ³²P-Labeling of Chinese Hamster Ovary Cell Phosphoproteins

Tissue culture plates (60-mm diameter) of CHO cells were grown to 100% confluency. The growth medium was removed, and cells were washed with phosphate-free Dulbecco's modified Eagle's medium (DMEM) (Gibco, Carlsbad, CA) three times. The cells were then incubated in 3 mL of phosphate-free DMEM with 100 μ Ci of $K_2H^{32}PO_4$ (Perkin Elmer, Boston, MA) for 4 to 18 h, with or without adding 5 μ L of 1

mM microcystin-LF (Sigma Aldrich, St Louis, MO). Following incubation, the ³²P-containing medium was removed, and the cells were washed three times with phosphate-buffered saline and extracted with 200 μL 1% of sodium dodecyl sulfate (SDS).

2.2.2 2D Electrophoretic Analysis

Protein extracts from cells were acetone-precipitated by addition of 9 volumes of ice-cold acid acetone (acidified with one drop of 6 N HCl in 10 mL of acetone) followed by vortexing and incubation at -80° C for at least 1 h. After spinning for 10 min at 13,400 X g at 4 ° C, acetone pellets were air dried and dissolved in rehydration buffer (7 M urea, 2 M thiourea, 15 mM dithiothreitol, 4% Triton X-100, and 1% pharmalytes). The first dimension (isoelectrofocusing) employed Amersham IPG strips (pH 3–10) on the Multiphor II apparatus (Amersham Pharmacia, Piscataway, NJ). Proteins in electrofocused IPG strips were reduced in 32 mM dithiothreitol and alkylated using 216 mM iodoacetamide. The second dimension was run on a 10% SDS-polyacrylamide gel electrophoresis (SDS-PAGE) gel. The 2D gels were stained with colloidal Coomassie (Pierce, Rockford, IL), equilibrated with 5% glycerol, and dried onto Whatman filter paper; radioactivity was visualized on a Storm 860 phosphorimager (Molecular Dynamics, Sunnyvale, CA).

2.2.3 Identification of Proteins from Excised Gel Spots

Spots that were excised from 2D gels were trypsinized in gel according to the developed method (Shevchenko et al., 1996) then desalted and concentrated using μC₁₈ ZipTips (Millipore, Billerica, MA). Samples were spotted on a matrix-assisted laser desorption/ionization (MALDI) plate with an equal volume of α-cyano-hydroxycinnamic

acid as the matrix. MS employed a QSTAR Pulsar i instrument equipped with an orthogonal MALDI (oMALDI) source (Applied Biosystems, Framingham, MA). MS spectra of the digests were obtained and parent ions selected from each digest for collision-induced fragmentation. The collision-induced fragmentation spectra were then submitted to the Mascot website (Matrix Science, London, UK) for database searching.

2.2.4 Pro-Q Diamond Stain of Chinese Hamster Ovary Cell Extract

Tissue culture plates (60-mm diameter) of CHO cells were grown to 100% confluency. Plates were washed with phosphate-buffered saline, extracted with 1% SDS or incubated with phosphate-free DMEM media overnight, and harvested with 1% SDS. Cell extracts were acetone precipitated and subjected to 2DE apparatus as above. Gels were stained with Pro-Q Diamond phosphoprotein gel stain (Molecular Probes, Eugene, OR) according to the manufacturer's protocol. These gels were visualized using the DarkReader DR45M Transilluminator (Clair Chemical Research, Doroles, CO). Subsequently, these gels were stained with Sypro Ruby stain (Bio-Rad, Hercules, CA) for total proteins.

2.2.5 2D Gel Image Processing

Images of gels stained with colloidal Coomassie, Sypro Ruby or Pro-Q Diamond were captured with the AlphaDigiDoc system (AlphaInnotech, San Leandro, CA). These images, as well as phosphorimages, were analyzed using the Melanie 4 software package (GeneBio, Geneva, Switzerland).

2.3 RESULTS AND DISCUSSION

2.3.1 Overview of the Phosphoproteome Compared with the Entire Proteome

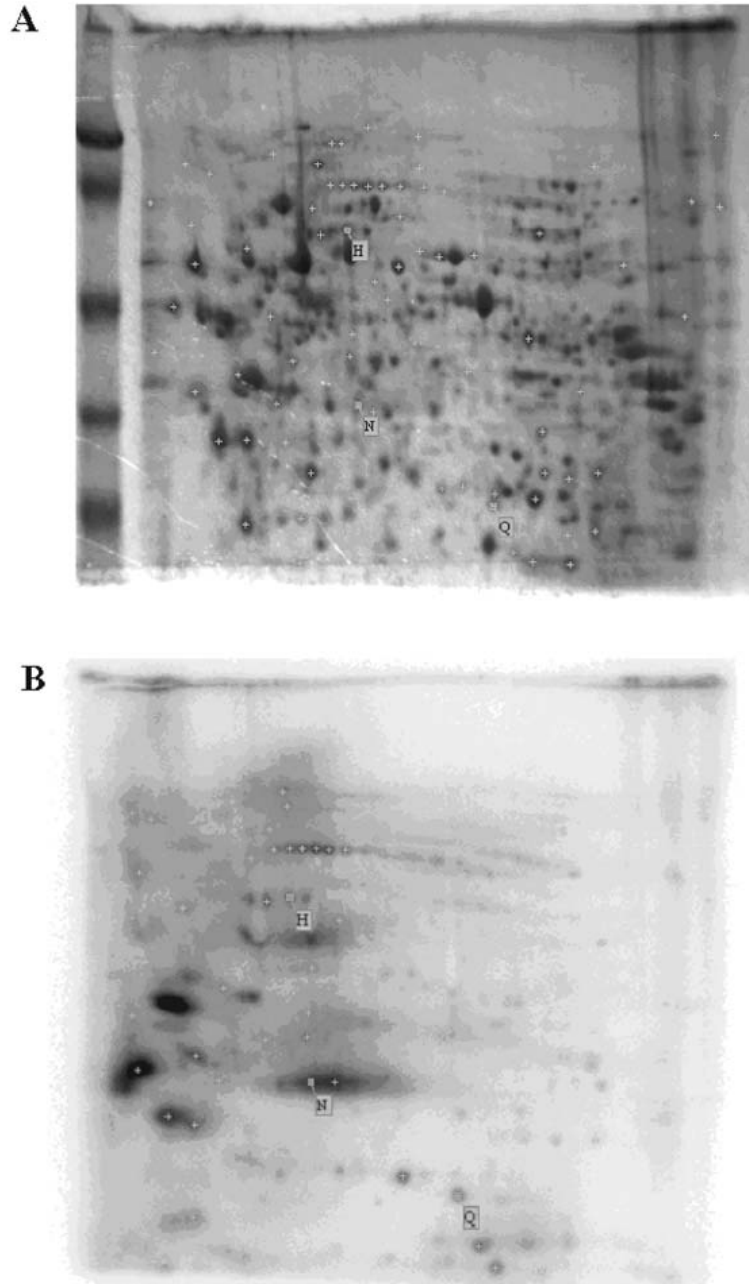


Figure 5. Two-dimensional electrophoresis of proteins and phosphoproteins of Chinese hamster ovary cells. Coomassie-stained gel (A) and corresponding phosphorimage (B) of proteins extracted from Chinese hamster ovary cells labeled for 4 h with ^{32}P -phosphate. Crosses indicate matched spots.

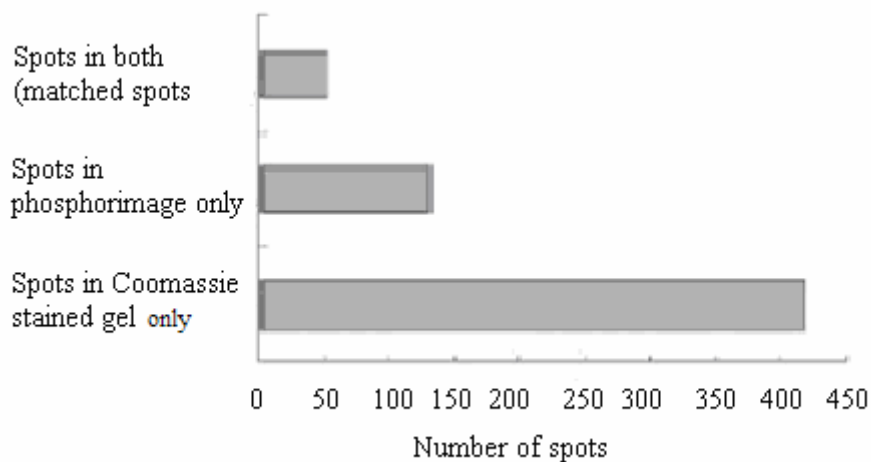


Figure 6. Number of spots in different categories. Proteins are grouped according to their appearance in phosphorimage, Coomassie-stained gel, or both.

Our initial objective was to examine the phosphoproteome as it compares with the abundance proteome (the abundant proteins, as detected by Coomassie blue stain). For this comparison, Melanie 4 detected 468 spots in the Coomassie-stained gel (Figure 5A), and 181 spots in the phosphorimage (Figure 5B). Thus, the observable phosphoproteome is about one third the size of the abundance proteome. However, this does not mean that one third of the proteome is phosphorylated. Low-abundance proteins are not visualized by Coomassie stain. In contrast, radiolabeling allows visualization of even fairly low abundance phosphoproteins (although we have not determined our limit of detection). Although the images in Figure 1 are from the same gel, only 51 spots in the phosphorimage match spots on the Coomassie-stained gel (indicated by crosses in Figure 5). Around 72% of phosphoproteins (130 out of 181, see Figure 6) cannot be matched with counterparts in the Coomassie-stained gel. Thus, most phosphoproteins are low-

abundance proteins, falling below the limit of detection of the Coomassie blue stain. It is tempting to use these data to determine the proportion of the proteome that is phosphorylated. Fifty-one of 468 (11%) proteins observed by Coomassie blue stain were apparently phosphorylated. Using this ratio one might extrapolate to the entire proteome, assuming that the ratio of phosphoproteins as a subset of protein observed is similar for the low-abundance proteins not observed with Coomassie blue. However, this assumption is questionable, for it is conceivable that phosphorylation is more common among low-abundance proteins. Ultimately, we cannot draw conclusions from this type of comparison in terms of the proportion of the entire proteome that is modified by phosphorylation.

2.3.2 Effects of Labeling Time on the Phosphoproteome Observed

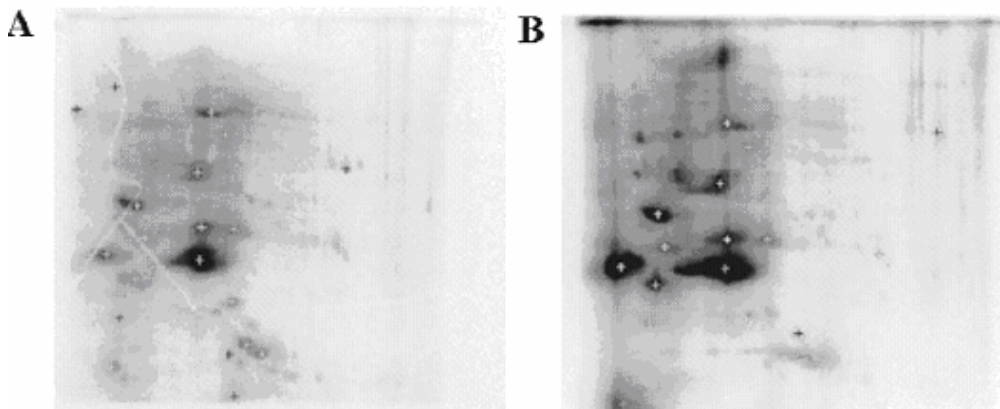


Figure 7. Effect of labeling time. Comparison of the Chinese hamster ovary phosphoproteome after (A) 4 h or (B) 16 h radiolabeling. Gels were exposed to the phosphorscreen for equivalent times. Gray crosses indicate matched spots.

The extent of labeling significantly limits the detection of radiolabeled phosphoproteins. We therefore examined the phosphoproteome observed using different labeling times. It should be noted that no discernable changes in the Coomassie-stained pattern were seen regardless of labeling time (data not shown). In a comparison between

4 h and 16 h of ^{32}P labeling (Figure 7), the longer labeling did allow detection of 22% more ^{32}P -labeled spots. However, the increased labeling time affected the number of

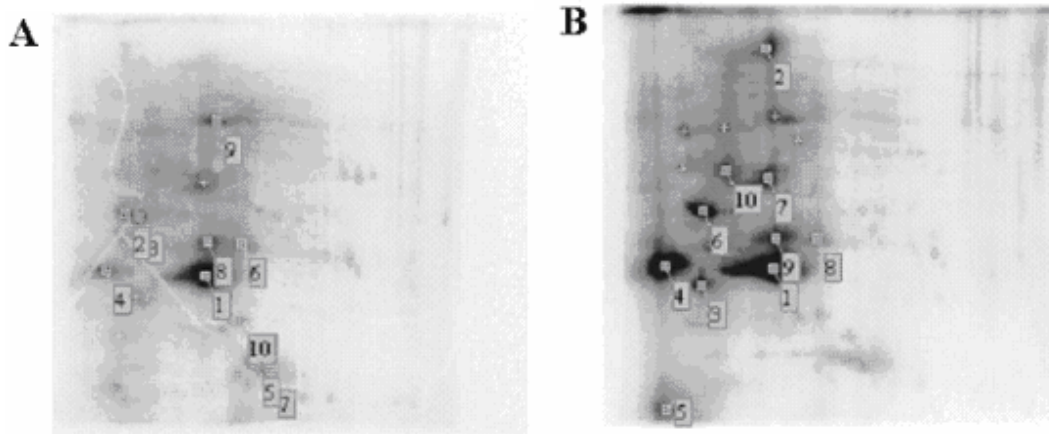


Figure 8. Spot intensities as a function of labeling time. Intensities of the 10 most intense spots are seen to change with different labeling times. Spots are numbered according to intensity as determined by the Melanie software.

spots as well as the relative intensities among spots. These two views of the phosphoproteome can be meaningfully compared by matching only the more intense spots (i.e., setting a high threshold for spot detection). When such a comparison was made, only 71% of the spots correlated between the two phosphorimages. This indicates that there are changes in the phosphoproteome pattern that are dependent on labeling, although the overall pattern is similar. These changes can also be seen by comparing the relative abundances of the 10 most intense spots from each of these two gel patterns (Figure 8). If increasing the labeling time had the straightforward effect of only increasing the signal of all phosphoproteins, then the relative intensities of the spots common to these two views would be conserved. The fact that the relative intensities are not conserved indicates that labeling time does not simply increase the sensitivity of the labeling. We assume that the changes in the phosphoproteome with variation in labeling time are due to the varied turnover rates of different phosphoproteins. Some proteins might not have reached equilibrium in terms of labeling in the shorter labeling period,

while others had. These kinetic considerations indicate that caution should be used in interpreting intensities from radiolabeling experiments. Unless we can be sure that we are at equilibrium conditions, we cannot be completely confident of relative stoichiometries of labeling. Additionally, changes may be due to the prolonged exposure to the low phosphate concentration in the media during labeling.

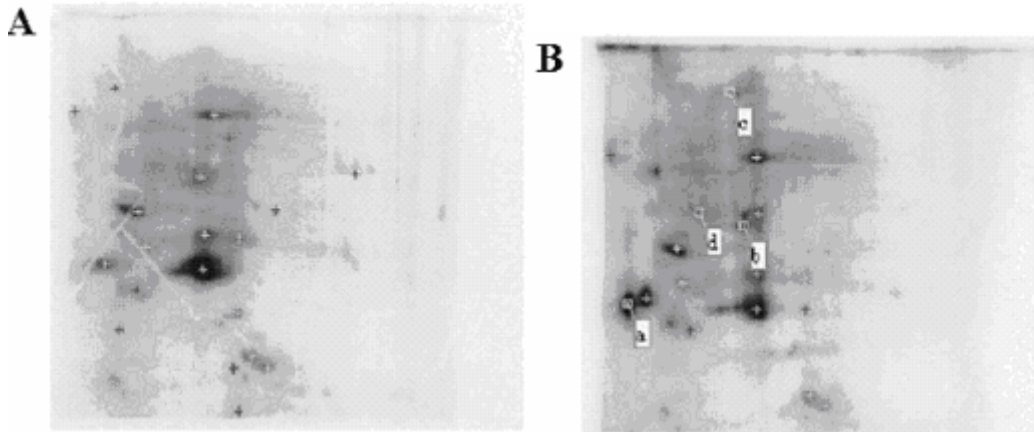


Figure 9. Effect of phosphatase inhibitor. Comparison of the Chinese hamster ovary phosphoproteome labeled 4 h in the absence (A) and presence (B) of microcystin an inhibitor of protein phosphatase type I and 2A. Spots labeled a-d show obvious changes; Indicating that these proteins likely represent substrates for one of these phosphatases.

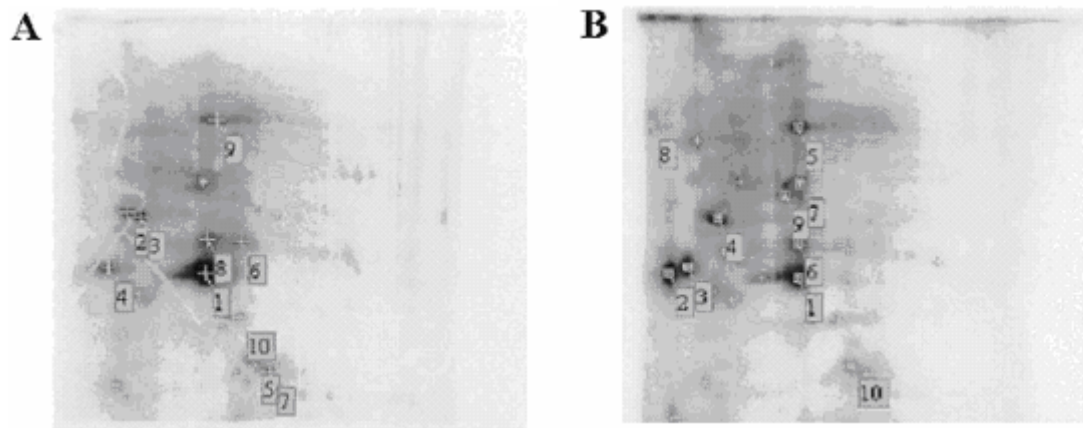


Figure 10. Spot intensities as a function of phosphatase inhibitor. Intensities of the 10 most intense spots change with microcystin (inhibitor of phosphatase I and 2A). Spots 1-10 are numbered according to intensity as determined by the Melanie software.

2.3.3 Effect of a Specific Phosphatase Inhibitor

Stoichiometry of phosphorylation is often maximized by the inclusion of phosphatase inhibitors during labeling. Additionally, information might be gained about the substrates of particular phosphatases by comparing labeled proteins with and without a specific inhibitor. We employed the inhibitor microcystin, which inhibits both type 1 and 2A protein phosphatases. As with varying labeling times, a good comparison can be made by matching only the more intense spots (using a high threshold for spot detection). Such a comparison was made between cells labeled in the presence or absence of microcystin added during labeling (Figure 9). Although the overall phosphoproteome pattern remains similar, 43% of the spots do not match. Obvious candidates for phosphatase 1/2A dephosphorylation are the spots labeled a–d in Figure 5B. These and more subtle changes can be seen when the 10 most intense spots from each gel are compared (Figure 10).

2.3.4 Identifying Phosphoproteins from 2D gels

A goal of phosphoproteome analysis is the identification of the proteins that are phosphorylated. Protein spots from 2D gels can be excised and the proteins identified using in-gel digestion followed by MS. Eighteen gel pieces that represented matches between spots on the Coomassie-stained gel and the phosphorimage shown in Figure 1 were selected as candidates to be identified and were cut out from the gel. These spots were then digested in-gel and analyzed by oMALDI quadrupole-time of flight MS. Fragmentation spectra (from collision-induced fragmentation) were submitted for

identification by comparison to fragmentation patterns predicted from the National Center for Biotechnology Information nonredundant database. Because of the incompleteness of the sequence database for Chinese hamsters, we were unable to identify several of the spots. Spots H, N, and Q were identified as the highly conserved proteins listed in Table 1. One of these, hRNP K, is known to be a phosphoprotein (Schullery et al., 1999). It is known that the pyruvate dehydrogenase E1 complex is phosphorylated (Korotchkina et al., 1995), although we could not find in the literature if the beta subunit has previously been determined to be phosphorylated. Because the majority of the phosphoprotein spots were of such low abundance that they were not observable by Coomassie stain, it is questionable whether or not identification of these spots would be possible, even if working with samples from an organism whose genome has been completely sequenced. Indeed, the correlation of the radioactive spots with Coomassie-stained spots is only tentative, and it is possible that a phosphoprotein might overlap on the gel with an abundant protein that is not phosphorylated but that would be identified from the excised gel piece. Our results suggest that this method is not a preferable method for identifying proteins that are phosphorylated.

Spot	Protein	Phosphoprotein?
H	Heterogeneous ribonucleoprotein K	Yes
N	Pyruvate dehydrogenase E1 beta subunit	Yes? Phosphorylated complex
Q	Proteasome subunit beta type 3	Unknown

Table 2. Identification of phosphoprotein spots cut from Coomassie-stained gel (Figure 5).

2.3.5 Use of a Phosphoprotein Stain for Visualization

Because of the inconvenience of working with radioactive material, we decided to investigate alternative ways of visualizing phosphoproteins after 2DE. We evaluated the commercially available phosphoprotein fluorescence stain Pro-Q Diamond. Following phosphor-specific staining, a fluorescent stain for total protein was employed. This staining showed that the overall proteome was similar to that seen using Coomassie (Figures 11A and B). We found that there is not perfect correlation between the

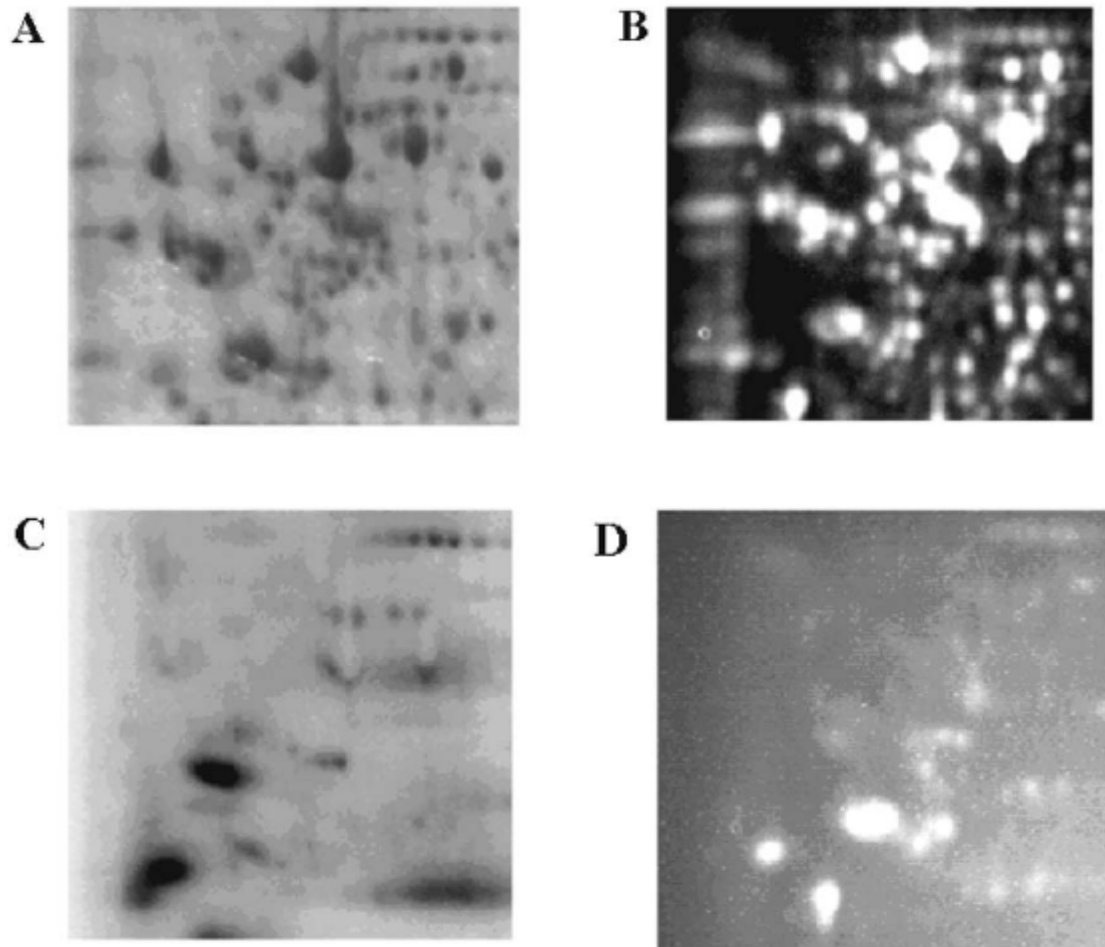


Figure 11. Comparison of radiolabeling and phosphoprotein staining for visualizing the phosphoproteome. Similar regions are shown from (A) Coomassie-stained gel, (B) Sypro Ruby stained gel, (C) phosphorimage of radiolabeled gel from A, and (D) Pro-Q Diamond-stained gel (subsequently stained for total protein and shown in B).

radiolabeled and Pro-Q Diamond-stained phosphoproteins (Figures 7C and D). The differences could be due to aspects of the radiolabeling, such as favoring phosphoproteins that experience rapid turnover. Alternatively, differences could be due to unequal staining among phosphoproteins or lack of complete specificity of the phosphoprotein stain. A further limitation to the use of this stain in many labs is that it serves only as a fair phosphoprotein stain when laser-based gel scanning is not available as a visualization method. Using transillumination as we did results in a lower-than-optimal signal-to-noise ratio with the stain, and a higher limit of detection. However, we have no reason to suspect that visualization using transillumination should affect the relative staining intensities of the phosphoproteins that are detected.

2.4 CONCLUSIONS

Because radiolabeling of phosphoproteins is very sensitive and straightforward to quantify, such analysis can give a clear picture of the relative phosphorylation of proteins present in a sample. However, care must be taken to determine that the proteins being labeled are in equilibrium with respect to the incorporation of label for this quantitation to be meaningful. The radiolabel approach is accessible to most labs because it does not require sophisticated instruments, although it does involve the inconvenience of working with radioactive materials. Because of the limitations of 2DE and Coomassie blue staining, many phosphoproteins cannot be visualized, especially low-abundance proteins. Our results show that most phosphoproteins are low abundance, including some of the most highly phosphorylated proteins. Furthermore, identification of phosphoproteins from this approach is difficult because even if a spot is visible to be cut out, it is not guaranteed that the protein identified is the radiolabeled protein seen to be

phosphorylated. Although these methods do enable comparative profiling, they do not allow facile identification of the phosphoproteins.

2.5 REFERENCES

- Fischer, E.H. and Krebs, E.G.(1955) Conversion of phosphorylase b to phosphorylase a in muscle extracts. *J Biol Chem*, **216**, 121–132.
- Ficarro, S.B., McClelland, M.L., Stukenberg, P.T., Burke, D.J., Ross, M.M., Shabanowitz, J., Hunt, D.F. and White, F.M.(2002) Phosphoproteome analysis by mass spectrometry and its application to *Saccharomyces cerevisiae*. *Nat Biotechnol*, **20**,301–305.
- Goochee, C.F., Gramer, M.J., Andersen, D.C., Bahr, J.B., Rasmussen, J.R.(1991) The oligosaccharides of glycoproteins: bioprocess factors affecting oligosaccharide structure and their effect on glycoprotein properties. *Biotechnology*, **9**, 1347–1355.
- Hayduk, E.J., Choe, L.H. and Lee, K.H.(2004)A two-dimensional electrophoresis map of Chinese hamster ovary cell proteins based on fluorescence staining. *Electrophoresis*, **25**, 2545–2556
- Khan, M., Takasaki, H. and Komatsu, S.(2005)Comprehensive phosphoproteome analysis in rice and identification of phosphoproteins responsive to different hormones/stresses. *J Proteome Res.*, **4**, 1592-1599.
- Korotchkina, L.G., Khailova, L.S. and Severin, S.E.(1995) The effect of phosphorylation on pyruvate dehydrogenase. *FEBS Lett*, **364**, 185–188.
- Schullery, S., Ostrowski, J., Denisenko, O.N., Stempka, L., Shnyreva, M., Suzuki, H., Gschwendt, M. and Bomsztyk, K.(1999) Regulated interaction of protein kinase C δ with the heterogeneous nuclear ribonucleoprotein K protein. *J Biol Chem*, **274**, 15101–15109.
- Shevchenko, A., Wilm, M., Vorm, O. and Mann, M.(1996) Mass spectrometric sequencing of proteins from silver-stained polyacrylamide gels. *Anal Chem*, **68**, 850–858.
- Walsh, G. (2003) Biopharmaceutical benchmarks *Nat. Biotechnol.*, **21**, 865–870.

CHAPTER THREE

NOVEL STRONG CATION EXCHANGE MONOLITHIC COLUMN AND PHOSPHOPEPTIDE ISOLATION

This chapter is a modified version of a published paper [Gu et al., 2006]

3.1 INTRODUCTION

Strong cation exchange (SCX) is an extremely important mode of ion-exchange chromatography for analyzing peptides and proteins (Mant et al., 1990). The utility of an SCX column, which often contains sulfonate groups, lies in its ability to maintain negative charge even under acidic buffer pH conditions (e.g., pH ~3). Under such conditions, most peptides bear positive charge due to the presence of positively charged basic residues (e.g., Arg, His, and Lys), terminal amino groups, uncharged acidic residues (e.g., Glu and Asp), and terminal carboxyl groups. SCX chromatography is, therefore, generally applicable for peptide analysis when operated in acidic buffer pH. On the other hand, when the buffer pH is in the neutral pH range, SCX can only be applied to the analysis of basic peptides or proteins.

In proteomics, the study of extreme complex protein and/or peptide mixtures requires the use of multidimensional liquid chromatography for separation prior to mass spectrometry analysis. The technique called MudPIT (multidimensional protein identification technology) was developed for this purpose. Rather than use traditional two-dimensional gel electrophoresis, MudPIT separates peptides using two-dimensional liquid chromatography, which usually uses an SCX column first, followed by a reversed-

phased column before ionization (Chen et al., 2006; Cagney et al., 2005; Vitali et al., 2005). The separation can be integrated directly with the MS ion source. An ideal SCX column with high separation capacity and no hydrophobic interaction will greatly benefit proteins identification by MS because of the high resolution of peptide/protein mixtures and compatibility with the downstream of reversed mobile phase. One example of MudPIT application is isolation of phosphopeptides using a SCX column (Beausoleil et al., 2004) and then application of the isolated eluant to LC (reversed phase)-MS/MS for large scale of identification phosphorylation sites. Most tryptic peptides usually have +2 charges at low pH (e.g. pH ~3). Attachment of one or more phosphate groups to peptides (as in phosphopeptides) will lower the charge stages of the phosphopeptides. By taking advantages of this property, phosphopeptides can be detached from other non-phosphopeptides. Of course there will be some phosphopeptides still in the +2 or more charge stages when there are histidine residues in tryptic peptides.

Particle-based SCX columns received considerable interest for peptide analysis in the 1980s because of the complementary selectivity to reversed-phase chromatography (Mant et al., 1985a; Mant et al., 1985b; Alpert et al., 1988; Crimmins et al., 1988). For example, the retention of peptides on a PolySulfoethyl A SCX column was found to be monotonically related to the charge of the peptides (Alpert et al., 1988; Crimmins et al., 1988). Several types of peptide standards were designed to evaluate three commercially available SCX columns (Burke et al., 1989). They found that retention of peptides was not only related to charge but also to peptide chain length. The retention of peptides was empirically linearized under conditions in which hydrophobic interactions were suppressed.

Monolithic materials, termed “continuous polymer bed” (Hjerten et al., 1989) offer an alternative to columns packed with small particles or beads. Excellent reviews have appeared describing applications of polymer monoliths in liquid chromatography of both small molecules and macromolecules (Svec et al., 2003; Svec et al., 2004a; Svec et al., 2004b). In addition to polymer monoliths, silica monoliths in which a silica sol-gel network is created by the gelation of a sol solution in a mold were introduced in 1996 (Fields et al., 1996; Minakuchi et al., 1996). Although silica monoliths are mechanically more stable than polymer monoliths, the pH stability of silica is inferior and column preparation requires multiple steps. In flow-through applications, such as chromatography, the throughpores of the polymer monolith must be optimized to allow passage of the mobile phase. Two methods have been developed for controlling the throughpores. One is to adjust the monomer solution ionic strength to prepare an acrylamide-based polymer monolith (Hjerten et al., 1999). The formation of throughpores was achieved by the promoted hydrophobic interaction of the polymer backbone in the presence of a high concentration of salt (e.g., ammonium sulfate). The other is to use porogens. By a combination of good solvent, poor solvent, and/or linear polymer as porogens, a broad range of medium throughpore diameters (500 nm-20 μm) can be readily achieved (Svec et al., 2004a; Svec et al., 2004b). This strategy has been used extensively and is a universal method to control the pore size distribution of a polymer monolith. Using appropriate porogens, a variety of polymer monoliths have been synthesized, e.g., based on acrylamide, acrylate, methacrylate, styrene, and norbornene (Palm et al., 1997; Ngola et al., 2001; Svec et al., 1992; Petro et al., 1996; Gusev et al., 1999; Premstaller et al., 2000) . Polymer monoliths have been extended to include SCX

chromatography. To introduce sulfonate groups into the monolith backbone, several approaches have been reported, including adsorption of surfactants (Paull et al., 2005; Liu et al., 2002; Wu et al., 2001), grafting of a sulfonate-containing monomer (Rohr 2003; Viklund et al., 1997; Viklund et al., 2000), functionalization of a reactive monolith with sodium sulfite (Ueki et al., 2004), and copolymerization (Palm et al., 1997; Ngola et al., 2001; Peters et al., 1997; Peters et al., 1998; Zakaria et al., 2005; Hilder et al., 2004; Wu et al., 2002). Among these, copolymerization is the most straightforward method because it requires one step only and it is easy to control the amount of sulfonate-containing monomer. For copolymerization, a sulfonate-containing monomer has been copolymerized with a cross-linker in the presence or absence (Wu et al., 2002) of a bulk monomer. Although direct copolymerization without the use of a bulk monomer is the simplest, the only reported example was the copolymerization of 2-(sulfooxy)ethyl methacrylate and ethylene glycol dimethacrylate for electrochromatography of peptides (Wu et al., 2002). However, due to the relatively low amount of 2-(sulfooxy)ethyl methacrylate used in the monolith recipe (~17% total monomers), the resulting monolith showed strong hydrophobicity. The separation of model peptides (2 or 3 residues) exhibited reversed-phase rather than ion-exchange behavior. The lack of reports on direct copolymerization of a sulfonate containing functional monomer with a cross-linker for SCX mainly results from two reasons. First, a new optimization must be performed in order to obtain a new polymer monolith although the composition of the monolith is simpler. Second, a sulfonate-containing monolith is believed to swell excessively in aqueous buffer (Ueki et al., 2004; Peters et al., 1997; Peters et al., 1998; Hilder et al., 2004). Thus, the stability of a monolith composed of a high percentage of sulfonate-

containing monomer is questionable. In this study, the preparation of a stable polymer monolith by direct copolymerization of a high amount (40%) of 2-acrylamido-2-methyl-1-propanesulfonic acid and poly(ethylene glycol) diacrylate was demonstrated for SCX liquid chromatography of peptides for the first time. It was hoped that this new polymer monolith could dramatically improve peak capacity of ion-exchange chromatography in which ion exchange of peptides is often considered relatively slow and less efficient than reversed-phase liquid chromatography for proteomics studies (Kimura et al., 2004).

3.2 MATERIALS AND METHODS

3.2.1 Chemicals and Reagents

2, 2-Dimethoxy-2-phenylacetophenone (DMPA, 99%), 3-(trimethoxysilyl)propyl methacrylate (98%), 2-acrylamido-2-methyl-1-propanesulfonic acid (AMPS), poly(ethylene glycol) diacrylate (PEGDA, Mn~258), and ethylene glycol dimethacrylate (EDMA) were purchased from Sigma-Aldrich (Milwaukee, WI) and used without further purification. Synthetic peptide standard CES-P0050 was obtained from Alberta Peptides Institute (Edmonton, Alberta, Canada). Bradykinin fragment 1-7, peptide standard P2693, and its nine components were from Sigma-Aldrich. Protein standards (myoglobin from equine skeletal muscle, cytochrome c from bovine heart, and lysozyme from chicken egg white) were also obtained from Sigma-Aldrich. Porogenic solvents for monolith synthesis and chemicals for mobile-phase buffer preparation were HPLC or analytical reagent grade.

For digestion of β -casein (Sigma-Aldrich), 1 mL of β -casein digestion solution, which contained 50 μ L of 1 M Tris pH 8.0 (99.9% purity, Fisher Scientific, Fair Lawn, NJ), 10 μ L of 0.1 M CaCl₂ (EM Science, Cherry Hill, NJ), 20 μ L of sequencing grade

modified trypsin (Promega, Madison, WI), 100 μ L of 2 mg/mL β -casein, and 820 μ L of MilliQ water, was incubated at 37 °C in a Shake' N' Bake hybridization oven (Boekel Scientific, Feasterville, PA) overnight. The digest was quenched by acidifying with formic acid. The β -casein digest was then desalted using a Strata-X 33 μ m polymeric sorbent column (Phenomenex, Torrance, CA), following the manufacturer's protocol. The eluent from the desalting column was lyophilized in a Centrivap cold trap (Lab-Conco, Kansas City, MO), resuspended in 20 μ L of gradient elution starting buffer, and centrifuged using an Eppendorf centrifuge (Brinkmann, Westbury, NY) at 10 000 rpm for 3 min before injection.

3.2.2 Polymer Monolith Preparation

Before filling the UVtransparent capillary (75- μ m i.d., 360- μ m o.d., Polymicro Technologies, Phoenix, AZ) with monomer solution, the capillary inner surface was treated with 3-(trimethoxysilyl)propyl methacrylate to ensure covalent bonding of the monolith to the capillary wall (Yu et al., 2001). The bulk monomer solution was prepared in a 1-dram (4 mL) glass vial by mixing 0.008 g of DMPA, 0.32 g of AMPS, 0.48 g of PEGDA, 0.20 g of water, 0.55 g of methanol, and 1.70 g of ethyl ether. The monomer mixture was vortexed and ultrasonicated for 5 min to help dissolve AMPS and eliminate oxygen. Because of its low viscosity, the monomer solution was introduced into the UV-transparent capillary by capillary surface action. The capillary (22-cm total length and 16.5-cm monolithic column length, unless otherwise specified) was then placed perpendicular to a UV dichroic mirror from Navitar (Newport Beach, CA), which was operated directly under a Dymax 5000AS UV curing lamp (Torrington, CT) for 3 min. The resulting polymer monolith inside the capillary was connected to an HPLC pump and

flushed with methanol and water sequentially to remove porogens and any unreacted monomers. The prepared polymer monolith was then equilibrated with buffer solution before use. Care was taken to avoid drying the monolith by storing it filled with water or mobile phase. After completion of all chromatographic experiments, a small section (2 cm) of the monolith inside the capillary was dried under vacuum for scanning electron microscopy (SEM) analysis (FEI Philips XL30 ESEM FEG, Hillsboro, OR) (Gu et al., 2005). The same procedure was also applied to synthesize poly(AMPS-*co*-EDMA) monoliths.

3.2.3 Capillary Liquid Chromatography (CLC)

CLC of peptides was performed using a system previously described, with some modifications (Gu et al., 2005). Briefly, two ISCO model 100 DM syringe pumps with a flow controller (Lincoln, NE) were used to generate a two-component mobile-phase gradient. Due to the nanoliter per minute flow required for the monolithic capillary, the gradient flow from the pump was split with the use of a Valco splitting tee (Houston, TX), which was installed between the static mixer of the syringe pumps and the 60-nL Valco internal loop sample injector. A 33-cm-long capillary (30- μm i.d.) was used as the splitting capillary, and a 5-cm-long capillary (30- μm i.d.) was connected between the splitting tee and the injector to minimize extracolumn dead volume. The mobile phase flow rate was set at 69 $\mu\text{L}/\text{min}$. The actual flow rate in the monolithic capillary column was measured by monitoring movement of a liquid meniscus through the 100-cm-long open tubular capillary (75- μm i.d.), which was connected to the monolithic capillary using a Teflon sleeve (Hamilton, Reno, NV). Depending on the mobile phase used, the flow rate in the monolithic capillary was 70-100 nL/min, resulting in split ratios from

700:1 to 1000:1. For CLC of peptides with gradient elution, mobile phase A was a 5 mM phosphate buffer (pH 2.7 or 7.0) with various amounts of acetonitrile. Mobile phase B was the same composition as mobile phase A plus 0.5 M NaCl, and a gradient rate of 1-5% B/min was typically used. All mobile phases were filtered through a 0.2 μm Nylon membrane filter (Supelco, Bellefonte, PA) and ultrasonicated before use. The apparent pH of the mobile phase was measured using a pH meter (Omego, Stamford, CT). On-column UV detection was performed at 214 nm. Chromatograms were transferred to an ASCII file and redrawn using Microcal Origin (Northampton, MA). The monolithic column was also used for CLC of proteins using aqueous buffers. For measurement of the dynamic binding capacity of the monolithic column, 1 mg/mL bradykinin fragment 1-7 in 5 mM phosphate containing 40% acetonitrile (pH 2.7) was pumped under constant pressure of 2000 psi through the monolithic column (18.6 cm long, 75- μm i.d.) using one syringe pump. No splitter was used for these measurements. Because of the low amount (<1 mL) of the bradykinin fragment 1-7 solution available, it was preloaded into a sample loop capillary (2 m long, 320- μm i.d.), with one end connected to the Valco injector and the other end to the monolithic column using Upchurch unions (Oak Harbor, WA). The flow rate was measured to be 91 nL/min. Following the same procedures, the dynamic binding capacity based on uptake of protein (cytochrome *c*) was also performed on a new monolithic column (7 cm long, 75- μm i.d.). A solution of 4 mg/mL cytochrome *c* in 5 mM phosphate (pH 6.2) was pumped through the column under constant pressure of 850 psi, resulting in a column flow rate of 91 nL/min. To study the swelling/shrinking properties of the polymer monolith, different organic solvents were pumped through a 10-cm-long monolith segment inside a capillary at different pressures. A splitter and

detector were not used for these measurements. The flow rate was measured as described above.

3.2.4 Synthesis and Characterization of Acrylamidomethanesulfonic Acid

To the solution of 2-aminoethanesulfonic acid (1.17 g, 10.5 mmol) in 10 mL of 1 N sodium hydroxide, was added acryloyl chloride (0.895 g, 10.0 mmol) and 3 N sodium hydroxide separately at such a rate that the solution is always slightly alkaline while stirring and cooling below 30°C with an iced-water bath. After the addition was completed, the mixture was stirred for another 2 h. It was then poured into a 100 mL beaker containing 3 mL of concentrated hydrochloric acid. The resulting precipitates were collected by suction filtration, washed with cold water, dried and recrystallized from ethanol-water.

The resulting product was dissolved in 100% methanol and analyzed using an LC-MSD-TOF (Agilent technologies, Santa Clara, CA) with a mobile phase of 75% methanol, 25% miliQ H₂O, and 5 mM ammonium formate. All columns were by-passed and the sample was directly introduced into the MSD-TOF detector.

3.2.5 Safety Considerations

AMPS monomer is listed as a suspected carcinogen, and PEGDA is a sensitizing agent. Appropriate MSDS information should be consulted for physical handling of these materials. Sunglasses that block UV light and gloves should be worn to avoid sunburns caused by the high-power UV-curing system during the preparation of the monolith.

3.3 RESULTS AND DISCUSSION

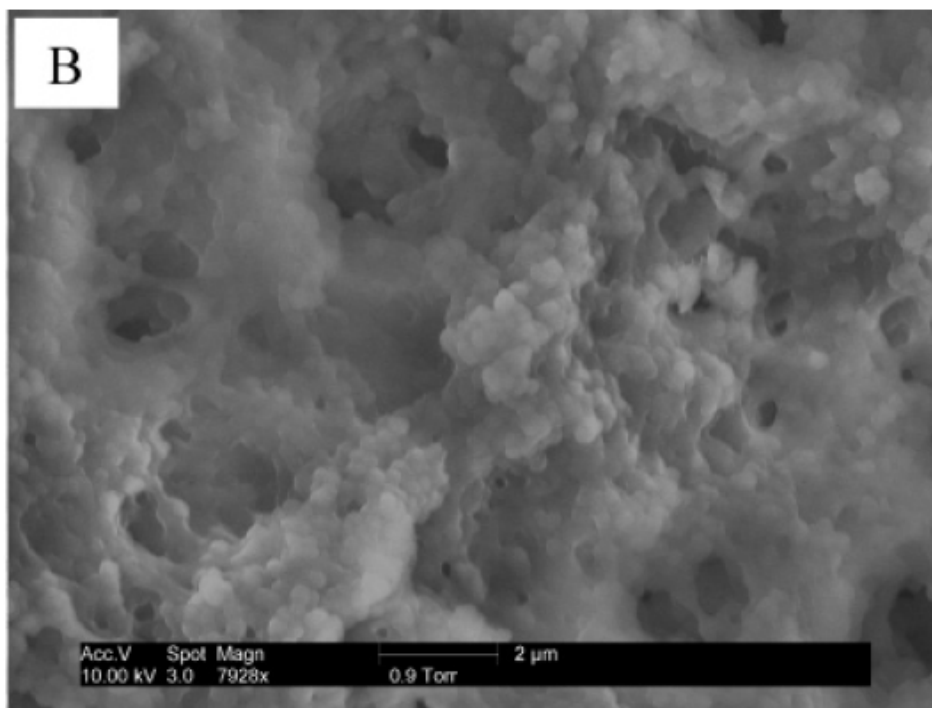
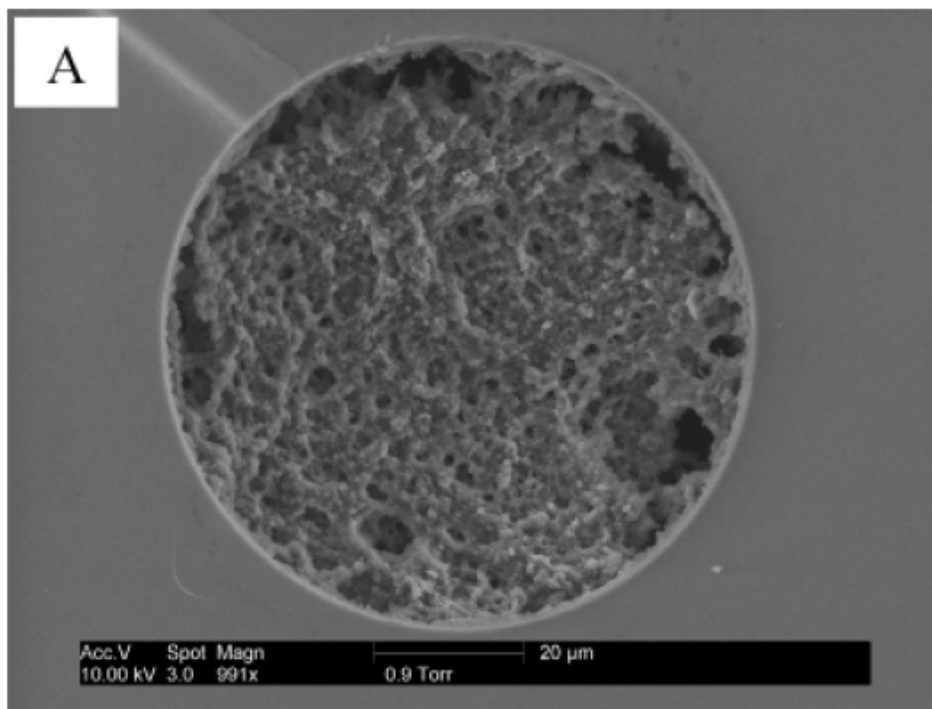
3.3.1 Polymer Monolith Preparation

AMPS, a commercially available acrylamido derivative, was chosen as monomer to synthesize the SCX monolithic column because it contains the desirable sulfonate group. PEGDA, which is an acrylate based cross-linker with three ethylene glycol units, has been shown to resist adsorption of peptides and proteins (Gu et al., 2005). Therefore, it was selected as cross-linker for the synthesis of the monolith. PEGDA was used instead of EDMA as cross-linker to prepare a monolith with more hydrophilicity. The most widely used porogen strategy was adopted to control the throughpores in the monoliths in this study. To date, choice of porogens has been mainly achieved by trial and error, although some theoretical aspects for porogen selection have been derived for macroporous particle synthesis using suspension polymerization (Guyot et al., 1982; Sederel et al., 1973; Kun et al., 1968). Because the solubility of AMPS in common organic solvents is low, water was selected as one of the porogens to help dissolve AMPS. Methanol was selected as another porogen because it was proven efficient for the formation of macroporous throughpores in a poly(PEGDA) monolith (Gu et al., 2005). Unfortunately, any combination of water and methanol (with 0.32 g of AMPS and 0.48 g of PEGDA) yielded a nonporous or microporous translucent gel structure that allowed no flow of mobile phase. The same results were also observed for combination of water, methanol, and 1-propanol. Since ethyl ether is another powerful porogen for PEG-based monoliths, it was finally chosen as the third porogen. After simple optimization, a recipe (25% monomers, composed of 40:60 wt % AMPS and PEGDA, and 75% porogens, composed of 8:23:69 wt % water, methanol, and ethyl ether) was finalized, and the

resulting monolith supported considerable flow under moderate pressure in aqueous buffer. Noteworthy was the incorporation of 40% AMPS, which represents the highest reported percentage of AMPS copolymerized into a polymer monolith backbone. Due to the one-step in situ synthesis protocol, the rate of success in preparing such monolithic capillary columns approached 100%. A scanning electron micrograph of the optimized monolith is shown in Figures 12A and B. It can be immediately observed that the morphology of the poly(AMPS-*co*-PEGDA) monolith is unique. It was composed of fused microglobules, with no distinct microspheres. It appeared intermediate between a conventional polymer monolith with a distinct particulate structure (Svec et al., 2003; Svec et al., 2004) and a silica monolith with a skeletal structure (Fields et al., 1996; Minakuchi et al., 1996). The throughpores of the monolith were obvious. Cracks along the circumference of the monolith (Figure 12A) were presumably due to shrinking of the monolith upon drying when SEM images were taken.

To explore variables that could result in the formation of this unique morphology, two other monoliths were prepared and their SEM photographs are shown in Figures 12C and D. With an increase in methanol in the porogen composition, conventional polymer monolithic morphology with discrete and more “regular” microglobules was formed (Figure 12C). If EDMA was used as crosslinker, the resulting poly(AMPS-*co*-EDMA) monolith exhibited similar fused but more porous structure (compare Figures 12B and D). Based on these micrographs, it seems that porogens rich in methanol or the use of EDMA as cross-linker favored the formation of conventional polymer monolithic morphology, while a monolith formed from porogens rich in ethyl ether or that used

PEGDA as cross-linker tended to form a fused structure. Both porogen and cross-linker are important factors that control the morphology of poly(AMPS) monoliths.



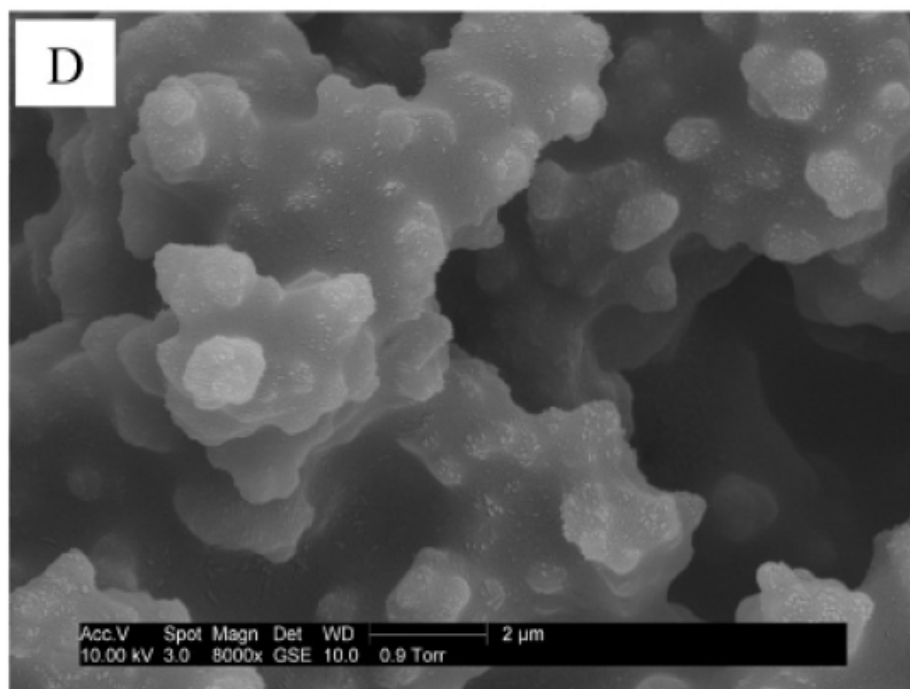
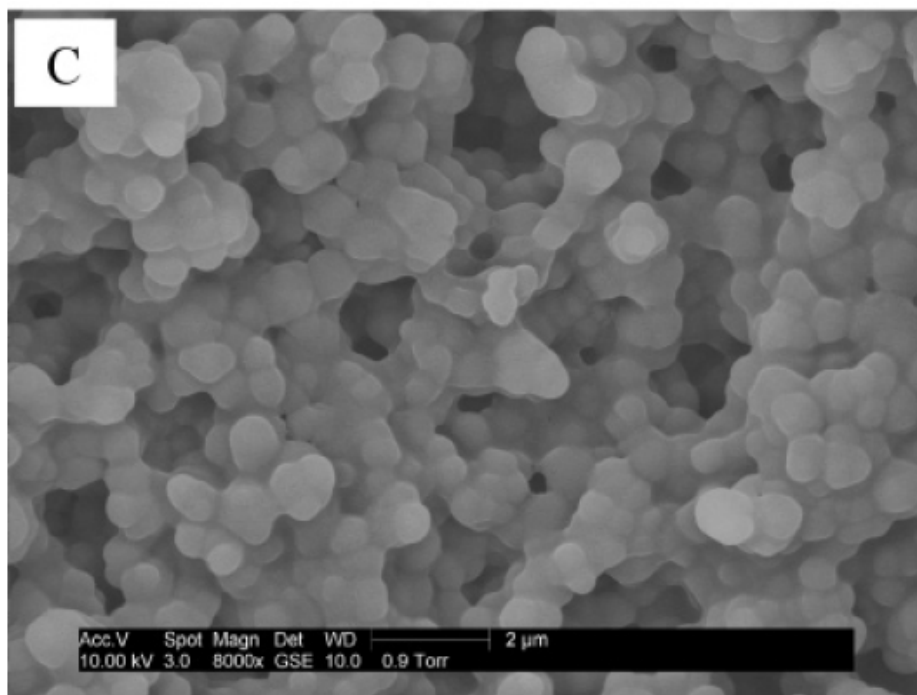


Figure 12. SEM photographs of several monoliths synthesized. (A) Optimized poly(AMPS-co-PEGDA) monolith used in this study (scale bar, 20 μm); (B) higher magnification of the monolith in (A) (scale bar, 2 μm); (C) poly(AMPS-co-PEGDA) monolith that has the same composition as (A) except that methanol and ethyl ether were 0.85 and 1.40 g, respectively (scale bar, 2 μm); (D) poly(AMPS-co-EDMA) monolith (recipe: 0.008 g of DMPA, 0.35 g of AMPS, 0.40 g of EDMA, 0.35 g of water, 1.10 g of methanol; scale bar, 2 μm).

3.3.2 Effect of Acetonitrile on the Elution of Synthetic Peptides.

An ideal SCX column for LC of peptides should be moderately hydrophilic, be able to retain weakly charged analytes (e.g., +1 charged peptides), and exhibit retention of analytes independent of buffer pH from acidic to neutral (Burke et al., 1989). In addition, high binding capacity is another favorable feature, which improves peptide resolution. Several synthetic peptides were designed to evaluate particle-based SCX columns (Burke et al., 1989; Mant et al., 1991). The synthetic peptide standard, CESP0050, was composed of four peptides (see Table 3), which possess certain characteristics for SCX column evaluation. These peptides are all undecapeptides having chain lengths similar to those most commonly encountered in protein tryptic digests, and they do not have any acidic residues (the C-terminal groups are amides), so they possess the same charges in acidic to neutral buffers. The hydrophobicity index of these peptide

analyte	amino acid sequence ^a	charge		hydrophobicity index	
		at pH 2.7	at pH 7.0	at pH 2.0 ^b	at pH 7.0 ^c
1	Ac-Gly-Gly-Gly-Leu-Gly-Gly-Ala-Gly-Gly-Leu-Lys-amide	+1	+1	14.7	18.6
2	Ac-Lys-Tyr-Gly-Leu-Gly-Gly-Ala-Gly-Gly-Leu-Lys-amide	+2	+2	17.5	23.4
3	Ac-Gly-Gly-Ala-Leu-Lys-Ala-Leu-Lys-Gly-Leu-Lys-amide	+3	+3	21.7	30.2
4	Ac-Lys-Tyr-Ala-Leu-Lys-Ala-Leu-Lys-Gly-Leu-Lys-amide	+4	+4	24.2	35.0

^a Amino acid sequence was from ref 42. Ac = Na-acetyl, amide = C_α-amide. Positively charged residues were indicated in boldface font. ^b Hydrophobicity index was calculated based on ref 43. ^c Data were from ref 42.

Table 3. Properties of Synthetic Peptides.

standards has been compiled for pH 7.0 (Mant et al., 1991). However, they were retabulated in Table 3 for easy reference, along with other properties (e.g., amino acid sequence).

Figure 13 shows a gradient elution chromatogram of the synthetic peptides under different buffer conditions using the poly(AMPS-*co*-PEGDA) monolithic SCX column. With an increase

in acetonitrile in the mobile phase from 0 to 40% (see Figure 13A-E), the elution times for peptides 1-4 were monotonically decreased. For peptide 4, addition of 40%

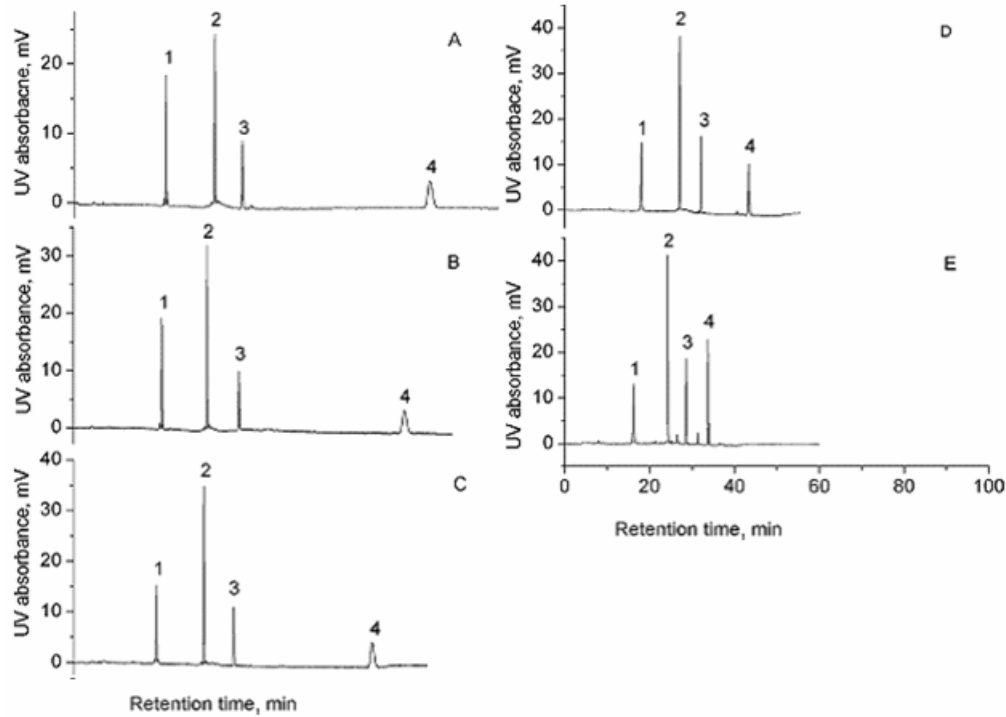


Figure 13. SCX chromatography of synthetic peptides. Conditions: 16.5 cm x 75 μ m i.d. monolithic column; buffer A was 5 mM NaH_2PO_4 (pH 2.7) and buffer B was buffer A plus 0.5 M NaCl, both buffers containing 0, 10, 20, 30, or 40% (v/v) acetonitrile (panels A-E, respectively); 2-min isocratic elution of 1% B, followed by a linear AB gradient (5% B/min, equating to 25 mM salt/min) to 100% B and various times of isocratic elution of 100% B until peptide 4 was eluted; ~10 min gradient delay time; mixture of peptides 1-4 (see Table 3 for sequence) in CES-P0050, which was dissolved in 400 μ L of buffer A with 0% acetonitrile, resulting in a concentration of 0.44 mM for peptide 3; 69 μ L/min pump master flow rate; 76, 83, 85, 89 or 100 nL/min column flow rates (panels A-E, respectively); online UV detection at 214 nm.

acetonitrile in the elution buffer was required to suppress hydrophobic interactions (compare Figures 13D and E). For the less hydrophobic peptides 2 and 3, 20-30% acetonitrile could effectively eliminate hydrophobic interactions, as evidenced by the very sharp peaks obtained. For the least hydrophobic peptide 1, no acetonitrile was required because no significant hydrophobic interactions were observed. The minor

differences in retention times for peptide 1 were likely due to differences in mobile-phase column flow rate. The dramatic decrease in retention time and improvement in peak shape for peptide 4 indicates relatively strong hydrophobicity of the poly(AMPS-*co*-PEGDA) monolith. This feature is not desirable for two dimensional LC (e.g., ion exchange followed by reversed phase) for proteomics, in which an aqueous buffer without acetonitrile is required in the first dimension to effect retention of peptides in the second dimension before separation. The relatively strong hydrophobicity of the poly(AMPS-*co*-PEGDA) monolith was surprising.

The biocompatible cross-linker PEGDA was specially designed and used to decrease unwanted polymer backbone hydrophobicity. To further confirm the biocompatibility of PEGDA, a poly(PEGDA) monolith was prepared following a previously published protocol (Gu et al., 2005), and peptides 1-4 were eluted from the monolith using buffers containing various amounts (0-40%) of acetonitrile. Results (data not shown) indicated negligible differences in peptide elution with the use of different buffers. Therefore, the relatively strong hydrophobicity of the poly(AMPS-*co*-PEGDA) monolith must be due to the monomer AMPS itself. In fact, the AMPS molecule contains an isobutyl arm, which connects the sulfonate group on one end and the acrylamido group on the other end was found that Poly-Sulfoethyl A columns were superior to the more hydrophobic sulfopropyl columns (Alpert et al., 1988). By analogy, it is expected that the monolithic sulfobutyl phase possesses stronger hydrophobicity than desired due to the butyl segment in the side groups. Despite the strong hydrophobicity of the poly(AMPS-*co*-PEGDA) monolith, it was shown to retain strongly the +1 charged peptide (see Figure 13E). This positive feature is uncommon for commercially available

particulate SCX columns where only the PolySulfoethyl A column could retain the peptide (Burke et al., 1989; Mant et al., 1991). For 40% acetonitrile, where any hydrophobic interaction was greatly eliminated, retention of the peptide on the monolith would be expected from ionic interaction only. This strong ionic interaction can be attributed to the use of a high amount of AMPS (40%) in the copolymerization. With hydrophobic interactions suppressed (i.e., with the use of 40% acetonitrile), the four synthetic peptides were eluted as extremely sharp peaks (see Figure 13E), with an average peak width at baseline of 0.28 min. According to the simple definition of peak capacity in gradient elution (peak capacity = time of gradient/peak width) (Stadalius et al., 1985), the peak capacity was calculated to be 71, a value surpassing most particulate based SCX columns (Burke et al., 1989; Mant et al., 1985; Alpert et al., 1988) (Peak capacities of 24-66 were estimated based on several chromatograms provided in these references) and other polymer monolithic SCX columns (Hjerten et al., 1989; Viklund et al., 1997; Ueki, et al., 2004) [Peak capacities of 5-32 were again estimated; in the case of isocratic elution, the peak capacity was calculated as $n = ((N)^{1/2}/4) \ln(t_2/t_1)$, where N is the column efficiency and t_2 and t_1 are the retention times of the last and the first eluting peaks, respectively]. The asymmetry factors calculated at 10% peak height for peptides 1-4 were 1.01, 0.94, 0.90, and 0.99, respectively. The sharp peaks together with minimal fronting or tailing indicated a highly efficient SCX monolithic column. The run-to-run reproducibility of the poly (AMPS-*co*-PEGDA) column was good. For three consecutive runs using conditions the same as in Figure 13E, the relative standard deviation (RSD) of the retention times for peptides 1-4 were 1.9, 0.7, 0.3, and 0.4%, respectively. For peak height, the RSD values for peptides 1-4 were 4.6, 2.3, 2.0, and 1.7%, respectively. These

data clearly demonstrate that good reproducibility could be readily achieved if the column was equilibrated with starting buffer for a sufficient period (typically ~10 column volumes) between runs, although the polymer monolith exhibited swelling in aqueous buffers (vide infra). Column-to-column reproducibility measurements gave retention time RSD values ($n=3$) for peptides 1-4 of 1.3, 1.6, 2.2, and 2.4%, respectively. However, significant deviation was observed for peak height measurements; the RSD values for peptides 1-4 were 18.5, 18.6, 34.6, and 21.9%, respectively.

3.3.3 Effect of Buffer pH on the Resolution of Synthetic Peptides

With an increase in buffer pH from 2.7 to 7.0, greater retention with similar sharp peaks was observed for synthetic peptides 1-4 under otherwise identical conditions as in Figure 13E (data not shown). Because the peptides bear the same charges in both buffer pHs (see Table 3), this indicates an increased negative charge density of the monolith upon an increase in buffer pH. Although AMPS is a strong organic acid with pK_a of 1.2 (Righetti et al., 1990), the pK_a of poly(AMPS) shifts to a higher value due to the absence of electron-withdrawing vinyl groups upon polymerization (Issa et al., 2003). An increase in metal-poly(AMPS) retention was observed with an increase in buffer pH from 1 to 7 (Rivas et al., 2001). Thus, the lower acidity of poly(AMPS) over AMPS accounts primarily for the increased retention of peptides at pH 7.0 compared to pH 2.7. Another contributing factor is the presence of acrylic acid, an impurity found in both AMPS and PEGDA monomers, which can be copolymerized into the monolith backbone. However, no confirmation of this was sought. The stronger retention of peptides upon increase of buffer pH was also observed for most particulate based SCX columns (Burke et al., 1989).

3.3.4 Dynamic Binding Capacity

One of the most important properties of an ion-exchange column is the binding capacity (Haddad et al., 1990), which determines the resolution, column loadability, and gradient elution strength. For the measurement of dynamic binding capacity of an SCX column, proteins (e.g., lysozyme or hemoglobin) are often used. Although the monolithic column could elute and separate proteins using buffers with high ionic strength (vide infra), it did not elute lysozyme, cytochrome *c*, or hemoglobin within 2 h under conditions typical for SCX chromatography of peptides [e.g., 5 mM phosphate (pH 2.7) containing 40% acetonitrile and 0.5 M NaCl]. Therefore, bradykinin fragment 1-7, which bears a +2 charge at pH 2.7, was used to determine the monolithic column dynamic binding capacity. During frontal analysis, a sharp increase in baseline was observed, indicating fast kinetic interaction of the peptide with the column. With the use of 1 mg/mL peptide, it took an amazingly long time (1074 min) to saturate the column. Based on the measured flow rate of 91 nL/min, the dynamic binding capacity was 119 mg/mL, corresponding to 157 μ equiv/mL. From the monolith recipe (see Experimental Section), this 40% MPS/60% PEGDA monolith had a theoretical binding capacity of 475 μ equiv/mL. This indicates that about 33% of AMPS in the monolith backbone was accessible for ionic interaction. The major portion (67% in this case) of AMPS is most likely buried in the polymer monolith, due to the direct copolymerization method used. Nevertheless, the dynamic binding capacity of the poly(AMPS-*co*-PEGDA) monolith was high. This was supported by the elution of the +4 charged peptide 4 as shown in Figure 13E after a 20-min gradient step.

For simple comparison with other SCX columns, the dynamic binding capacity was also measured based on cytochrome *c* uptake although such measurement might be inappropriate and inaccurate due to hydrophobic binding. It took 282 min to saturate the 7-cm-long monolith, resulting in a binding capacity of 332 mg/mL. The dynamic binding capacity of our monolith was compared with other columns. The PolySulfoethyl A column had a dynamic binding capacity of 100 mg of hemoglobin/mL of packing material, corresponding to ~ 3 μ equiv/mL (Alpert et al., 1988). Because 157 μ equiv of peptide/mL or 332 mg of protein/mL was achieved for the current monolithic column, the binding capacity was greater than that of the PolySulfoethyl A column. For the poly(glycidyl methacrylate-*co*-ethylene glycol dimethacrylate) monoliths (Viklund et al., 1997; Viklund et al., 2000) grafted with AMPS for SCX chromatography of proteins, the dynamic binding capacity was found to be typically lower than 100 mg of protein/g of monolith. For the functionalized poly(glycidyl methacrylate-*co*-ethylene glycol dimethacrylate) monolith (Ueki et al., 2004), the dynamic binding capacity was 90-300 μ equiv/mL, albeit based on copper ion uptake. The binding capacity was very low (~ 1 μ equiv/mL) for the anion-exchange polymer monolith (Zakaria et al., 2005), which was prepared by agglomeration of aminated latex particles to a monolith prepared through the copolymerization of a small amount of AMPS, a large amount of butyl methacrylate, and EDMA. This was presumably due to the lower amount of AMPS used in the copolymerization. In summary, the dynamic binding capacity of the current monolith, which was prepared from direct copolymerization of 40% AMPS and 60% PEGDA, was greater than the particulate-based SCX PolySulfoethyl A column and most of the other

polymer monolithic SCX columns.

no	analyte	amino acid sequence ^a	MW	no. of residues	charge at pH 2.7	hydrophobicity index at pH 2.0 ^b
1	oxytocin	Cys-Tyr-Ile-Gln-Asn-Cys-Pro-Leu-Gly-NH ₂	1007.19	9	+1	19.5
2	methionine enkephalin	Tyr-Gly-Gly-Phe-Met	573.70	5	+1	10.0
3	leucine enkephalin	Tyr-Gly-Gly-Phe-Leu	555.62	5	+1	12.6
4	bombesin	pGlu-Gln- Arg -Leu-Gly-Asn-Gln-Trp-Ala-Val-gly- His -Leu-Met-NH ₂	1619.85	14	+2	34.9
5	luteinizing hormone Releasing hormone	pGlu- His -Trp-Ser-Tyr-Gly-Leu- Arg -Pro-Gly	1183.27	10	+2	20.4
6	[Arg ⁸]-vasopressin	Cys-Tyr-Phe-Gln-Asn-Cys-Pro- Arg -Gly-NH ₂	1084.23	9	+2	11.5
7	bradykinin fragment 1-5	Arg -Pro-Pro-Gly-Phe	572.66	5	+2	7.5
8	substance P	Arg -Pro-Lys-Pro-Gln-Gln-Phe-Phe-Gly-leu-Met-NH ₂	1347.70	11	+3	27.9
9	bradykinin	Arg -Pro-Pro-Gly-Phe-Ser-Pro-Phe- Arg	1060.20	9	+3	16.8

^a Amino acid sequence was from sigma web site. Positively charged residues were indicated in boldface font. Free N-terminal bears +1 charge while pyroded N-terminal with glu(pGlu) is neutral. ^b Hydrophobicity index was calculated based on ref 43.

Table 4. Properties of the Nine Peptides in the P2693 Standard.

3.3.5 SCX Chromatography of a Complex Peptide Mixture

To demonstrate the general utility of the poly(AMPS-*co*-PEGDA) monolith for peptide analysis, a more complex peptide mixture P2693 composed of nine natural peptides (see Table 4) was chromatographed using buffer containing 40% acetonitrile under different gradient rates (Figure 14). As seen in Figure 14A, seven out of the nine peptides were resolved when 5% B/min gradient rate was used. By decreasing the gradient rate to 2% B/min, eight peaks were baseline separated (Figure 14B). A further decrease in the gradient rate to 1% B/min resolved all nine peptides, although peptides 2 and 3 were not baseline separated (Figure 14C and inset). Thus, it is convenient to use a shallow gradient to improve resolution for analyzing complex samples. The separation shown in Figure 14C was governed by an ion-exchange mechanism. Following the empirical relationship

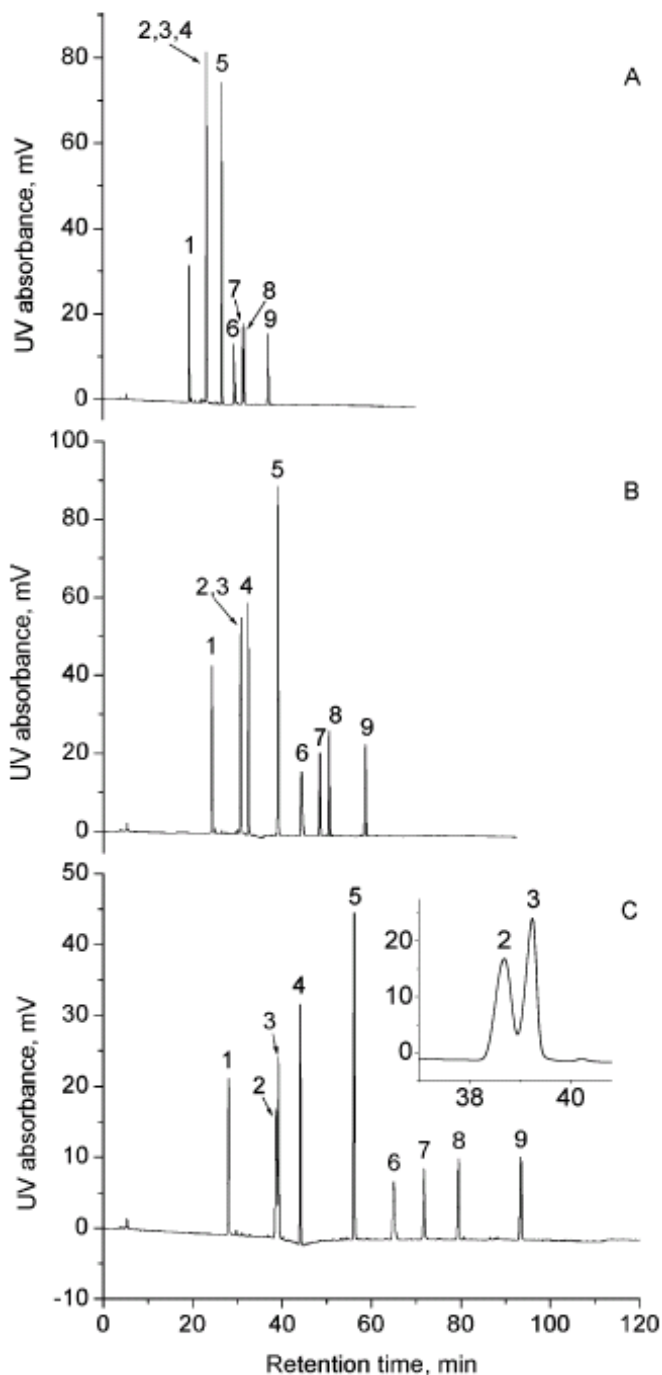


Figure 14. SCX chromatography of natural peptides. Conditions were the same as those in Figure 13E with the following exceptions: mixture of nine natural peptides (see Table 4) dissolved in 25 μ L of buffer A to make each peptide \sim 1 mg/mL; gradient rate of (A) 5, (B) 2, and (C) 1% B/min.

between retention time and charge-to-chain length ratio (Burke et al., 1989), a straight line $[t_R) 66.03N/\ln(n) - 2.05]$ was obtained with a regression coefficient of 0.96, where t_R

is the peptide retention time, N is the charge, and n is the number of amino acid residues. This confirmed a pure ionic interaction of the polymer monolith for SCX of natural peptides with 5-14 residues and a hydrophobicity range from 7.5 to 34.9 (see Table 4). It is interesting that the elution order in Figure 14C is the reverse of that in capillary zone electrophoresis (CE) (cf. technical bulletin for P2693 from Sigma, <http://www.sigmaaldrich.com/sigma/datasheet/p2693dat.pdf>) except for peptides 7 and 8. This is not unexpected because retention in SCX is based on the charge-to- $\ln(\text{chain length})$ ratio, while in CE migration is determined by analyte charge-to-size ratio. Thus, an analyte with more charge and smaller size will migrate earlier in CE and elute later in SCX. As compared with separation in CE, better resolution (with the exception of peptides 2 and 3) was generally obtained for SCX chromatography, although longer time was required. Peak widths were somewhat narrower in SCX chromatography than in CE. This demonstrates that comparable or better resolution and efficiency was achieved for peptide analysis with the use of the poly(AMPS-*co*-PEGDA) monolithic column than for CE. The average peak width at baseline in Figure 14A (excluding the second peak due to coelution of three peptides), Figure 14B (excluding the second peak due to coelution of two peptides), and Figure 14C (excluding the second and third peaks due to incomplete resolution) were 0.27, 0.38, and 0.56 min, resulting in peak capacities of 74, 130, and 179 for the gradient rates of 5, 2, and 1% B/min, respectively. As discussed above, the peak capacity calculated from Figure 13E was 71, where a gradient rate of 5% B/min was used for SCX of four synthetic peptides. It seems that the peak capacity depends on the salt gradient rate and not on the analytes used. A shallower gradient resulted in a greater peak capacity. This was due to the use of the unique monolith, for which the peak width

increased less proportionally upon an increase in the gradient elution time. This feature is attractive for resolving complex peptide samples (e.g., protein digests). Noteworthy was the resolution between methionine enkephalin and leucine enkephalin (inset in Figure 14C). These two peptides bear the same charge and have the same chain length (see Table 4). They also have very similar molecular weight and hydrophobicity. Due to the use of 40% acetonitrile in the mobile phase, it is not likely that the resolution was based on differences in hydrophobicity. Instead, the separation was primarily due to differences in ionic interaction resulting from a minor difference in molecular weight. Because methionine enkephalin has a greater molecular weight than leucine enkephalin, the ionic interaction between methionine enkephalin and the monolith would be expected to be somewhat smaller, leading to earlier elution. The successful separation of methionine enkephalin and leucine enkephalin emphasizes the exceptional resolution provided by the poly(AMPS-*co*-PEGDA) monolith. Further evaluation of the monolith was conducted for SCX chromatography of a β -casein digest (Figure 15). Once again, very nice separation was obtained. Based on several completely resolved peaks (indicated in Figure 15), the peak capacity was estimated to be 167, close to 179 measured using peptide standard P2693. This confirmed that peak capacity was not dependent on the sample analyzed, but on the gradient rate. It should be mentioned that the protein digest had to be desalted. If the β -casein digest was not desalted (see Experimental Section), the peptides coeluted in 15 min (data not shown). This is expected because peptides will not be strongly retained if they are dissolved in a high concentration of salt buffer. During the experiment, it was also important to use freshly prepared peptides and to store them in a refrigerator. For

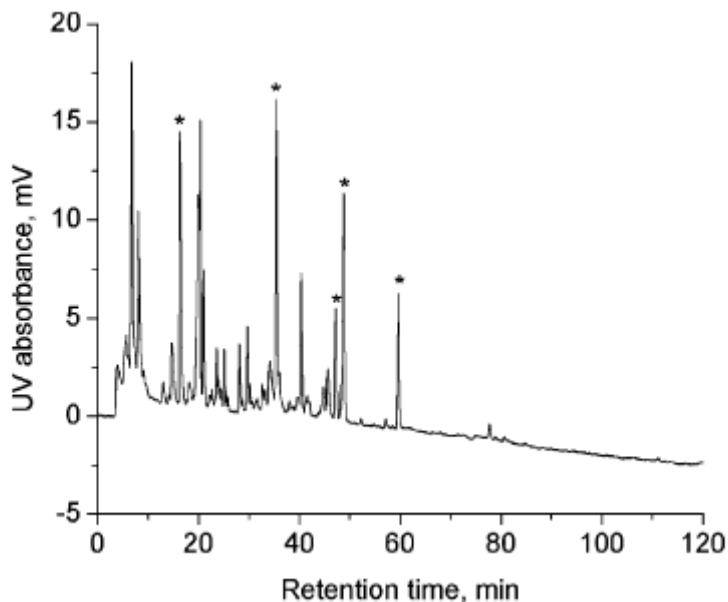


Figure 15. SCX chromatography of a β -casein digest. Conditions were the same as in Figure 14C.

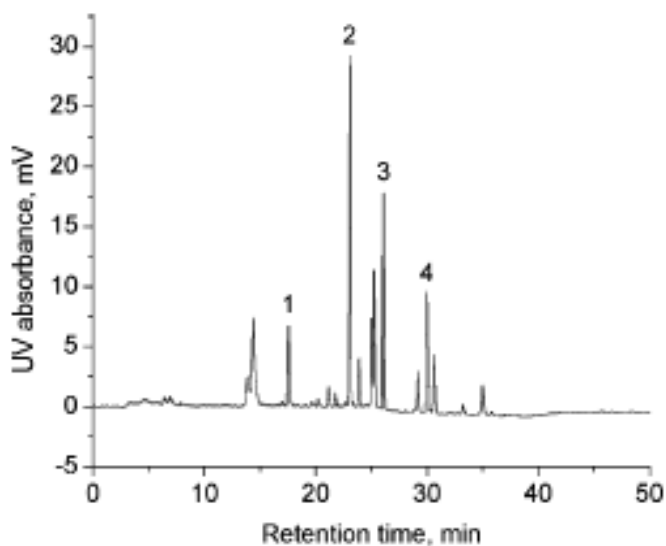


Figure 16. SCX chromatography of an old synthetic peptide sample. Conditions were the same as in Figure 13E.

example, peptide standard CES-P0050 degraded if dissolved in the starting buffer and stored at 2-8 °C for more than 2 months. Figure 16 shows a separation of a degraded sample. In addition to the main four peptides, eight other peptides could be clearly seen. This, once again, demonstrates the high resolution of the poly(AMPS-*co*-PEGDA)

monolith for SCX liquid chromatography of peptides. It opens the possibility of using SCX chromatography for quality analysis (e.g., purity) of peptides, although such analyses are almost exclusively performed using reversed-phase liquid chromatography.

3.3.6 SCX Chromatography of Protein Standards

An attempt was also made to perform SCX chromatography of basic proteins, and the result is shown in Figure 17. As mentioned before, proteins did not elute from the monolithic column when 5 mM phosphate (pH 2.7) containing 40% acetonitrile and 0.5 M NaCl was used as eluent. This is likely due to stronger binding of proteins than peptides, as confirmed by the elution of proteins when NaCl concentration was increased to 2.0 M. However, due to the poor solubility of NaCl in 40% acetonitrile, a buffer that

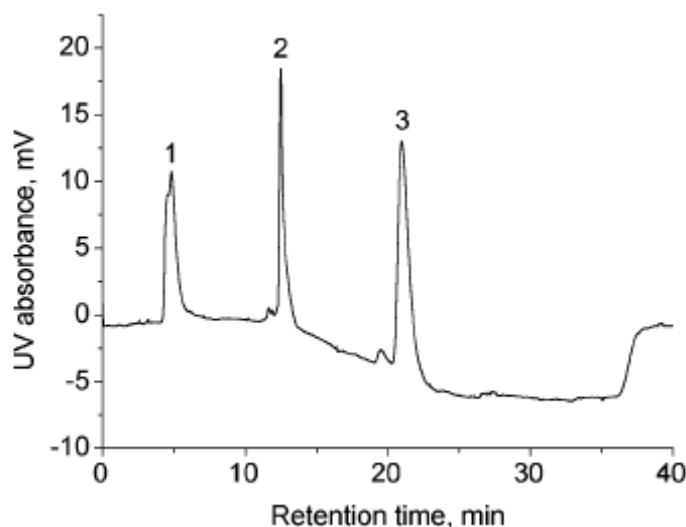


Figure 17. SCX chromatography of proteins. Conditions were the same as in Figure 13E except that different buffers were used; buffer A was 5 mM phosphate (pH 6.2) and buffer B was buffer A plus 2.0 M NaCl. Analytes: (1) myoglobin, (2) cytochrome c, and (3) lysozyme. The baseline drift during gradient elution and the rise of the baseline at the end of the gradient were due to the difference in UV absorbances of buffers A and B.

contains no acetonitrile must be used. Thus, the separation in Figure 17 was based on a mixed-mode mechanism. An increase in buffer salt concentration resulted in a decrease

in ionic interaction and an increase in hydrophobic interaction. As a result, protein peaks were broadened by the increased nonspecific hydrophobic interaction during salt gradient elution. Although the SCX column exhibited worse chromatographic performance for proteins than for peptides, it was comparable to other monolithic SCX columns for protein analysis (Viklund et al., 1997).

3.3.7 SCX Chromatography Application for the Separation of Model Phosphopeptides

A mixture of one tryptic phosphopeptide and two other non-phosphopeptides was used as a model to show the utility of this column in isolation of phosphopeptides from non-phosphopeptides. Even under isobaric buffer B, the +1 charged phosphopeptide ($E_t = 4.20$ min in Figure 18) is well separated from the other two non-phosphopeptides ($E_t = 7.11$ and 12.25 min, respectively, for +2 and +3 non-phosphopeptides in Figure 18).

3.3.8 Stability of the Poly(AMPS-*co*-PEGDA) Monolith

Permeability is a good index to reflect swelling or shrinking of the monolith. If a monolith swells, its throughpores will decrease in size, resulting in lower permeability, and vice versa. From Table 5 the permeability was ~1 order of magnitude lower in aqueous buffer than in some organic solvents. With the use of organic solvents, the permeability decreased roughly with an increase in solvent relative polarity, except that ethyl ether and acetone had the highest permeability. This indicates that the monolith swells in more polar solvents and shrinks in less polar solvents. Although the poly(AMPS-*co*-PEGDA) monolith swelled in aqueous buffer and shrank in organic

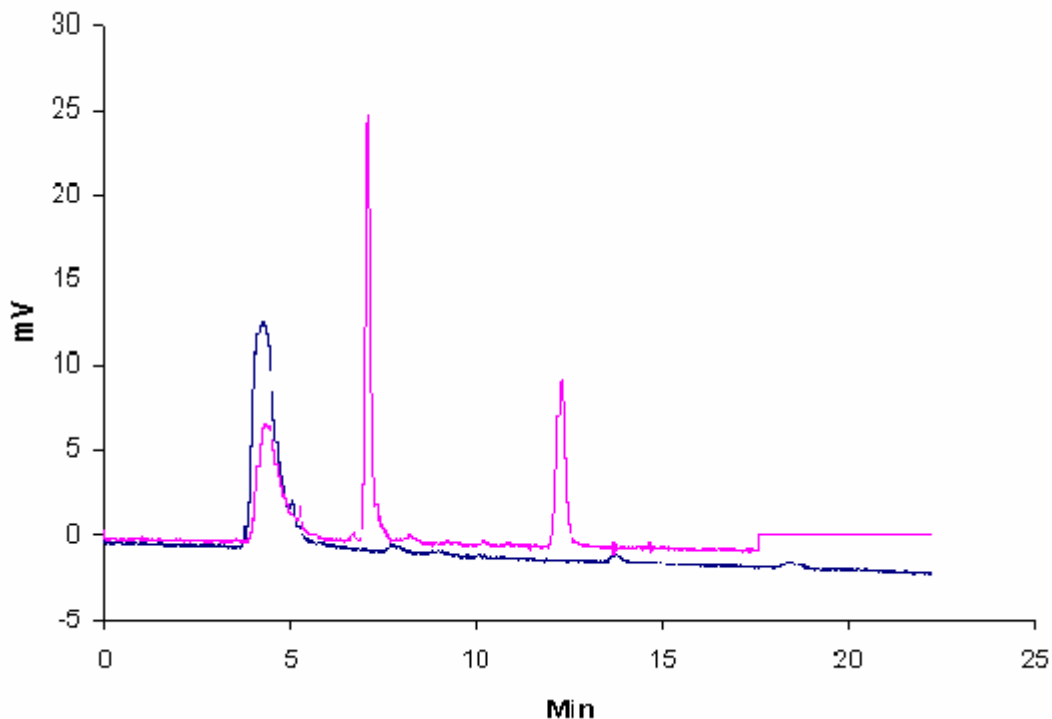


Figure 18. SCX chromatography of a phosphopeptide and a mixture of three peptides. Isocratic Buffer B was used to separate the real peptides (blue chromatogram) 60 nL of 2 mg/mL monophosphopeptide from β -casein (T6) was loaded, the retention time for this +1 charged peptide is 4.20 min (red chromatogram) 60 nL of a mixture of three peptides monophosphopeptide (+1), bradykinin fragment 1-7 (+2) and angiotensin fragment 1-7 (+3) at 1 mg/mL was loaded. The retention times are 4.32 min, 7.11 min and 12.25 min for T6, bradykinin fragment 1-7, and angiotensin fragment 1-7, respectively.

solvents, no detachment of the monolith from the capillary wall was observed under any condition, likely due to covalent attachment to the capillary wall. Furthermore, the column flow rate reached a constant value after equilibration with a new solvent. This indicated reversible shrinking or swelling of the monolith under a variety of solvent conditions. For the SCX liquid chromatography of peptides reported in this study, the column flow rate measured was 70-100 nL/min when the back pressure read from the pump panel was between 2000 and 2300 psi during the gradient run. This indicates that a considerable flow was generated at moderate pressure even though the monolith swelled. The polymer monolith could be used continuously over 1 month under a pressure of

flushing fluid	relative polarity ^a	viscosity, η (cP) ^b	column back pressure, Δp (psi)	linear velocity, u (mm/s)	permeability, k ($\times 10^{-15} \text{m}^2$) ^c
hexane	0.009	0.300	800	5.52	30.0
ethyl ether	0.117	0.224	800	12.09	49.1
THF	0.207	0.456	800	2.51	20.8
acetone	0.355	0.306	800	9.09	50.4
acetonitrile	0.460	0.369	800	3.30	22.1
methanol	0.762	0.544	800	1.17	11.5
water	1.000	0.890	1200	0.27	2.9
buffer A	/	0.846	1200	0.33	3.4
buffer B	/	0.890	1200	0.47	5.1

^a Relative polarity data were from <http://virtual.yosemite.cc.ca.us/smurow/orgsoltab.htm>. ^b Viscosity data were from online *CRC Handbook of Chemistry and physics*, 85th ed.; Boca Raton, 2004-2005. For buffer A, which contains 40% acetonitrile, the viscosity is ~95% water (Sadek, P.C. *HPLC Solvent Guide*, 2nd ed.; John Wiley and Sons: New York, 2002). For buffer B, which contains both 40% acetonitrile and 0.5 M NaCl, the viscosity is assumed to be $0.89 \times 0.95 \times 1.052 = 0.890$ because 0.5 M NaCl is 1.052 times the viscosity of pure water. ^c Permeability $k = \eta L u / \Delta p$, where η is the viscosity, L is the column length (10 cm in this case), u is the solvent linear velocity, and Δp is the column back pressure.

Table 5. Permeability of the Poly(AMPS-co-PEGDA) Monolith

2000 psi. Excessive swelling of the sulfonate-containing polymer monolith in aqueous buffer, which would result in no flow, was not observed for the poly(AMPS-co-PEGDA) monolith reported in this study.

3.3.9 Tentative Explanation of the Sharp Peaks Obtained

It is interesting that the permeabilities of the monolith in aqueous buffers A and B were different (see Table 5). An increase in permeability was observed with the use of the same buffer with 0.5 M NaCl additive. This reflects a responsive property of the poly(AMPS-co-PEGDA) monolith upon contact with salt. Poly(trimethylolpropane trimethacrylate) monolith [poly(TRIM)] with a surface grafted with *N,N*-dimethyl-*N*-methacryloxyethyl-*N*-(3-sulfopropyl) ammonium betaine (SPE) showed a salt-dependent

permeability (Viklund et al., 2000). However, the permeability decreased with an increase in NaCl concentration in the range of 0-0.2 M. Interestingly, no such trend was observed for the monolith prepared by copolymerization of TRIM and SPE. The salt-dependent permeability of the poly (AMPS-*co*-PEGDA) monolith is expected to have an influence on the chromatography of peptides. The mobile phase flow rate in the monolithic column increased in our system during the salt gradient run because the nanoflow gradient in the column was generated by a passive splitter (see Experimental Section). As seen in Figure 14, the sharper the salt gradient, the narrower the peak widths. Double gradient elution was previously demonstrated in ion-exchange liquid chromatography of small ions, where a flow gradient was intentionally employed to achieve fast separation (Paull et al., 2005). It should be emphasized that although a natural flow rate gradient existed in these studies, it did not contribute significantly to the sharpening of peptide bands, especially under shallow (e.g., 1% B/min) salt gradient conditions, where a flow rate increase of ~1.4 times (see Table 5) was estimated for a 100-min interval. It is hypothesized that the extremely sharp peaks achieved in this study are primarily due to the nature of the poly(AMPS-*co*-PEGDA) monolith. While the poly(AMPS-*co*-PEGDA) monolith was shown to exhibit strong hydrophobicity, the hydrophobicity was mainly derived from the side chains of the monolith that attached the functional AMPS monomer. The backbone of the polymer monolith contributed negligible hydrophobicity due to the use of both a biocompatible cross-linker PEGDA and a biocompatible acrylamido group in the AMPS. Thus, no nonspecific hydrophobic interaction between the polymer backbone and peptide would occur. Because the side chains are located on the surface of the polymer monolith upon contact with aqueous

buffer, mass-transfer resistance would be small, resulting in high column efficiency. To test this hypothesis, SCX chromatography of synthetic peptides 1-4 on a poly(AMPS-co-EDMA) monolith was performed under the same conditions as in Figure 13E. Although well separated, the peaks for all four peptides were broad and tailing (data not shown). This observation confirms that the extremely narrow peaks obtained in this study were primarily due to the use of the biocompatible cross-linker PEGDA.

3.3.10 Synthesis of Acrylamidomethanesulfonic Acid

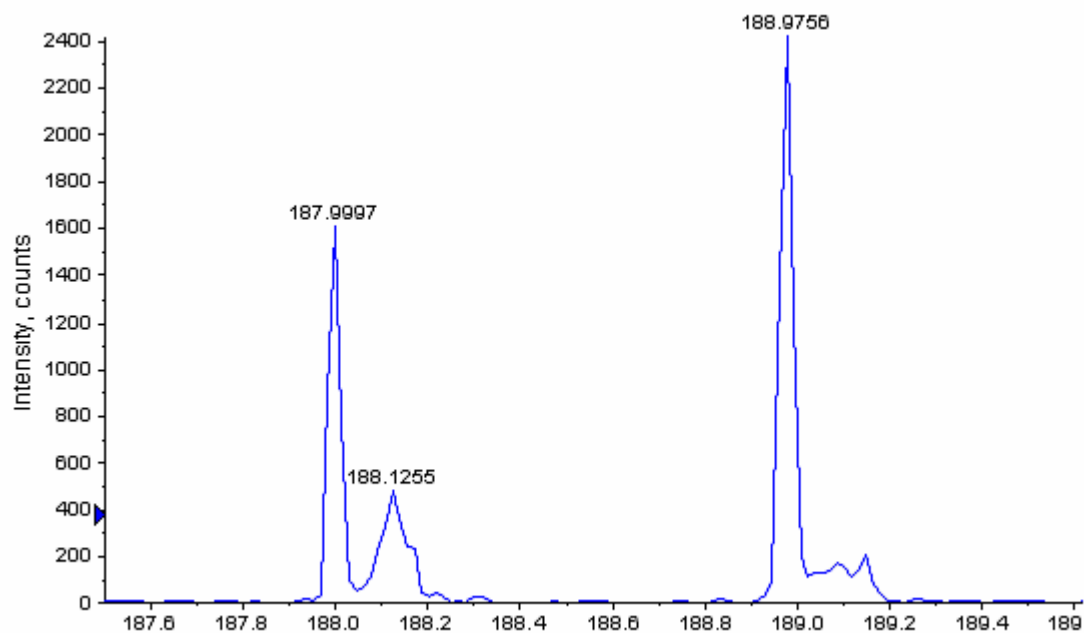


Figure 19. LC-MSD-TOF confirmation of acrylamidomethanesulfonic acid. The reaction mixture (0.1 g) was dissolved in methanol. The sample was carried directly to TOF detector without any chromatographic separation.

The desired product, acrylamidomethanesulfonic acid, was confirmed by LC-MS detection of peak 187.9997 Da, which is the $[M+Na]^+$ ion (M^+ refers to +1 charged molecular ion). It was 1.34 ppm error to the theoretical molecular weight value (187.9988 Da). In order to obtain a quantitative ratio of product acrylamidomethanesulfonic acid

and reactant 2-aminoethanesulfonic acid, the resulting reaction mixture was also dissolved in D₂O and analyzed using 500MHz NMR. The ratio of desired produce/reactant (2-aminoethanesulfonic acid) is about 1:3 (data not shown). Due to the similarity of the two molecules, I have not been able to separate them from each other so as to achieve a pure acrylamidomethanesulfonic acid monomer.

3.4 CONCLUSIONS

A poly(AMPS-*co*-PEGDA) monolith containing as high as 40% AMPS was prepared by one-step copolymerization. The monolith had several favorable features, such as high binding capacity, extraordinary high resolution, and high peak capacity, making it ideal for resolving complex peptide samples, such as protein digests. Due to its excellent chromatographic performance and ease of preparation, the poly(AMPS-*co*-PEGDA) monolith is expected to find many applications. A unique structural feature of the new monolith is the use of PEGDA instead of the conventional EDMA cross-linker, which is believed to result in the high resolution and sharp peaks obtained for peptide analysis. Due to the hydrophobicity of the AMPS monomer, a better monolith could be obtained if a more hydrophilic functional monomer was used. For example, if acrylamidomethanesulfonic acid or 2-acrylamido-1-ethanesulfonic acid was used in place of AMPS, the hydrophobicity of the resulting monolith would be dramatically decreased. This should, in turn, provide even better separation of peptides and make efficient SCX of proteins possible with aqueous buffers containing no acetonitrile. Unfortunately, neither of the two monomers is commercially available. The synthesis of acrylamidomethanesulfonic acid was carried out. Analysis confirmed the formation of the desired product by both the molecular weight (by LC-MS) and structure (by NMR). It

is hard to purify the product from the reaction mixture because of the similarity between the reactant (2-aminoethanesulfonic acid) and the product (acrylamidomethanesulfonic acid). Another possible alternative functional monomer is the commercially available vinylsulfonic acid. Unfortunately, it may be challenging to design suitable porogens to copolymerize vinylsulfonic acid and PEGDA because it is well known that the polymerization rate of vinyl and acrylamido groups is different. Another difficulty is the unavailability of pure vinylsulfonic acid. For example, sodium vinylsulfonate, a sodium salt of vinylsulfonic acid, is available through Sigma as ~30% solution in H₂O. This further complicates the porogen design because the ratio of vinylsulfonic acid to water is fixed at 3 to 7 if 30% sodium vinylsulfonate is used.

3.5 REFERENCES

- Alpert, A.J. and Andrews, P.C.(1988) Cation-exchange chromatography of peptides on poly(2-sulfoethyl aspartamide)-silica. *J. Chromatogr.*, **443**, 85-96.
- Beausoleil, S.A., Jedrychowski, M., Schwartz, D., Elias, J.E., Villen, J., Li, J., Cohn, M.A., Cantley, L.C. and Gygi, S.P.(2004) Large-scale characterization of HeLa cell nuclear phosphoproteins. *PNAS*, **33**,12130-12135.
- Burke, T.W., Mant, C.T., Black, J.A. and Hodges, R.S.(1989) Strong cation-exchange high-performance liquid chromatography of peptides. Effect of non-specific hydrophobic interactions and linearization of peptide retention behaviour. *J. Chromatogr.*, **476**, 377-389.
- Cagney, G., Park, S., Chung, C., Tong, B., O'Dushlaine, C., Shields, D.C. and Emili A.(2005) Human tissue profiling with multidimensional protein identification technology J Proteome Res., 4, 1757-1767.
- Chen, E.I., Hewel, J., Felding-Habermann, B. and Yates, J.R. 3rd.(2006) Large scale protein profiling by combination of protein fractionation and multidimensional protein identification technology (MudPIT). *Mol Cell Proteomics.*, 5, 53-56.
- Crimmins, D.L., Gorka, J., Thoma, R.S. and Schwartz, B.D.(1988) Peptide characterization with a sulfoethyl aspartamide column. *J. Chromatogr.*, **443**, 63-71.
- Fields, S.M.(1996) Silica Xerogel as a Continuous Column Support for High-Performance Liquid Chromatography. *Anal. Chem.*, **68**, 2709-2712.
- Gu, B., Armenta, J.M. and Lee, M.L.(2005) Preparation and evaluation of poly(polyethylene glycol methyl ether acrylate-co-polyethylene glycol diacrylate) monolith for protein analysis. *J. Chromatogr. A*, **1079**, 382-391.
- Gu, B., Chen, Z., Thulin, C. D., Lee, M. L. (2006) Efficient Polymer Monolith for Strong

- Cation-Exchange Capillary Liquid Chromatography of Peptides *Anal. Chem.* **78**, 3509-3518
- Guo, D.; Mant, C. T.; Taneja, A. K.; Parker, J. M. R.; Hodges, R. S. *J. Chromatogr.* 1986, **359**, 499-517.
- Gusev, I., Huang, X. and Horvath, C. (1999) Capillary columns with in situ formed porous monolithic packing for micro high-performance liquid chromatography and capillary electrochromatography. *J. Chromatogr. A*, **855**, 273-290.
- Guyot, A. and Bartholin, M.(1982) Design and properties of polymers as materials for fine chemistry. *Prog. Polym. Sci.*, **8**, 277-332.
- Haddad, P. R.; Jackson, P. E. *Ion Chromatography: Principles and Applications*; Elsevier: New York, 1990.
- Hilder, E.F., Svec, F. and Frechet, J.M.(2004) Latex-functionalized monolithic columns for the separation of carbohydrates by micro anion-exchange chromatography. *J. Chromatogr. A*, **1053**, 101-106.
- Hjerten, S. *Ind. Eng. Chem. Res.* 1999, **38**, 1205-1214.
- Hjerten, S.; Liao, J. L.; Zhang, R. J. (1989) High-performance liquid chromatography on continuous polymer beds. *J. Chromatogr.*, **473**, 273-275.
- Issa, R. M.; El-Sonbati, A. Z.; El-Bindary, A. A.; Kera, H. M. *J. Inorg. Organomet. Polym.* 2003, **13**, 269-283.
- Kimura, H., Tanigawa, T., Morisaka, H., Ikegami, T., Hosoya, K., Ishizuka, N., Minakuchi, H., Nakanishi, K., Ueda, M., Cabrera, K. and Tanaka, N.(2004) Simple 2D-HPLC using a monolithic silica column for peptide separation. *J. Sep. Sci.*, **27**, 897-904.
- Kun, K. A.; Kunin, R. J. *Polym. Sci., Part A1* 1968, **6**, 2689-2701.
- Liu, Z., Wu, R. and Zou, H.(2002) Recent progress in adsorbed stationary phases for capillary electrochromatography. *Electrophoresis*, **23**, 3954-3972.
- Mant, C. T. and Hodges, R. S.(1991) In *High-Performance Liquid Chromatography of Peptides and Proteins: Separation, Analysis, and Conformation*; Mant, C. T., Hodges, R. S., Eds.; CRC Press: Boca Raton, FL, pp 171-185.
- Mant, C.T.; Hodges, R.S. (1990) In *High-Performance Liquid Chromatography of Biological Macromolecules: Methods and Applications*; Gooding, K., Regnier, F., Eds.; Marcel Dekker: New York, pp 301-332.
- Mant, C.T.; Hodges, R.S.(1985) General method for the separation of cyanogen bromide digests of proteins by high-performance liquid chromatography. Rabbit skeletal troponin I. *J. Chromatogr.*, **326**, 349-356.
- Mant, C.T.; Hodges, R.S.(1985) Separation of peptides by strong cation-exchange high-performance liquid chromatography. *J. Chromatogr.*, **327**, 147-155.
- Minakuchi, H., Nakanishi, K., Soga, N., Ishizuka, N. and Tanaka, N.(1996) Octadecylsilylated Porous Silica Rods as Separation Media for Reversed-Phase Liquid Chromatography. *Anal. Chem.*, **68**, 3498-3501.
- Ngola, S.M., Fintschenko, Y., Choi, W.Y. and Shepodd, T.J.(2001) *Anal. Chem.*, **73**, 849-856.
- Palm, A. and Novotny, M.V.(1997) Macroporous Polyacrylamide/Poly(ethylene glycol) Matrixes as Stationary Phases in Capillary Electrochromatography. *Anal. Chem.*, **69**, 4499-4507.
- Paull, B. and Nesterenko, P.N.(2005) New possibilities in ion chromatography using porous monolithic stationary-phase media. *TrAC-Trends Anal. Chem.*, **24**, 295- 303.

- Paull, B., Riordain, C.O. and Nesterenko, P.N.(2005) Double gradient ion chromatography on a short carboxybetaine coated monolithic anion exchanger. *Chem. Commun.*, **2**,215-217.
- Peters, E.C., Petro, M., Svec, F. and Frechet, J.M.(1997) Molded rigid polymer monoliths as separation media for capillary electrochromatography. *Anal. Chem.*, **69**, 3646-3649.
- Peters, E.C., Petro, M., Svec, F. and Frechet, J.M.(1998) Molded rigid polymer monoliths as separation media for capillary electrochromatography. 2. Effect of chromatographic conditions on the separation. *Anal. Chem.*, **70**, 2288-2295.
- Petro, M., Svec, F. and Frechet, J.M.(1996) Comparison of the chromatographic properties of the monolithic rod with columns packed with porous and non-porous beads in high-performance liquid chromatography of polystyrenes. *J. Chromatogr, A*, **752**, 59-66.
- Premstaller, A., Oberacher, H. and Huber, C.G.(2000) High-performance liquid chromatography-electrospray ionization mass spectrometry of single- and double-stranded nucleic acids using monolithic capillary columns. *Anal. Chem.*, **72**, 4386- 4393.
- Righetti, P. G.(1990) In Immobilized pH Gradients. Theory and Methodology; Burdon,R. H., van Knippenberg, P. H., Eds.; Elsevier: New York, p 17.
- Rivas, B.; Martı́nez, E.; Pereira, E.; Geckeler, K. E. *Polym. Int.* 2001, **50**, 456-462.
- Rohr, T., Hilder, E.F., Donovan, J.J., Svec, F. and Frechet, J. M. J.(2003) Photografting and the Control of Surface Chemistry in Three-Dimensional Porous Polymer Monoliths. *Macromolecules*, **36**, 677-684.
- Sederel, W. L. and Jong, G. J.(1973) Styrene-Divinylbenzene Copolymers: Construction of Porosity in Styrene Divinylbenzene Matrices. *J. Appl. Polym. Sci.*, **17**, 2835-2846.
- Sinner, F. and Buchmeiser, M.R.(2000) A New Class of Continuous Polymer Supports Prepared by Ring-Opening Metathesis Polymerization: A Straightforward Route to Functionalized Monoliths. *Macromolecules*, **33**, 5777-5786.
- Stadalius, A. A.; Quarry, M. A.; Snyder, L. R. *J. Chromatogr.* 1985, **327**, 93-113.
- Svec, F.LC-GC *Eur.* 2003, **16**, 24-28.
- Svec, F.(2004) Organic polymer monoliths as stationary phases for capillary HPLC. *J. Sep. Sci.*, **27**, 1419-1430.
- Svec, F.(2004) Preparation and HPLC applications of rigid macroporous organic polymer monoliths. *J. Sep. Sci.*, **27**, 747-766.
- Svec, F.; Frechet, J. M. J. *Anal. Chem.* 1992, **54**, 820-822.
- Ueki, Y., Umemura, T., Li, J., Odake, T. and Tsunoda, K.(2004) Preparation and application of methacrylate-based cation-exchange monolithic columns for capillary ion chromatography. *Anal. Chem.*, **76**, 7007-7012.
- Viklund, C. and Irgum, K.(2000) Synthesis of Porous Zwitterionic Sulfobetaine Monoliths and Characterization of Their Interaction with Proteins. *Macromolecules*, **33**, 2539-2544.
- Viklund, C., Svec, F., Frechet, J.M. and Irgum, K.(1997) Fast ion-exchange HPLC of proteins using porous poly(glycidyl methacrylate-co-ethylene dimethacrylate) monoliths grafted with poly(2-acrylamido-2-methyl-1-propanesulfonic acid). *Biotechnol. Prog.*, **13**, 597-600.
- Vitali, B., Wasinger, V., Brigidi, P. and Guilhaus, M.(2005) A proteomic view of *Bifidobacterium infantis* generated by multi-dimensional chromatography coupled with tandem mass spectrometry. *Proteomics.*, **5**, 1859-1867.
- Wu, R., Zou, H., Fu, H., Jin, W. and Ye, M.(2002) Separation of peptides on mixed mode of reversed-phase and ion-exchange capillary electrochromatography with a monolithic column. *Electrophoresis*, **23**, 1239-1245.

- Wu, R., Zou, H., Ye, M., Lei, Z. and Ni, J.(2001) Separation of basic, acidic and neutral compounds by capillary electrochromatography using uncharged monolithic capillary columns modified with anionic and cationic surfactants. *Electrophoresis*, **22**, 544-551.
- Yu, C., Davey, M.H., Svec, F. and Frechet, J.M.(2001) Monolithic porous polymer for on-chip solid-phase extraction and preconcentration prepared by photoinitiated in situ polymerization within a microfluidic device. *Anal. Chem.*, **73**,5088-5096.
- Zakaria, P., Hutchinson, J.P., Avdalovic, N., Liu, Y. and Haddad, P.R.(2005) Latex-coated polymeric monolithic ion-exchange stationary phases. 2. Micro-ion chromatography. *Anal. Chem.*, **77**, 417-423.

CHAPTER FOUR

ANALYSIS OF PHOSPHORYLATION OF SYNTAXIN 1A AND 4A BY AMPK

4.1 INTRODUCTION

In large scale phosphoproteome studies, the goal is to identify as many phosphorylation sites from as many phosphoproteins as possible. So far, only a subset of a phosphoproteome can be observed due to limitations mentioned in the introduction. Furthermore not every single phosphorylation site can be identified in this type of study. When examining a single phosphorylated protein, different strategies should be applied for different phosphorylation scenarios, depending on conditions such as the phosphorylation stoichiometry, the availability of proteins and instrumental conditions. All means should be applied to the study because, for any single protein, no one method ensures success. All our phosphorylation studies employed a Qstar Pulsar I (Applied Biosystems, Foster City, CA) triple quadrupole-time-of-flight mass spectrometer. Usually, information-dependent acquisition (IDA) was used to collect MS/MS spectra. Phosphopeptides, due to poor stoichiometry and/or low ionization in the positive mode, are seldomly automatically chosen for fragmentation. Even when they are, their fragmentation spectra are usually not adequate for phosphorylation site identification purposes. In this chapter, enrichment of phosphopeptides by TiO₂ resins was used to study a quadruply phosphorylated peptide from phosphducin-like protein (PhLP), and peptide-level mapping was used to study the phosphorylation of syntaxin 1a.

Protein phosphorylation plays a major role in signal transduction. The work undertaken here involved the phosphorylation of syntaxins by AMPK (AMP-activated protein kinase). AMPK serves as an energy sensor and metabolic switch in cells by phosphorylating key target proteins that control flux through metabolic pathways of hepatic ketogenesis, cholesterol synthesis, lipogenesis, triglyceride synthesis, adipocyte lipolysis, and skeletal muscle fatty acid oxidation. It has been also shown that AMPK was activated (Vavvas et al., 1997; Winder et al., 1996) and glucose uptake was increased (Goodyear et al., 1998; Hayashi et al., 1997; Holloszy et al., 1996) under muscle contraction. Glucose uptake, which is part of the effect of insulin, was shown to be increased by chemical activation of AMPK (Hayashi et al., 1998). Winder et al proposed a novel mechanism for stimulation of glucose uptake in skeletal muscle under muscle contraction as shown in Figure 20 (Winder et al., 1999). Briefly, muscle contraction activates AMPK, which stimulates glucose uptake through the phosphorylation of one or more SNARE (soluble N-ethylmaleimide-sensitive fusion protein attachment protein receptor) proteins involved in the vesicle membrane fusion process by AMPK.

The AMPK substrate(s) that are responsible for the increased fusion of microvesicles to the membrane have not been identified yet. An examination of the elements involved in vesicle membrane fusion, such as VAMP, SNAP-25 (counter part of SNAP-23 found in skeletal muscle cell) and syntaxin 1a (counterpart of syntaxin 4 found in muscle cell) in neuron cells by Dr. William W. Winder (Dept. of Physiology and Developmental Biology, BYU, Provo UT) showed that syntaxin 1a was the only substrate found for AMPK. Because of the availability of syntaxin 1a and its similarity to syntaxin 4 (the protein of interest; the form of syntaxin expressed in muscle), a study of the

phosphorylation of syntaxin 1a was performed. The localization of the phosphorylation site is the first step toward elucidating the role of syntaxin 4 phosphorylation by AMPK in the glucose uptake mechanism. Elucidation of this mechanism is significant in our understanding of diabetes mellitus. Activation of AMPK has the same effect as insulin on glucose uptake. Drugs that activate AMPK in muscle cells will alleviate symptoms of diabetes patients.

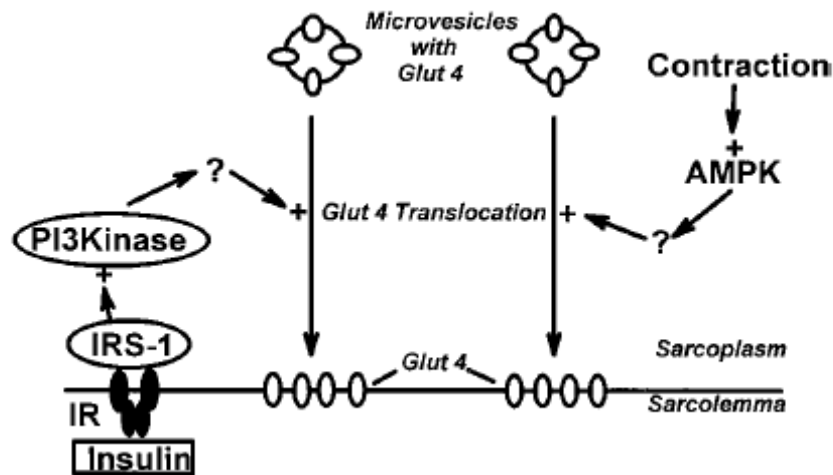


Figure 20. Two mechanisms for stimulation of glucose uptake in skeletal muscle, one mediated by insulin and one triggered by muscle contraction. The hypothesis of mediation of the contraction effect by AMPK is based on the observations that exercise and electrical stimulation increase AMPK activity and glucose uptake and that glucose uptake is increased by chemical activation of AMPK with AICA-riboside. IR, insulin receptor; IRS-1, insulin receptor substrate 1; PI 3-kinase, phosphatidylinositol 3-kinase (Winder et al., 1999).

Through the course of these studies, the need for a positive control phosphoproteins became evident. Phosducin-like protein (PhLP) was chosen for this role. PhLP, a protein homologous to phosducin, acts as a co-chaperone for G_{β} folding and assembly of the $G_{\beta\gamma}$ dimer in GPCR signal pathways. *In vitro* phosphorylation of PhLP

by CK2 and analysis of its phosphorylation sites has been reported (Lukov et al., 2006). Here phosphorylated PhLP tryptic peptides served as a positive control for MonoTip® TiO Pipette Tip enrichment studies.

4.2 MATERIALS AND METHODS

4.2.1 Syntaxin 1a (1a1, 1a7, 1a9, 1a11, 1a12) Expression and Protein Purification

Syntaxin 1a and its different truncated forms of recombinant proteins were provided by Dr. Woodbury (Department of Physiology and Developmental Biology, BYU, Provo, UT), which were prepared as previously reported (Woodbury et al., 2006). The plasmids of syntaxin 1a and its truncated forms (syntaxin 1a7, 1a8, 1a9, 1a11, 1a12) were gracious gifts from Dr. Mark K. Bennett (University of California, Berkeley).

4.2.2 PhLP Expression and Purification

The bacterial expression vector pET15b (Novagen, Madison, WI) containing hPhLP-myc-His construct was from Dr. Willardson's Lab (Dept. Chemistry and Biochemistry, Brigham Young University, Provo, UT). The integrity of all constructs was confirmed by sequence analysis. The construct was transformed into RbC₁₂ competent DE3 Escherichia coli by heat shock. The protein was expressed and purified using a Pro-bond nickel-chelate column (Qiagen, Valencia, CA) as described previously (Savage et al., 2000). The purified protein was exchanged into 20 mM HEPES, pH 7.2, 150 mM NaCl buffer using an ultrafree centrifuge concentrator (Millipore, Billerica, MA) and the protein concentration was assayed by the Bradford method. The protein was stored with 50% glycerol at -20 ° C.

4.2.3 *In vitro* Phosphorylation of PhLP, Syntaxin 1a and Syntaxin 4a

PhLP phosphorylation by CK2. A 500 µg amount of purified PhLP was phosphorylated by CK2 (10 unit/µl, Calbiochem) in 20 mM HEPES, pH 7.5, 100 mM KCl, 20 mM NaCl, 5 mM MgCl₂, 5 mM dithiothreitol, and 1 mM ATP for 1 h at 37°C. The phosphorylation was confirmed by mobility shift in SDS-PAGE using 12% gels.

Syntaxin 1a and syntaxin 4a phosphorylation by AMPK and LKB1/STRAD/MO25 (AMPKK). On the day of the assay, ATP, AMP and DTT were added to the stock solution (100 mM Hepes, 200 mM NaCl, 20% glycerol, 2 mM EDTA, and 12.5 mM MgCl₂, pH 7.0) to make a working assay mix of final concentration of 40 mM Hepes, 0.2 mM SAMS, ± 0.2 mM AMP, 80 mM NaCl, 8% glycerol, 0.8 mM EDTA, 0.8 mM DTT, 5 mM MgCl₂, and 0.2 mM ATP, pH 7.0. AMPK was phosphorylated by adding LKB1/STRAD/MO25 (AMPKK), which will then phosphorylate syntaxin 1a or syntaxin 4a. The reaction mixture was incubated for two hours at 30 °C. ³²P-labeled ATP was used instead of ATP to assay the phosphorylation rate of syntaxin 1a by this method.

4.2.4 In-gel Digestion of Syntaxin 1a Containing Gel Bands

Gel bands containing syntaxin 1a were cut out and transferred to 1.5 mL eppendorf tubes. Then they were equilibrated in 1.5 mL of 50% acetonitrile and 50 mM ammonium bicarbonate buffer for 30 min at room temperature on a micro mixer. After aspirating off the buffer, proteins in the gel bands were reduced with 150 µl of 5 mM DTT, 100 mM ammonium bicarbonate reduction buffer for 30 min at 60° C. After removing the reduction buffer, the gel bands were cooled to room temperature and the proteins alkylated by incubating 30 min with 150 µl of 20 mM iodoacetamide, 100 mM ammonium bicarbonate in the dark. The gel bands were then equilibrated with 1 mL of

100 mM ammonium bicarbonate again and cut into six smaller pieces. They were dehydrated with 500 μ l 50% acetonitrile and 50 mM ammonium bicarbonate for 30 min under rotation, then speed vacuumed to dryness. Proteins in the gel pieces then were digested with trypsin digestion solution (0.02 mg/mL trypsin, 25 mM ammonium bicarbonate) by gradually adding 10 μ l aliquots until they were fully rehydrated and then covered with an additional 30 μ L 25 mM ammonium bicarbonate. They were then incubated at 37 ° C with motion overnight (16-24 h) in a hybridization oven. The digestion reaction was quenched by adding 1 μ l 88% formic acid followed by sonication for 20 min. The supernatants were separated from the gel pieces by brief centrifugation for LC-MS/MS analysis.

4.2.5 Enrichment of Phosphopeptides from Tryptic Peptides

Enrichment of phosphopeptides from tryptic peptides of phosphorylated PhLP and syntaxin 1a were performed with MonoTip® TiO Pipette Tip (GL Sciences, Tokyo, Japan) according to the manufacturer's procedure. Briefly this titanium dioxide-containing silica monolith was conditioned with an acetonitrile phosphate buffer and equilibrated with 50% acidic acetonitrile. Tryptic peptides from phosphorylated PhLP and phosphorylated syntaxin 1a were absorbed to the tip by passing them through the tip several times. The tip was rinsed with 50% acetonitrile 100 mM KCl buffer and eluted either with 200 mM phosphate pH 7.0 buffer or 2% aqueous ammonia buffer.

4.2.6 LC-MS/MS Analysis of Tryptic Peptides or Enriched Samples

Samples were analyzed on an Applied Biosystems (Framingham, MA) API Qstar Pulsar i mass spectrometer with an online LC Packings (Dionex, Sunnyvale, CA)

UltiMate Plus Capillary LC System. Tryptic digests of each protein sample were run through a 15 cm x 250- μ m-ID column hand-packed with Jupiter C18 10- μ m reversed-phase resin (Phenomenex, Torrence, CA). An initial gradient of 2.2%/min to a concentration of 60% acetonitrile in 0.1% formic acid was applied to the column, followed by a 3.5%/min gradient up to a concentration of 95% organic phase. The HPLC was controlled by the mass spectrometer software (Analyst, Applied Biosystems) and incorporated a FamOS autosampler (Dionex, Sunnyvale, CA). The column effluent was analyzed in information-dependant acquisition (IDA) mode on the mass spectrometer. In this mode, a survey scan (full MS scan) is performed and then the three most intense peaks from the survey scan are automatically chosen for fragmentation to obtain MS/MS spectra, as long as they have not been chosen for fragmentation in the last 2 min (timed exclusion). Data were collected for m/z 500–2500 over a 55-min interval. The IDA spectra were reconstructed using the Bio-Analyst software and searched in the Mascot database with and without an extra 80 Da corresponding to phosphorylation. Molecular ions of m/z predicted for possible phosphorylation sites were selected as parent ions in manual selection LC-MS/MS experiments. CID spectra were compared with theoretical peptide fragments to deduce specific phosphorylation sites.

4.3 RESULTS AND DISSCUSSION

4.3.1 Study of PhLP Phosphorylation with Phosphopeptide Enrichment

Study of the PhLP phosphorylation by casein kinase II has been previously reported (Lukov et al., 2006). The phosphorylation was confirmed by site-directed mutagenesis analysis (Lukov et al., 2006). As a positive control for the TiO₂ enrichment method, these phosphorylation sites were analyzed with the enrichment procedure using

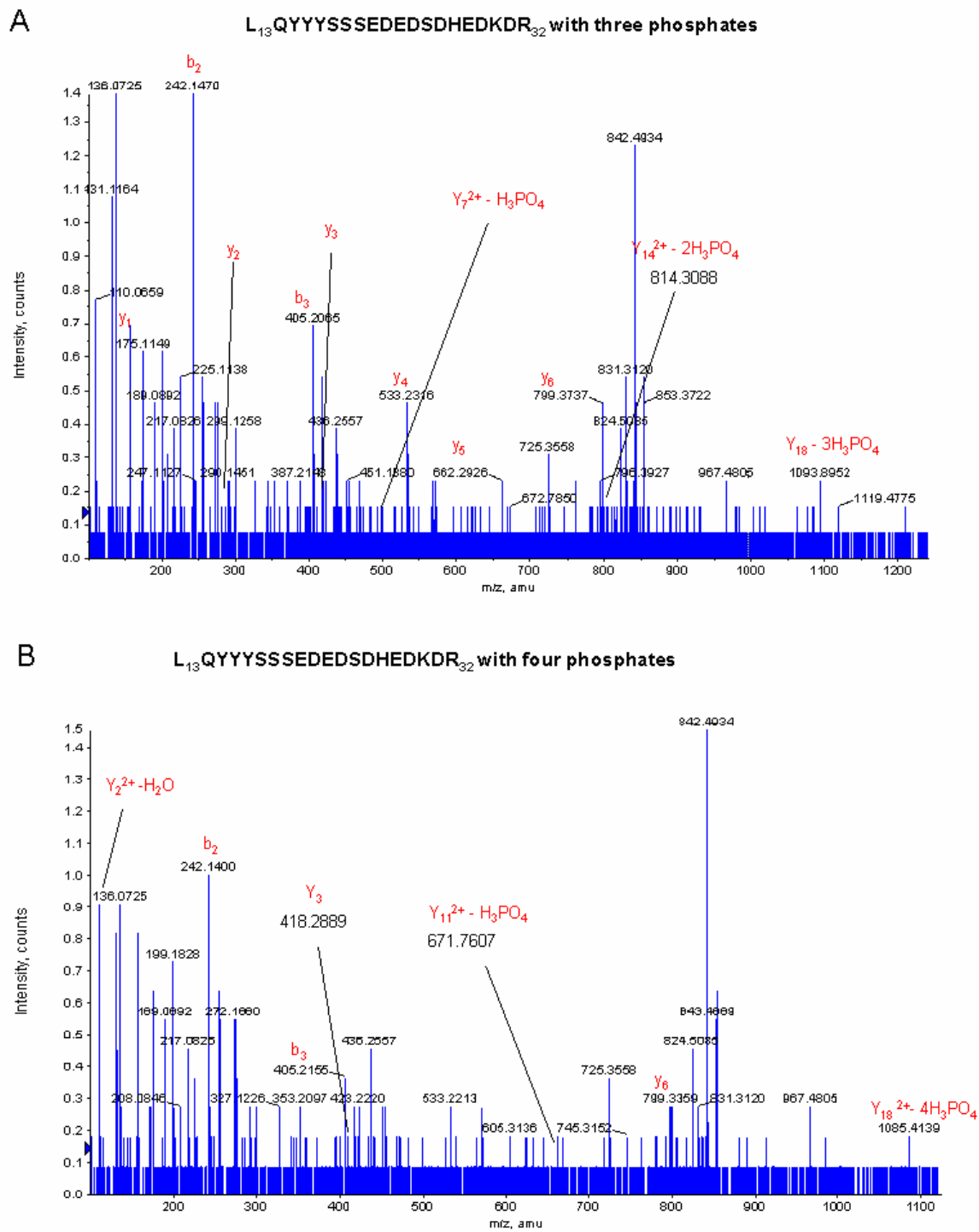


Figure 21. MS/MS spectra of T3 of phosphorylated PhLP by CKII. (A), Tryptic peptides T3 in triply phosphorylated form from the phosphopeptide enriched sample of 50 μ g of tryptic phosphorylated PhLP. (B), Tryptic peptides T3 in quadruply phosphorylated form from the same sample.

the TiO₂ pipette tip. One of the phosphopeptides (Trypsin digestion fragment 3, T3) with quadruply phosphorylated sites was enriched and was chosen for fragmentation by information-dependent acquisition. The triply phosphorylated form and quadruply phosphorylated form of this T3 were both detected, as shown in spectra A and B of Figure 21, respectively. Although there are possibilities of three phosphorylation sites out of seven possible candidate sites in Figure 21A, phosphorylation of S18, S19 and S25 had the highest Mowse Score (82.7) compared with the other two possibilities (LQYYYSSSEDEDEDSDHEDKDR, Mowse Score 73.3; LQYYYSSSEDEDEDSDHEDKDR, Mowse Score 71.7; underline indicates phosphorylation), which were also observed in the samples of phosphorylated PhLP tryptic peptides without TiO₂ enrichment. The data show that phosphorylation on S25 with any combination of phosphorylation of two out of the three consecutive serines could be possible. The quadruply phosphorylated form of the same tryptic peptide was also observed and fragmented. Although the Mowse Score is low for the fragmentation (35.0), the combination of phosphorylation of S18-20 and S25 gives the highest Mowse score. In light of observation of the triply phosphorylated form of the same peptide, it is reasonable to conclude that S25 is the site that is phosphorylated along with any two or all three phosphorylation sites from the three consecutive serines (S18-20). In concert with data from the report of Lukov et al. (2006) noting the observation of singly or doubly phosphorylated form of the same peptide, phosphorylation of one to four sites among the four serine residues (S18-20, S25) is suggested, with some sites preferred over others. The MonoTip® TiO Pipette Tip did not successfully enrich T37 of PhLP (N₂₈₇SATCHSESDLEIDALEGPR; ALEGPR is part of the myc tag on PhLP C-terminus), which was reported in the same paper (Lukov et al.,

2006). It seems that MonoTip® TiO Pipette Tip tends to enrich multiply phosphorylated peptides in preference over singly phosphorylated peptides. The same conclusion was also drawn in other reports (Kweon et al., 2006).

4.3.2 Study of Syntaxin 1a Phosphorylation

The study of syntaxin 1a phosphorylation instead of syntaxin 4 phosphorylation was done due to availability of syntaxin 1a and the similarity of these two proteins (shown in Figure 22). The stoichiometry of phosphorylation of syntaxin 1a by AMPK is 7%, as quantified by a ³²P-labeled ATP *in vitro* reaction (W. Winder, unpublished results).

As the first step towards elucidation of syntaxin 1a phosphorylation,

syn1a,	1	MKDRTQELRTAKDSDDDD--VAVTVDRDRFM-----DEFFEQVEEIRGFIDKIAENVE
syn4a,	1	MRDRTHELRQGDDSSDEEDKERVALVVHPGTARLGSPDEEFFHKVRTIRQTIVKLGKQVQ
		* *
syn1a,	53	EVKRKHSAILASPNPDEKTKEELEELMSDIKKTANKVRSKLKSI EQSIEQEGLNRSSAD
syn4a,	61	ELEKQQVTILATPLPEESMKQELQNLRDEIKQLGREIRLQLKAIEPQ-KEEADENYNSVN
		* *
syn1a,	113	LRIRKTQHSTLSRKFVEVMSEYNATQSDYRERCKGRIQRQLEITGRITTS-EELEDMLLES
syn4a,	120	TRMRKTQHGVLSSQQFVELINKNSMQSEYREKNVERIRRQLKITNAGMVSDEELEQMLDS
		* *
syn1a,	172	GNPAIFASGLIMDSSISKQALSEIETRHSEIIKLENSIRELHDMFMDMAMLVESQGEMID
syn4a,	180	GQSEVFSVSNILKDTQVTRQALNEISARHSEIQQLERSIRELHDIFTFLATEVEMQGEMIN
		* *
syn1a,	232	RIEYNVEHAVDYVERAVSDTKKAVKYQSKAR
syn4a,	240	RIEKNILSSADYVERGQEHVKTALENQKKAR
		* *

Table 6. Sequence alignments of syntaxin 4a (syn4a) and syntaxin 1a (syn1a) by Sim software program (available for free at <http://ca.expasy.org/tools/sim-prot.html>). 124 Amino acids are identical (or 45.8%) in 271 amino acids overlap as shown by asterix (*).

the enrichment of phosphopeptides by MonoTip® TiO Pipette Tip was carried out. A 7.2 µg amount of syntaxin 1a was phosphorylated *in vitro*, trypsin digested and

phosphopeptides were enriched as described above (4.2.5). IDA acquisition was used to collect tandem MS spectra. No phosphopeptide candidates were chosen for fragmentation. With the experience of analysis of phosphorylated PhLP, single phosphorylation of peptides might be one of the reasons that no candidates were chosen for fragmentation here. Phosphorylation stoichiometries below 20% pose a challenge to the identification of phosphorylation sites.

As a result, a second approach was applied. This approach involved the mapping of possible phosphorylation candidates by taking advantage of the post-translational modification mapping program provided with the Analyst software. False positives were ruled out by employing several criteria [including: existence of the unphosphorylated form (in the case of low phosphorylation rate), peptide/phosphopeptide retention time on reverse-phased liquid chromatography and non-specific noise by comparing with controls] and then, chosen candidates (of specific m/z) were fragmented by manual selection LC MS/MS for confirmation. In this case, phosphorylated syntaxin 1a and controls (from reactions without LKB1/STRAD/MO25, the AMPKK) were run on an SDS-PAGE gel in order to purify the samples (Table 7). Samples from in-gel digestion of four lanes (two samples and two controls) were run on the Qstar MS as described (materials and methods section) using the IDA acquisition mode. Mapping modification was carried out on all four samples. Only tryptic peptide number 32 (T32, T₁₅₉TTSEELEDMLESGNPAIFASGIIMDSSISK₁₈₉) of syntaxin 1a was identified as a phosphopeptide found after ruling-out false positives.

The unphosphorylated form of T32 ($m/z=1092.4967$ of average mass, +3 charge, retention time between 21.0-22.0 minute) was found among all four samples. But the

phosphorylated form of T32 ($m/z=1119.2$ of average mass, +3, $t_R = 21.0-21.7$ min) was only found in the two samples, not in controls, as shown in ion extraction (XIC) of ions with m/z between 1118.7 and 1119.7 (Figure 22). With the availability of the several truncated forms of syntaxin 1a, experiments were designed to narrow down the possible

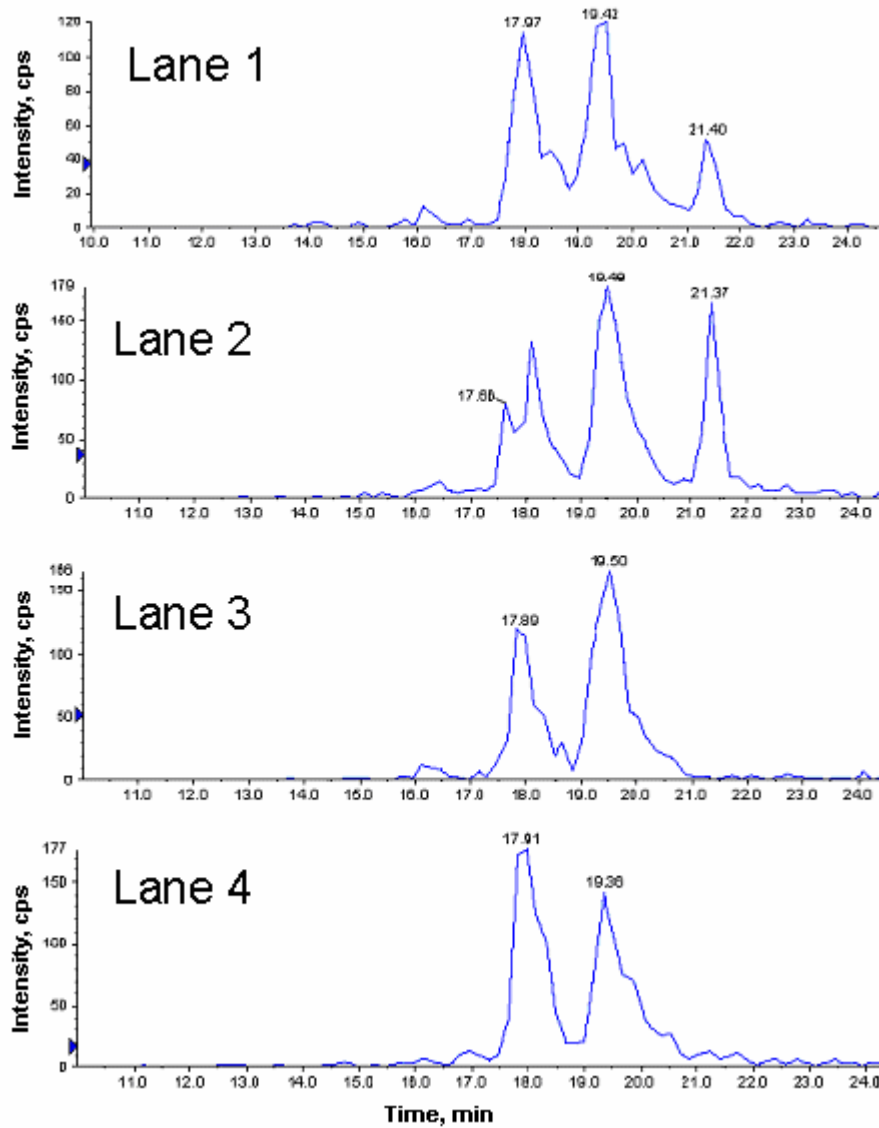


Figure 22. Ion extractions of m/z (1118.7-1119.7) of TOF MS experiments from syntaxin 1a phosphorylation samples and controls. The phosphorylated form of T32 of syntaxin 1a is eluted between 21.0-21.7 min. The two samples (Lane 1 and Lane 2) were added with strain 8 phosphorylated AMPK and the two controls (Lane 3 and Lane 4) were without strain 8 phosphorylated AMPK.

Lane	1	2	3	4
Cocktail Buffer with ATP, DTT, AMP	10	10	10	10
Syn1A1 (100 $\mu\text{g/mL}$)	5	5	5	5
Strain 8 phosphorylated AMPK	2	2	0	0
Water	8	8	8	8
Incubation time	2h	2h	2h	2h

Table 7. *In vitro* phosphorylation of syntaxin 1a for in-gel digestion. All volume units are in μL .

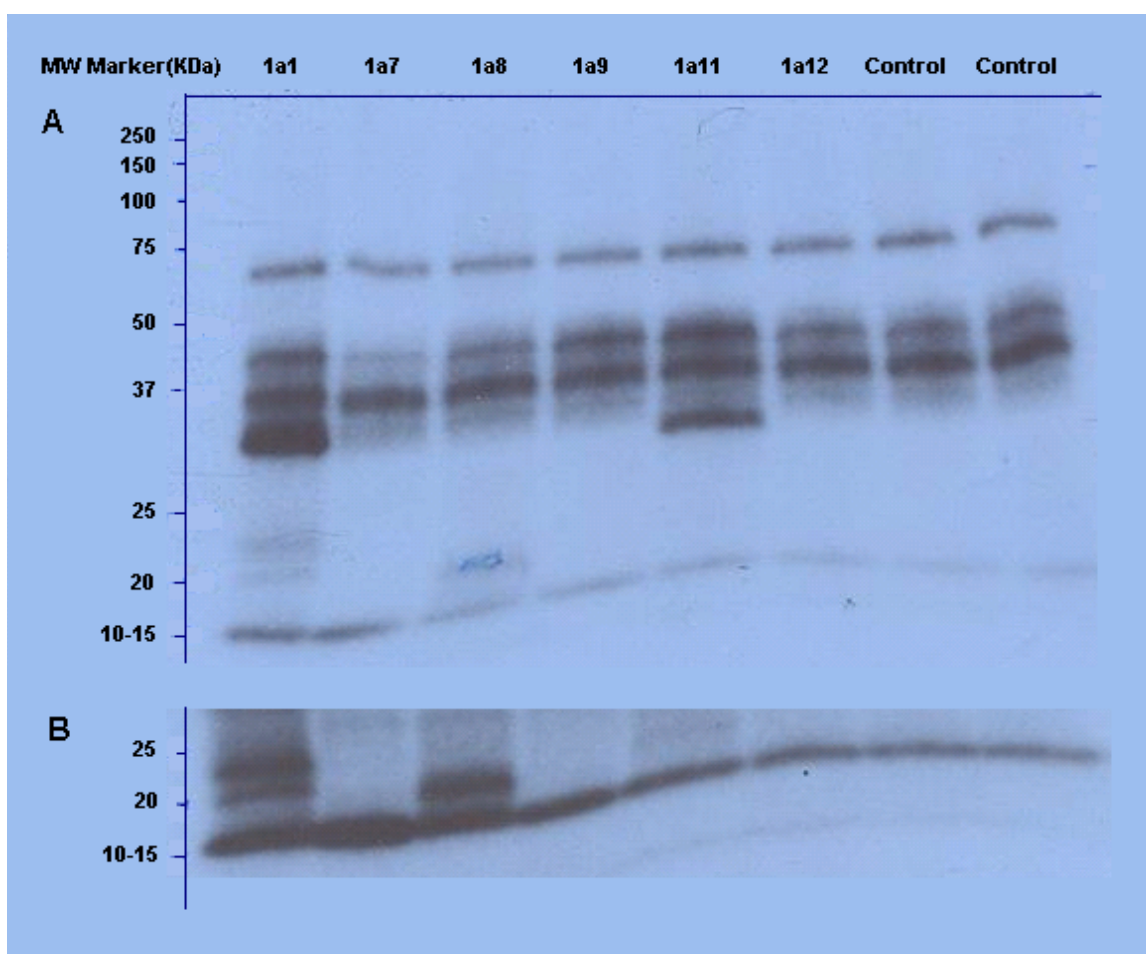


Figure 23. Autoradiography of *in vitro* phosphorylated syntaxin 1a and its truncated forms by activated AMPK. (A) The film was incubated about four hours. (B) The film was developed overnight for the same region from the dye front to 25 KDa molecular maker. Sequences of syntaxin 1a1, 1a7, 1a8, 1a9, 1a11, and 1a12 are 1-288, 8-288, 77-288, 115-288, 194-288, and 221-288, respectively.

phosphorylation sites by their *in vitro* phosphorylation with ^{32}P -labeled ATP to roughly verify the mapping result.

The different truncated forms (about 0.2 μg of each, with the exception of syntaxin 1a7 with a lower amount) of syntaxin 1a were *in vitro* phosphorylated as was syntaxin 1a, shown in Table 7. In this experiment syntaxin 1a, syntaxin 1a1, syntaxin 1a7, syntaxin 1a8, and syntaxin 1a9 were phosphorylated while syntaxin 1a11 and syntaxin 1a12 were not. With the sequences of truncated forms of syntaxin 1a (listed in the caption of Figure 23), we can conclude that the phosphorylation site(s) should be between amino acids 115-193, which is consistent with peptide T32₁₅₉₋₁₈₉ suggested by mass spectrometry. The fragmentation of phosphorylated T32 was not successful due to

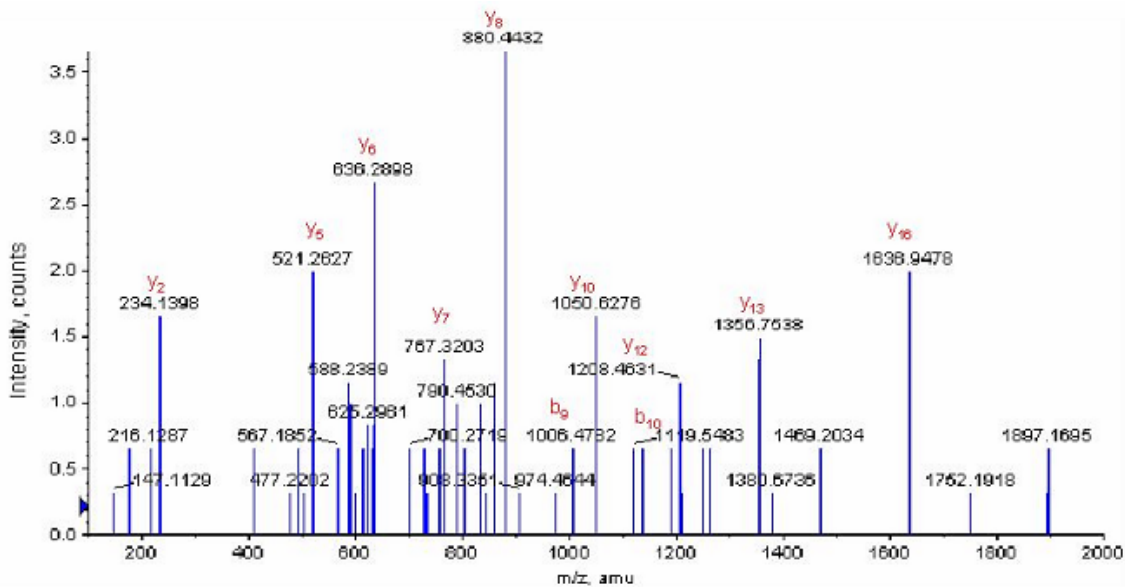


Figure 24. MS/MS spectrum of unphosphorylated T32 (1637.7, +2,) with strong b, y ions labeled.

its extremely low signal intensity. Its unphosphorylated form, however, was successfully fragmented and its sequence was confirmed as shown in Figure 24 (with a Mowse Score

of 66). The +2 charged form of phosphorylated T32 was also found in the phosphorylated samples. Despite this accumulated evidence that T32 is a phosphopeptide, the exact phosphorylation site remains unknown. Site-directed mutagenesis of potential phosphorylation sites would be necessary to pinpoint the exact sites, which would also serve as *in vivo* verification. It would be wise to start with highly likely sites such as S162, S186, S188, T160 and T161 (predicted by Netphos 2.0). With the observation of S188 minus water in the fragmentation of unphosphorylated T32, S188 might be the first choice for a site-directed mutagenesis study.

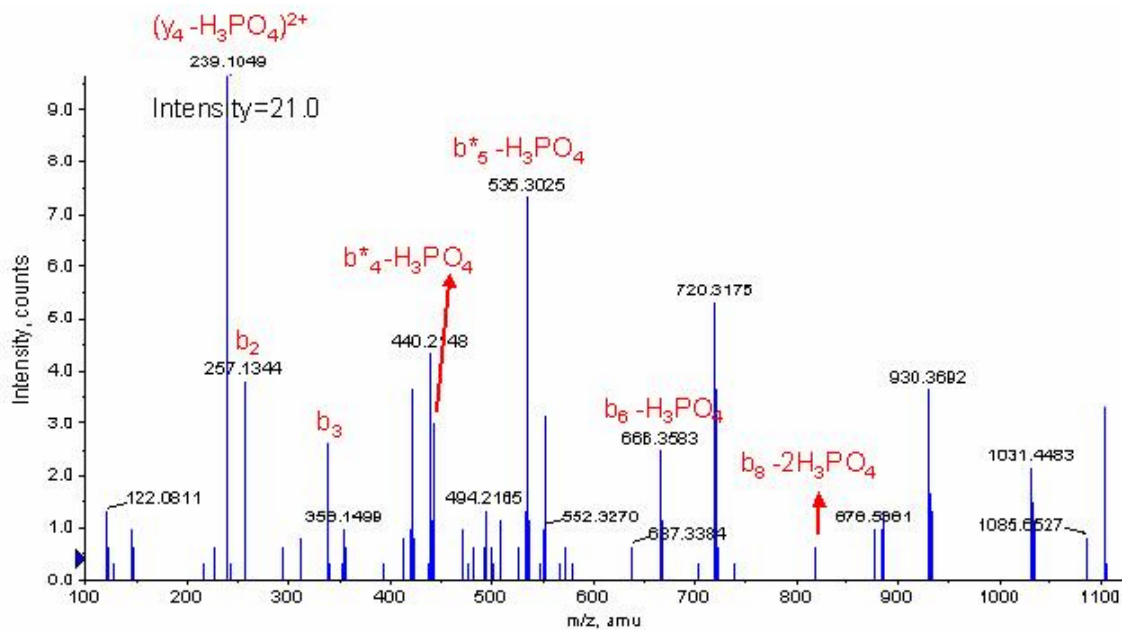


Figure 25. MS/MS spectrum of T12 of syntaxin 4a (1012.5, +2, Mowse score, 20) with strong b, y and their de-ammonia (b^*) form labeled.

With the surprise finding of the difference in syntaxin 1 and syntaxin 4 phosphorylation by PKA (cAMP-dependent protein kinase), it is necessary to study syntaxin 4 phosphorylation by AMPK. Above all, this is because it is syntaxin 4 that is present in the muscle cells, and thus, more relevant to the physiology of interest. Pure syntaxin 4a (amino acid sequence, 1-273, without the membrane spanning region,

residues 274-293) was purchased (Synaptic system, Goettingen, Germany) and *in vitro* phosphorylated in the same manner as syntaxin 1a. A candidate for the phosphorylated peptide T12 (Q₆₅QVTILATPLPEESMK₈₀) was chosen for fragmentation in the IDA mode. Three possible phosphorylation sites (T68, T72 and S78) were identified based on the fragmentation (Figure 25). The Mowse score was 20, which means further verification of these sites will be needed by site-directed mutagenesis or other methods. Site-directed mutagenesis will also be needed for *in vivo* confirmation of phosphorylation and study of the role of this phosphorylation.

4.4 CONCLUSIONS

Different strategies were applied for different cases of protein phosphorylation analysis. Although PhLP phosphorylation by CK2 has been previously studied, more detailed characterization of its multiply phosphorylated peptide was enabled after it had been enriched using the MonoTip® TiO Pipette Tip. All four serine phosphorylation sites in the peptide were identified with high confidence by MS. Analysis of syntaxin 1a phosphorylation was very difficult due to the low phosphorylation stoichiometry. Enrichment by MonoTip® TiO Pipette Tip was unsuccessful. Taking one step back, peptide level mapping for phosphorylation of syntaxin 1a was carried out. Some general rules for phosphopeptide mapping are 1) the non-phosphopeptide form should always be observed when the phosphorylation rate is low, 2) clean samples should be used to reduce false positives and a control with a phosphatase would be recommended, and 3) retention time can also be used to rule out false positives. Increased polarity from the phosphate group leads to shorter retention time on reverse-phased LC. Only one peptide, T32, was identified as a potential phosphopeptide under these rules. Further work such as site-

directed mutagenesis will be required in order to pinpoint the exact phosphorylation location. Analysis of phosphorylation of the more relevant protein syntaxin 4 by AMPK seemed to be more successful than analysis of syntaxin 1a. Three phosphorylation sites ((T68, T72 and S78) were suggested on the same peptide by IDA acquisition with a Mowse score of 20. The good fragmentation of its unphosphorylated form gives more confidence to the possible identification of these phosphorylation sites. Still, further confirmation will be required. The next step will be the study of the role of this phosphorylation in AMPK activation and glucose uptake.

4.5 REFERENCES

- Goodyear, L. J., and B. B. Kahn. (1998) Exercise, glucose transport, and insulin sensitivity. *Annu. Rev. Med.* 49: 235–261
- Hayashi, T., J. F. P. Wojtaszewski, and L. J. Goodyear. (1997) Exercise regulation of glucose transport in skeletal muscle. *Am. J. Physiol.* 273 (Endocrinol. Metab. 36): E1039–E1051,
- Hayashi, T., M. F. Hirshman, E. J. Kurth, W. W. Winder, and L. J. Goodyear. (1998) Evidence for 58-AMP-activated protein kinase mediation of the effect of muscle contraction on glucose transport. *Diabetes* 47: 1369–1373
- Holloszy, J. O., and P. A. Hansen. (1996) Regulation of glucose transport into skeletal muscle. *Rev. Physiol. Biochem. Pharmacol.* 128: 99–193
- Kweon HK, Hakansson K. (2006) Selective zirconium dioxide-based enrichment of phosphorylated peptides for mass spectrometric analysis. *Anal Chem.* 78:1743-9
- Lazarov, M. E., Martin, M. M., Willardson, B. M. & Elton, T. S. (2000) Molecular cloning and characterization of the human phosducin-like protein promoter. *Biochimica et Biophysica Acta* 1492, 460–464
- Lukov GL, Baker CM, Ludtke PJ, Hu T, Carter MD, Hackett RA, Thulin CD, Willardson BM. (2006) Mechanism of assembly of G protein betagamma subunits by protein kinase CK2-phosphorylated phosducin-like protein and the cytosolic chaperonin complex. *J Biol Chem.* 281:22261-74.
- Savage JR, McLaughlin JN, Skiba NP, Ha HE, Willardson BM. (2000). Functional roles of the two domains of phosducin and phosducin-like protein. *J Biol Chem* 275, 30399–407.
- Vavvas, D., A. Apazidis, A. K. Saha, J. Gamble, A. Patel, B. E. Kemp, L. A. Witters, and N. B. (1997) Ruderman. Contraction-induced changes in acetyl-CoA carboxylase and 58-AMP-activated kinase in skeletal muscle. *J. Biol. Chem.* 272: 13256–13261

- Winder WW, Hardie DG. (1999) AMP-activated protein kinase, a metabolic master switch: possible roles in type 2 diabetes. *Am J Physiol.* Jul;277(1 Pt 1):E1-10.
- Winder, W. W., and D. G. Hardie. (1996) Inactivation of acetyl-CoA carboxylase and activation of AMP-activated protein kinase in muscle during exercise. *Am. J. Physiol.* 270 (Endocrinol. Metab. 33): E299–E304
- Woodbury , D. J., J. M. McNally, J. R. Lemos. (2006) SNARE-induced fusion of vesicles to a Planar Bilayer. Chapter 10 *in* "Advances in planar lipid bilayers and liposomes", edited by A. Leitmannova-Liu. (Elsevier) Vol. 5:287-313. (in press).

CHAPTER FIVE

FUTURE WORK

Future work involves finishing up the incomplete part of syntaxin 4 phosphorylation by AMPK and its role in the signal pathway, as well as synthesizing a more hydrophilic monomer, such as acrylamidomethanesulfonic acid, for the monolithic SCX column to achieve a less hydrophobic property.

5.1 APPLIED SITE-DIRECTED MUTAGENESIS TO CONFIRM THE IDENTIFIED PHOSPHORYLATION SITES IN VIVO AND ROLES OF PHOSPHORYLATION ON THESE SITES

5.1.1 Confirmation of the Identified Phosphorylation Sites *in vivo*

Confirmation of these possible phosphorylation sites *in vivo* can be done in three steps. First, plasmids containing the desired mutation of syntaxin 4 and a tag (such as myc tag) can be transfected to a rat cell line. Cells will be serum starved and then incubated with serum and radio label (^{32}P -labeled phosphate). Immunoprecipitation with an antibody against the tag will be performed to pull down syntaxin 4 mutants. No radioactivity should be detected if the mutation on these identified sites successfully blocks the phosphorylation. Otherwise, phosphorylation site(s) other than the identified could be phosphorylated.

5.1.2 Role of Phosphorylation on the Identified Sites

After the phosphorylation sites are confirmed *in vivo*, study of the role of this phosphorylation in the process of AMPK activation and glucose uptake will be carried out. According to the proposed mechanism, phosphorylation potentially increases the

vesicle-membrane fusion process. If it is true, mutation of these sites should block the process. The role of this phosphorylation in the fusion process can be deduced by the degree that the fusion process is blocked by mutation of these sites.

5.1.3 Examination of the Possibility of other SNARE Proteins Involved in This Vesicle-membrane Fusion Process

Although Dr. Winder has ruled out the possibility of SNAP-25 and VAMP protein phosphorylation by AMPK, it is possible that their counterparts SNAP-23 and VAMP-2 might behave differently as substrates for AMPK, especially when considering that syntaxin 1a and syntaxin 4a are phosphorylated differently by AMPK. Initial examination can be done by using recombinant SNAP-23 and VAMP-2 proteins *in vitro* phosphorylated by AMPK. Further experiments will be carried out if there is any sign of phosphorylation of these proteins *in vitro*. It is not hard to tell if they can be phosphorylated or not with the ^{32}P -labeled *in vitro* phosphorylation experiment.

5.2 FUTURE WORK ON THE MONOLITHIC SCX COLUMN

Either the synthesis of acrylamidomethanesulfonic acid through new approaches or the separation of acrylamidomethanesulfonic acid from 2-aminoethanesulfonic acid will be recommended for future work to achieve a more hydrophilic monomer for the monolithic SCX column.